

Electronic Thesis and Dissertation Repository

---

4-10-2024 2:00 PM

# Physical and Geometrical Modulation of Human Fibroblast Behaviour

Sarah M. Brooks, *Western University*

Supervisor: Hamilton, Douglas W., *The University of Western Ontario*

Co-Supervisor: Mittler, Silvia, *The University of Western Ontario*

A thesis submitted in partial fulfillment of the requirements for the Doctor of Philosophy degree in Biomedical Engineering

© Sarah M. Brooks 2024

Follow this and additional works at: <https://ir.lib.uwo.ca/etd>



Part of the [Biomaterials Commons](#)

---

## Recommended Citation

Brooks, Sarah M., "Physical and Geometrical Modulation of Human Fibroblast Behaviour" (2024).  
*Electronic Thesis and Dissertation Repository*. 10042.  
<https://ir.lib.uwo.ca/etd/10042>

This Dissertation/Thesis is brought to you for free and open access by Scholarship@Western. It has been accepted for inclusion in Electronic Thesis and Dissertation Repository by an authorized administrator of Scholarship@Western. For more information, please contact [wlsadmin@uwo.ca](mailto:wlsadmin@uwo.ca).

## Abstract

This thesis investigates the impact of mechanical stimuli, specifically substratum topography and elastic modulus, on dermal and gingival fibroblast behaviour associated with scarring and regeneration. Scar formation presents a significant issue for implanted biomaterials often leading to device failure. Even though scar formation is a normal end point to adult human dermal wound healing, gingival wounds are capable of tissue regeneration or scarless wound healing. Understanding how these cells respond to environmental cues, including substratum topography and elastic modulus, is central to the development of novel biomaterials for stimulation of tissue regeneration. It was hypothesized that topographic features, with submicron periodicity, will inhibit increased cell contraction and excessive extracellular matrix deposition on materials with a high stiffness.

The first aim quantifies and compares adhesion behaviors of human dermal and gingival fibroblasts on materials patterned with anisotropic sub-micron topographies. I reveal distinct responses between the two cell types including the necessity of integrin  $\beta 1$  in human dermal fibroblast (HDF) contact guidance. The second aim investigates the impact of varying elastic moduli on fibroblast physiology, highlighting differences in adhesion size and composition, F-actin arrangement, myofibroblast differentiation, and extracellular matrix production. The third aim introduces a novel, combined, elastic modulus-varied, topographic cell culture device, incorporating sub-micron topographies into a tunable elastic modulus material for the first time. This device will facilitate the study of how cells integrate mechanical stimuli, offering insights into their effects in vivo, specifically within soft tissue environments.

This work identifies the tissue of origin as a crucial determinant in fibroblast response to topography and elastic moduli, challenging existing theories on adhesion formation, and providing insights into integrin engagement mechanisms. The interplay between topography and elastic modulus is explored, suggesting a potential strategy for reducing fibrotic events related to implanted biomaterials.

Overall, this thesis enhances our understanding of fibroblast responses to microenvironmental cues, emphasizing the importance of tissue-specific considerations in biomaterial design and paving the way for future research in tissue engineering and wound healing.

## Keywords

Human dermal fibroblasts, Human gingival fibroblasts, Fibrillar adhesions, Tensin-1, Integrin  $\beta$ 1, Myofibroblast, Extracellular matrix, Mechanosensation, Submicron topography, Elastic modulus, Fibrosis.

## Summary for Lay Audience

Currently, a number of bone interfacing biomaterials, including dental and orthopaedic implants, possess varying surface geometries and topographies to optimize tissue repair and integration, implant efficacy and longevity. In contrast, there is less research existing on the effects of surface modifications upon the behaviour of soft-tissue residing cells which is important for implants such as catheters, stents and grafts. Scar formation and fibrosis remain a significant clinical problem in many tissues and organs including skin. Formation of a collagen dense tissue with little cellular presence is the normal response to injury of soft tissues such as skin in adults, but failure of the wound healing process to terminate results in fibrosis, which affects up to 90% of patients and can lead to a significant reduction in physical and psychological quality of life. Scar formation also inhibits the integration of various medical devices including dental and hip implants, leading to device failure. Interestingly, unlike adult skin, fetal and gingival tissues exhibit scarless healing after injury, but the underlying cell and molecular differences in these cells that result in different healing profiles is unknown.

In this thesis, I investigated the molecular behaviours associated with scar formation in dermal and gingival fibroblasts on surfaces incorporating a topography and surfaces with variable stiffness. I determined that human gingival fibroblasts use a different adhesion mechanism when sensing and responding to surface topography compared to human dermal fibroblasts. I also demonstrated that human gingival fibroblasts and human dermal fibroblasts behave differently on surfaces of low stiffness. Finally, I created a means to investigate cell behaviour on a surface of variable, but defined topography and stiffness, combined. The results of this study provided further insight into cell-material interactions and allow optimization of biomaterials to promote regeneration of soft tissues, rather than scar formation and fibrosis.

# Co-Authorship Statement

## **Chapter 1**

Sarah Brooks wrote the chapter. Douglas Hamilton and Silvia Mittler contributed to the design of the chapter and provided critical feedback during preparation of this chapter.

## **Chapter 2**

Sarah Brooks performed the experiments, data analysis, and prepared the figures. The original topographic surfaces were fabricated by Erden Ertorer under the supervision of Silvia Mittler. Nie Heng-Yong of Surface Science Western completed the AFM and sessile drop goniometry. Douglas Hamilton established the direction of the study and contributed to the ongoing experimental design. Douglas Hamilton obtained ethical approval for all tissue collection used to obtain human dermal and gingival fibroblast primary cell lines. Sarah Brooks wrote the chapter with critical feedback from Douglas Hamilton and Silvia Mittler. This chapter is published in ACS Applied Materials & Interfaces: Brooks S, Mittler S, Hamilton DW. Contact Guidance of Connective Tissue Fibroblasts on Submicrometer Anisotropic Topographical Cues Is Dependent on Tissue of Origin,  $\beta$ 1 Integrins, and Tensin-1 Recruitment, 2023; 15 (16), 19817-19832, DOI: 10.1021/acsami.2c22381.

## **Chapter 3**

Sarah Brooks performed the experiments, data analysis, and prepared the figures. Douglas Hamilton established the direction of the study and contributed to the ongoing experimental design. Douglas Hamilton obtained ethical approval for all tissue collection used to obtain human dermal and gingival fibroblast primary cell lines. Sarah Brooks wrote the chapter with critical feedback from Douglas Hamilton and Silvia Mittler. This chapter is in preparation for manuscript submission.

## **Chapter 4**

Sarah Brooks performed the experiments, data analysis, and prepared the figures. The original topographic surfaces were fabricated by Erden Ertorer under the supervision of

Silvia Mittler. Nie Heng-Yong of Surface Science Western completed the AFM and sessile drop goniometry. Douglas Hamilton established the direction of the study and contributed to the ongoing experimental design. Douglas Hamilton obtained ethical approval for all tissue collection used to obtain human dermal and gingival fibroblast primary cell lines. Sarah Brooks wrote the chapter with critical feedback from Douglas Hamilton and Silvia Mittler.

## **Chapter 5**

Sarah Brooks wrote the chapter. Douglas Hamilton and Silvia Mittler contributed to the design of the discussion and provided critical feedback during preparation of this chapter.

## Acknowledgments

I would like to express my sincere gratitude to my co-supervisors, Dr. Douglas Hamilton, and Dr. Silvia Mittler, for their invaluable guidance and unwavering support throughout the completion of my thesis. Their expertise, insightful feedback, and encouragement have been instrumental in shaping this work. Thank you for fostering my scientific independence and journey of personal growth and development.

To my advisory committee, Dr. Lauren Flynn, Dr. Cheryle Seguin, and Dr. Amin Rizkalla, thank you for the invaluable contributions to the completion of my thesis. Each member brought a unique perspective and expertise to the table, enriching the depth and quality of my research.

It goes without saying this thesis could not have been completed without the funding provided by the Natural Sciences and Engineering Research Council (NSERC). I recognize the privilege of living in a country that enables intellectual curiosity.

Thank you to all the members of the Hamilton Lab, past and present, for their unwavering support and camaraderie. The shared challenges, triumphs, and countless discussions have created a vibrant intellectual environment that has shaped and enriched my research experience. To Georgia, thank you for your guidance and friendship.

Finally, I would not be here today without the endless support of my parents, siblings, and husband. Thank you all for being incredible role models, a voice of reason and the light of my life.

# Table of Contents

Abstract.....	ii
Summary for Lay Audience.....	iv
Co-Authorship Statement.....	v
Acknowledgments.....	vii
Table of Contents.....	viii
List of Tables.....	xiv
List of Figures.....	xv
List of Abbreviations.....	xviii
1 Rationale, Literature Review and Thesis Overview.....	1
1.1 Rationale, Hypothesis and Objectives.....	1
1.2 Soft Tissue Injury and Healing: Role of the fibroblast in wound resolution.....	3
1.2.1 Scar Formation.....	8
1.2.2 Scarless wound healing.....	8
1.2.3 Human gingival wound healing.....	9
1.3 The cellular microenvironment and modeling the influence of external stimuli on cell behaviour in vitro.....	10
1.4 Mechanotransduction: How cells sense their external environment.....	11
1.4.1 Cellular adhesion formation.....	11
1.5 A mechanism of migration: Contact guidance.....	13
1.6 Controlling environmental parameters to regulate cell behaviour.....	14
1.6.1 Elastic modulus.....	14
1.6.2 Topography.....	15
1.7 Thesis Overview.....	19
1.8 References.....	21



2	Quantification and comparison of human dermal and gingival fibroblast behaviours, associated with fibrosis, upon materials of various topographies. ....	30
2.1	Introduction.....	30
2.2	Materials and Methods.....	31
2.2.1	Dermal and gingival fibroblast isolation and culture.....	31
2.2.2	Fabrication of topographical cues .....	31
2.2.3	Atomic force microscopy.....	35
2.2.4	Sessile Drop Goniometry .....	35
2.2.5	Submicron topographic substrate cell culture.....	35
2.2.6	Immunocytochemistry of adhesion formation and extracellular matrix deposition analysis .....	36
2.2.7	Focal and fibrillar adhesion quantification .....	36
2.2.8	Statistical Analysis.....	37
2.3	Results.....	38
2.3.1	Submicron repeating grooves induce alignment of vinculin, tensin-1 and F-actin in HDFs and HGFs without altering adhesion site quantity or area.....	38
2.3.2	Fibronectin deposition and organization.....	49
2.3.3	Inhibition of integrin $\alpha\beta3$ and integrin $\beta1$ influence HDF and HGF spreading.....	54
2.3.4	Inhibition of integrin $\alpha\beta3$ and integrin $\beta1$ reduce HDF orientation/alignment, but not in HGFs at 24 h post seeding .....	59
2.4	Discussion.....	66
2.4.1	HGFs and HDFs exhibit morphological and adhesion alignment to sub-micron groove topographies.....	66
2.4.2	HDFs and HGFs require both integrin $\alpha\beta3$ and integrin $\beta1$ adhesion sites for cell spreading and elongation up to 6 hours post-seeding.....	68
2.4.3	Inhibition of integrin $\alpha\beta3$ and integrin $\beta1$ illustrates an essential role for $\beta1$ integrins in contact guidance of HDFs, but not HGFs. ....	69

2.4.4	HDFs recruit tensin-1 to focal adhesion in the absence of $\beta$ 1 integrin adhesion sites .....	71
2.4.5	Sub-micron grooves as an anti-fibrotic surface: Disruption of fibronectin fibril formation .....	72
2.4.6	Conclusions.....	73
2.5	References.....	74
3	Comparison of human dermal and gingival fibroblast behaviour in response to varying elastic modulus. ....	80
3.1	Introduction.....	80
3.2	Materials and Methods.....	81
3.2.1	Dermal and gingival fibroblast isolation and culture.....	81
3.2.2	Varied elastic modulus substratum cell culture .....	82
3.2.3	Adhesion and proliferation quantification .....	82
3.2.4	Immunofluorescent labelling .....	83
3.2.5	Western Blot .....	83
3.2.6	Analysis of underlying mechanotransduction signalling pathways.....	83
3.2.7	Statistical analysis.....	84
3.3	Results.....	84
3.3.1	HDFs and HGFs exhibit differential adhesion and proliferation on surfaces of differing elastic modulus .....	84
3.3.2	HDF and HGF focal and fibrillar adhesion associated protein localization is altered by varying surface elastic modulus.....	89
3.3.3	Extracellular matrix is differentially deposited upon surfaces of varying elastic modulus .....	103
3.3.4	HDF and HGF are capable of myofibroblast differentiation in a manner dependent on elastic modulus. ....	108
3.3.5	Exogenous TGF- $\beta$ 1 treatment alters HGF adhesion composition .....	115
3.3.6	HDF and HGF intracellular signaling differs across substratum of varying elastic modulus .....	120

3.4	Discussion.....	125
3.4.1	Tissue culture plastic reduces HDF and HGF initial cell adhesion and proliferation rate.....	125
3.4.2	Influence of elastic modulus on HDF and HGF adhesion and cytoskeletal F-actin arrangement are population specific.....	126
3.4.3	HDFs and HGFs quickly alter low elastic modulus surfaces with extracellular matrix deposition .....	128
3.4.4	HGF myofibroblast differentiation is dependent upon the elastic modulus of the substratum, adhesion formation and TGF- $\beta$ 1. ....	129
3.4.5	Intracellular signaling in human dermal and gingival fibroblasts downstream of variation in elastic moduli.....	130
3.4.6	Conclusions.....	131
3.5	References.....	132
4	Fabrication of a novel, elastic moduli varied-topographic cell culture surface .....	138
4.1	Introduction.....	138
4.2	Materials and Methods.....	139
4.2.1	Elastic Moduli Varied-Topographical Substratum Fabrication .....	139
4.2.2	Material Characterization.....	144
4.2.3	Dermal and Gingival Fibroblast Isolation and Culture.....	145
4.2.4	Elastic Moduli Varied-Topographic Substratum Cell Culture .....	145
4.2.5	Immunofluorescence.....	145
4.3	Results.....	146
4.3.1	Silicone provides an optically translucent, structural polymer with negligible swelling to fabricate topographic surfaces of various elastic modulus.....	146
4.3.2	Silicone reliably fabricates submicron topographic cell culture substrata .....	149
4.3.3	Silicone allows reliable fabrication of submicron topographic cell culture substrata of varying elastic modulus.....	154

4.3.4	Plasma treated silicone with submicron topographic features are hydrophilic .....	157
4.3.5	Silicone surfaces with submicron topographic details provides a viable means of cell culture .....	161
4.4	Discussion .....	164
4.4.1	Silicone provides an optically translucent, structural polymer with negligible swelling to fabricate topographic surfaces of various elastic modulus.....	164
4.4.2	The fabricated topographic silicone elastomers establish development of a novel cell culture device. ....	167
4.5	References .....	168
5	Discussion .....	171
5.1	General Discussion .....	171
5.1.1	Quantification and comparison of human dermal and gingival fibroblast adhesion composition and behaviours on materials patterned with anisotropic sub-micron topographies.....	171
5.1.2	Quantification and comparison of human dermal and gingival fibroblast adhesion composition and behaviours on materials of varying elastic moduli.....	173
5.1.3	The fabrication of a novel, combined, elastic modulus varied, topographic cell culture device to quantitate human dermal and gingival fibroblast behavior. ....	175
5.2	Contributions to the Literature.....	176
5.2.1	Tissue of Origin as a Variant in Fibroblast response to topography and variations in elastic moduli .....	176
5.2.2	Hierarchical Adhesion Theory: Are $\beta 1$ integrins the real determinant of contraction, but not necessarily of adhesion maturity? .....	177
5.2.3	How to engage an Integrin.....	178
5.2.4	Topography VS Elastic Modulus: Is one more important than the other?.....	179
5.3	Experimental Limitations.....	179
5.4	Future Directions .....	180

5.5 Conclusions.....	182
5.6 References.....	183
Appendix A: Supplementary Tables & Figures.....	191
Appendix B: Human Ethics Approvals.....	192
Curriculum Vitae .....	194

## List of Tables

Table 2-1: Average quantity and area of vinculin containing focal adhesions.....	47
Table 2-3: Average quantity and area of tensin-1 containing fibrillar adhesions.....	48
Table 4-1: Silicone elastomer polymerization specifications .....	141
Table 4-2 Surface contact angle determined through sessile drop goniometry .....	160

## List of Figures

Figure 1-1: Fibroblast involvement in traditional stages of adult dermal wound healing: hemostasis, inflammation, proliferation, and remodeling. ....	7
Figure 1-2: Scanning electron microscopy images of (A) nanogrooves, and (B) discontinuous nanogroove dot topographies employed in topographical studies of cell physiology.....	18
Figure 2-1: Schematic of submicron topographical silicon surface fabrication .....	34
Figure 2-2: HDFs and HGFs orient with respect to the long axis of the groove topographies.....	40
Figure 2-3: Nanogrooves effect adhesion site and intracellular cytoskeletal protein expression of HGFs and HDFs. ....	42
Figure 2-4: Submicron grooves orient HGF and HDF adhesion proteins. ....	44
Figure 2-5: Submicron grooves orient HGF and HDF cytoskeletal proteins. ....	46
Figure 2-6: HDF and HGF fibronectin fibril assembly is disrupted by anisotropic repeating groove topographies.....	51
Figure 2-7: Association of $\alpha 5$ and $\beta 1$ integrin dimers are disrupted on anisotropic repeating groove topographies.....	53
Figure 2-8: Inhibition of integrin $\alpha \nu \beta 3$ and integrin $\beta 1$ has a differential effect upon HGF and HDF spreading. ....	56
Figure 2-9: HDF and HGF cell area and circularity are affected by $\alpha \nu \beta 3$ and integrin $\beta 1$ blocking antibodies. ....	58
Figure 2-10: Independent inhibition of integrin $\alpha \nu \beta 3$ and integrin $\beta 1$ demonstrates contrast in alignment between HDF and HGF.....	61

Figure 2-11: Independent inhibition of integrin $\alpha\beta3$ and integrin $\beta1$ demonstrates a functional disparity amongst HDF and HGF. ....	63
Figure 2-12: Inhibition of integrin $\beta1$ results in tensin-1 recruitment to $\alpha\beta3$ peripheral adhesion sites in HDFs, but not HGFs. ....	65
Figure 3-1: HDF and HGF adhesion is effected by substratum elastic modulus. ....	86
Figure 3-2: HDF and HGF proliferation increases upon surfaces of low elastic moduli .	88
Figure 3-3: A substratum of 0.2 kPa elastic modulus inhibits HDF F-actin stress fiber formation. ....	92
Figure 3-4: Substrata of low elastic modulus inhibit HGF F-actin stress fiber formation. ....	94
Figure 3-5: HDF and HGF vinculin protein expression is unchanged by substratum elastic modulus. ....	96
Figure 3-6: HDF and HGF tensin-1 expression is centrally located upon TCP .....	98
Figure 3-7: HDF and HGF focal and fibrillar adhesion quantity and area is dependent upon substratum elastic modulus .....	100
Figure 3-8: HDF and HGF focal and fibrillar adhesions decrease in size upon substrata of low elastic modulus. ....	102
Figure 3-9: HDF and HGF quickly establish fibronectin fibrils upon low elastic modulus surfaces .....	105
Figure 3-10: A substrate elastic modulus of 0.2 kPa inhibits HDF and HGF extracellular matrix production following 2 weeks .....	107
Figure 3-11: HDF Myofibroblast differentiation is unaffected by substratum elastic modulus. ....	110
Figure 3-12: TGF- $\beta1$ induces HGF myofibroblast differentiation upon TCP .....	112



Figure 3-13: $\alpha$ -SMA expression by HDFs and HGFs shows minimal change by culturing on substrata of various elastic moduli.....	114
Figure 3-14: Integrin $\beta$ 1 and Tensin-1 exhibit greater co-localization upon TCP than 0.2 kPa elastic modulus surface among HGFs.....	117
Figure 3-15: TGF- $\beta$ 1 treatment switches integrin $\alpha$ v $\beta$ 3 adhesion engagement for integrin $\beta$ 1 in HGFs.....	119
Figure 3-16: HDF ERK1/2 and GSK3 $\alpha$ $\beta$ phosphorylation is effected by culturing on surfaces of varying elastic moduli .....	122
Figure 3-17: HGF ERK1/2 phosphorylation is upregulated upon 64 kPa elastic modulus surface.....	124
Figure 4-1: Schematic detailing the fabrication process of the topographic silicone elastomers .....	143
Figure 4-2: Fabrication process of topographic, silicone elastomers .....	148
Figure 4-3 Atomic force microscopy images of the elastic modulus varied topographic silicone elastomers.....	151
Figure 4-4: Periodicity of peak-to-peak topographic structures within silicone elastomers with varied elastic modulus. ....	153
Figure 4-5: Elastic modulus of the fabricated silicone elastomers patterned with topographic features.....	156
Figure 4-6: Contact angle measurement upon plasma cleaned 5:1 and 10:1 topographic silicone elastomers .....	159
Figure 4-7: HDF and HDF upon silicone surfaces with a sub-micron topography .....	163

## List of Abbreviations

AA	Antibiotic and antimycotic
AFM	Atomic force microscopy
$\alpha$ SMA	$\alpha$ -smooth muscle actin
DMEM	Dulbecco's Modified Eagle Medium
dPBS	Dulbecco's Phosphate Buffered Saline
ECM	Extracellular matrix
EGF	Epidermal growth factor
ERK1/2	Extracellular signal-regulated kinases-1/2
FAK	Focal adhesion kinase
FBS	Fetal bovine serum
GSK-3ab	Glycogen synthase kinase 3
HDF	Human dermal fibroblast
HGF	Human gingival fibroblast
IL	Interleukin
INF	Interferon
MMP	Matrix metalloproteinases
PBS	Phosphate buffered saline
PDGF	Platelet-derived growth factor
PECAM	Platelet endothelial cell adhesion molecule

PEG	Polyethylene glycol
PVS	Polyvinylsiloxane
TCP	Tissue culture plastic
TGF $\beta$ 1	Transforming growth factor- $\beta$ 1
TNF- $\alpha$	Tumor necrosis factor- $\alpha$

# 1 Rationale, Literature Review and Thesis Overview

## 1.1 Rationale, Hypothesis and Objectives

Currently, bone interfacing biomaterials, such as dental and joint implants, possess varying specific surface geometries and topographic features to optimize tissue repair and regeneration by osteoblasts and fibroblasts through improved osseointegration, reduced fibrotic events, and ultimately increased implant longevity<sup>1,2</sup>. However, there is relatively little research on the effects of biomaterial surface modifications on the control and regulation of fibroblast behaviour to optimize healing and incorporation of biomaterials that interface with soft tissues, e.g. abutments of dental implants<sup>3</sup>. Scar formation characterized by increased cell contraction and excessive extracellular matrix (ECM) deposition, represents a normal response to soft tissue injury in postnatal life, as well as during integration of biomaterials into host tissues. Scar tissue exhibits reduced function, increased stiffness, and decreased strength<sup>4</sup>. Strategies that reduce scar formation are a persistent obstacle in the design of biomaterials to facilitate efficacy and longevity of implanted materials. As postnatal tissue injury response often results in scarring, it is important to understanding the cellular and molecular processes that cause fibrotic tissue formation and how they are controlled by physical factors to develop methods of controlling fibrosis development. Of great significance is that both prenatal and adult oral tissues exhibit an ability to regenerate, leading to scarless healing<sup>4</sup>. Fibrotic cell behaviours are known to be influenced directly by how cells interact with their surrounding environment, whether that is extracellular matrix or a biomaterial surface. Specifically, topography and the elastic moduli of the matrix/material are known to influence cell adhesion and downstream molecular events that regulate cell phenotype and control cell contractility<sup>4-6</sup>. *Understanding how cells respond to such environmental cues is central to the development of novel biomaterials for stimulation of tissue regeneration.* Currently, model systems to study these physical cues in combination *in vitro* are not available, which we will address in this thesis, with the long-term goal of implementing the results of this study to design novel biomaterials that promote soft tissue healing.

Of great clinical significance, biomaterials of a higher stiffness promote cellular behaviours associated with fibrosis (increased adhesion, adoption of a contractile phenotype, excessive extracellular matrix production) <sup>7,8</sup>. However, our group has previously shown that specific topographic features that limit adhesion formation in mammalian cells can reduce fibrotic cell behaviours independent of the substratum stiffness <sup>3</sup>. This work demonstrates that topographical cues could be used to limit the fibrotic response on biomaterials with a high stiffness. The goal of this thesis was to quantify the mechanistic influence of substratum topography and elastic moduli, alone and in combination, on fibrotic cell behaviours.

*The overall hypothesis was that topographical and elastic modulus modulation will differentially affect human dermal and gingival fibroblast behaviour including cellular adhesion, proliferation, extracellular matrix production, and cell contractility. This hypothesis will be tested using the following specific aims:*

*Aim 1: Quantification and comparison of human dermal and gingival fibroblast adhesion composition and behaviours, associated with fibrosis, on materials patterned with anisotropic sub-micron topographies.*

*Aim 2: Quantification and comparison of human dermal and gingival fibroblast adhesion composition and behaviours, associated with fibrosis, on materials of varying elastic moduli.*

*Aim 3: The fabrication of a novel, combined, elastic modulus varied, topographic cell culture device to quantitate human dermal and gingival fibroblast behavior, associated with fibrosis.*

The objective of this study was to develop, optimize and utilize a unique cell culture surface combining variable elastic moduli with topographic features to investigate the molecular behaviours associated with scar formation in dermal and gingival fibroblasts. Cellular adhesion, morphology, migration, differentiation, proliferation, and extracellular matrix production was investigated using this novel cell culture device of varying topographical structure and elastic modulus. The increase of substratum elastic modulus was hypothesized to increase cellular behaviour associated with fibrosis including an increase

in cellular adhesion, proliferation, extracellular matrix production, and cell contractility. The presence of a substratum topography was hypothesized to work in opposition to the high elastic modulus; the aforementioned fibrosis associated behaviours will decrease due to geometrical limitation of adhesion site formation. Human dermal and gingival fibroblasts were hypothesized to exhibit different responses to substratum topography and elastic moduli; human gingival fibroblasts will exhibit less sensitivity, through a minimal effect of substratum topography and elastic modulus upon the investigated behaviours, as compared to human dermal fibroblast populations. The quantification of adhesion patterns, extracellular matrix deposition, cell proliferation, and myofibroblast differentiation upon various sub-micrometer topographical substrata, elastic modulus altered substrata and the elastic modulus varied-topographic cell culture surface aimed to assess mechanistic differences between the two fibroblast cell lineages.

## 1.2 Soft Tissue Injury and Healing: Role of the fibroblast in wound resolution

Mammalian wound healing is characterized by four temporally consecutive, overlapping phases (visualized in Figure 1-1); hemostasis, inflammation, proliferation and remodeling with the goal of repairing the site of injury and restoring the native tissue function <sup>4</sup>.

Hemostasis is initiated immediately following the injury. A platelet plug is formed, followed by a fibrin matrix for infiltrating cells to adhere to in the subsequent stages <sup>4</sup>. The combined fibrin matrix and platelet plug establish a thrombus which halts bleeding, and releases growth factors and cytokines such as platelet-derived growth factor (PDGF), transforming growth factor- $\beta$  (TGF $\beta$ 1) and epidermal growth factor (EGF) <sup>9</sup>. In response to these growth factors, fibroblasts undergo chemotaxis, migrating towards the wound site, where they proliferate, differentiate into myofibroblasts, and synthesize collagen <sup>10</sup>.

The inflammatory stage occurs over the first three to five days following the injury <sup>11</sup>. Neutrophils are recruited to the wound bed along with monocytes which subsequently differentiate into macrophages of varying phenotypes <sup>4</sup>. Neutrophils and macrophages

serve to phagocytize debris and contaminants from the wound bed in preparation for new tissue growth. They also release inflammatory mediators such as interleukin-1 (IL-1), interleukin-6 (IL-6), tumor necrosis factor- $\alpha$  (TNF- $\alpha$ ) and reactive oxygen species <sup>12</sup>. As a result, the immune response is heightened by the recruitment and activation of more neutrophils and macrophages, in addition to fibroblasts and other cell populations involved in the subsequent healing processes. Fibroblasts also contribute to the immune response by upregulating adhesion molecules necessitated by immune cells and producing pro-inflammatory cytokines including TNF- $\alpha$ , interferon- $\gamma$  (INF- $\gamma$ ), IL-6 and interleukin 12 (IL-12) <sup>13</sup>. The provisional fibrin matrix is augmented by fibroblasts to facilitate the migration of immune cells through the production of matrix metalloproteinases <sup>13</sup>.

The third phase of wound healing, proliferation, occurs for up to 6 weeks following the initial tissue injury <sup>11</sup>. A variety of cell types including keratinocytes, fibroblasts and immune cells continue to proliferate and migrate within the wound bed. Macrophages influence cell maturation and differentiation. Keratinocytes restore the epithelial barrier and angiogenesis occurs <sup>4</sup>. Fibroblasts differentiate and transition into contractile myofibroblasts, primarily as a result of increased mechanical forces acting upon the fibroblasts resulting in TGF $\beta$ 1 release, the upregulation of smooth muscle  $\alpha$ -actin ( $\alpha$ SMA) and deposition of collagen type III abundant extracellular matrix known as granulation tissue <sup>4,14</sup>. Granulation tissue essentially provides an interim scaffold for newly deposited ECM and neovasculature, a means of wound contraction by myofibroblasts in a positive feed-back loop, providing tensile strength within the wound bed, and leads to the poor structural organization of the wound site <sup>15</sup>.

In the final stage of wound healing, remodeling occurs of the granulation tissue for years following the initial injury as the body attempts to re-establish the native architecture of the uninjured tissue <sup>11</sup>. Myofibroblasts continue to contract the wound site and turn over the preliminary extracellular matrix from collagen type III into collagen type I via matrix metalloproteinases (MMPs) <sup>4</sup>. As a result of the remodeling process and continued myofibroblast activation, the extracellular matrix increases in stiffness, complexity, and order <sup>12</sup>. Many cells deemed no longer necessary within the wound bed undergo apoptosis. The decellularization process begins with the immune cells, followed by the endothelial

cells and fibroblast populations in effort to re-establish pre-injury tissue cellularity <sup>16</sup>. The resultant tissue does not possess the mechanical or physiological properties of uninjured skin as normal adult wound healing results in scar formation <sup>4</sup>.



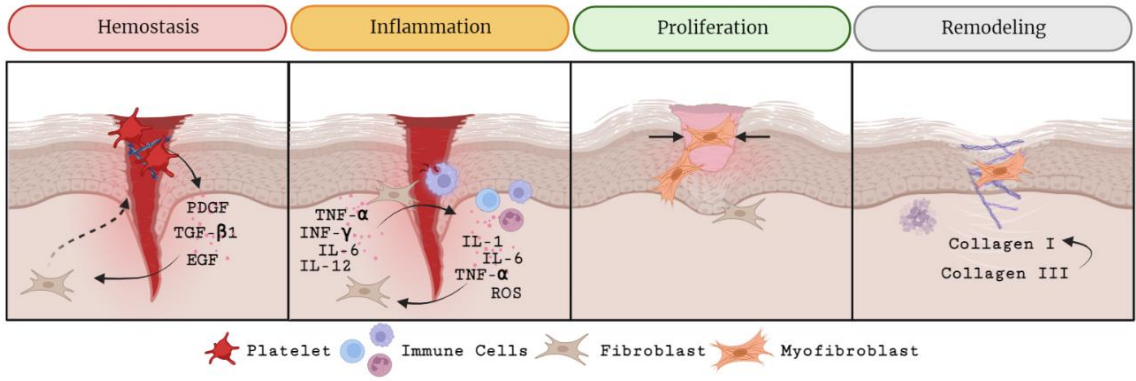


**Figure 1-1: Schematic visualization of fibroblast involvement in traditional stages of adult dermal wound healing: hemostasis, inflammation, proliferation, and remodeling.**

Cytokines produced in hemostasis by the thrombus induces fibroblast chemotaxis to the wound site. During the inflammation stage, fibroblasts upregulate adhesion molecules necessitated by immune cells, produce pro-inflammatory cytokines and augment the fibrin matrix with matrix metalloproteinases to facilitate the immune response. Fibroblasts establish a preliminary extracellular matrix and differentiate into myofibroblasts in the proliferative phase of wound healing. Remodeling can occur for years following an injury as the body attempts to re-establish the native architecture and function of the uninjured tissue.

Created with BioRender.com.

### 1.2.1 Scar Formation

Scar formation is a normal response to adult wound healing in soft connective tissues. Keloids and hypertrophic scars are characterized by abnormal wound healing and an excess of fibrotic tissue<sup>11,17</sup>. Leading to significant impairments of physical and psychological quality of life, keloids and hypertrophic scars are treated with corticotherapy, botulinum toxin and laser therapy, resulting in a billion-dollar burden upon the United States health care system<sup>4,11</sup>. Although the process of excessive healing as seen in the formation of keloids and hypertrophic scars is not completely understood, a prolonged inflammatory stage, excessive collagen deposition and remodeling, maintenance of fibroblast hypercellularity, persistence of myofibroblast activity, and excessive mechanical stress have all been implicated in the process<sup>8,11,14,17-19</sup>. It has been suggested that both the chemical and physical environment influence the cell's ability for normal wound healing<sup>4</sup>. An environment controlling the expression of pro-inflammatory mediators, such as IL-6, PDGF, and TGF- $\beta$ 1, as well as the differentiation, proliferation and maturation of cells including fibroblasts and macrophages, may be necessary to evade pathologies involving excessive scarring<sup>4-6,8,20</sup>. There are, however, exceptions to this rule, tissues where fibroblast activity does not result in scarring as a result of healing.

### 1.2.2 Scarless wound healing

Scarless wound healing is a form of tissue regeneration resulting in tissue identical to the native uninjured tissue. With regards to skin, complete regeneration is evident in some instances including embryos, adult human gingiva, and the African spiny mouse, *Acomys*<sup>12</sup>. In general, when comparing the processes of wound healing resulting in scar formation and tissue regeneration, tissue regeneration demonstrates less inflammation, lower levels of chemokines and TGF- $\beta$ 1, higher collagen type III/type I ratio, higher production of MMPs and fewer myofibroblasts<sup>12</sup>. The mechanistic differences underlying tissue regeneration, when compared to traditional adult wound healing resulting in scar formation, have yet to be fully elucidated and remain a major focus of wound healing

research. Current research has a focus on the recapitulation of behaviours associated with scarless wound healing, by scar forming adult fibroblasts, to determine the mechanism underlying scarless wound healing <sup>21</sup>.

### 1.2.3 Human gingival wound healing

The human gingiva is a soft connective tissue lined with epithelium overlying the alveolar bone, encapsulating the dentition, within the oral cavity. Human gingival tissue, much like fetal tissues, are capable of scarless healing through the classic four stage wound healing process, hemostasis, inflammation, proliferation, remodeling, exhibited in human dermal wound healing. Human gingival and dermal cells exhibit many differences including embryonic origin, neural crest and mesoderm respectively, as well as distinctive gene expression, extracellular matrix molecules, response to inflammatory mediators and reduced focal adhesion kinase (FAK) expression <sup>6,22,23</sup>. In comparison with dermal cells, gingival cells display fetal cell like characteristics including faster wound healing kinetics, cell migration into a collagen matrix and remodeling of a fibrin lattice as compared to dermal fibroblasts <sup>22</sup>. As the stimuli present in these collagenous dense tissues, dermis and gingiva, are similar during healing, the differences in fibroblast phenotypes during the healing processes is unexpected.

As fibroblasts are central to the wound healing process in both tissues, and how these cells behave in relation to the microenvironment is still poorly understood, further investigation is necessary to determine the mechanisms underlying scarless versus scarring healing in human tissues. *How gingival fibroblasts behave during healing at the cell and molecular level compared to dermal fibroblasts is largely unknown due to a lack of appropriate model systems for direct comparison of different cell types to the same external stimuli.*

### 1.3 The cellular microenvironment and modeling the influence of external stimuli on cell behaviour *in vitro*

The *in situ* extracellular environment, often referred to as the cellular microenvironment, includes extracellular molecules, growth factors, cytokines, cells, and interstitial fluid <sup>24</sup>. The extracellular matrix functions to provide strength, direct cell behaviours and sequester growth factors and cytokines for cellular processes. The extracellular matrix is a diverse substratum whose varying type, cellular and molecular components, greatly influence the cellular response to their local environment <sup>25</sup>. Among many others, tyrosine kinase receptors, CD44, RHAMM and integrin  $\alpha$  and  $\beta$  subunits influence cellular adhesion, proliferation, migration, invasion, and matrix remodeling through binding to the native collagen and glycosaminoglycan hyaluornan assembly of the extracellular matrix <sup>26-28</sup>.

The ECM also provides cells with topographic and mechanical cues in the structural organization and elastic moduli of the extracellular matrix respectively. Despite being primary stimuli governing resident cell response, how factors such as elastic moduli and topography of the matrix influence cell behavior is often overlooked. Therefore, understanding cell response to these stimuli is of great importance, particularly in combination, and is one of the foci of this thesis.

Cell behavior and phenotype is known to be influenced and modified by mechanical, chemical, and electrical stimuli within the cell's surrounding environment <sup>29</sup>. The scale and complexity of these external signals is difficult to integrate and model *in vitro* to investigate cell behavior. Although topographical, chemical, and electrical cues have been investigated in isolation, combinations of these stimuli have yet to be modelled in an accurate and controllable manner <sup>30,31</sup>. The establishment of a tunable, experimental model incorporating stimuli such as elastic moduli and topographical patterning within a cell culture environment, could provide essential information about mechanotransduction and cell phenotype during healing or tissue augmentation.

## 1.4 Mechanotransduction: How cells sense their external environment

Cells constantly receive input from the mechanical, and chemical cues present in their extracellular environment. Mechanotransduction, the molecular processes transforming extracellular mechanical stimuli (e.g. pressures or stresses) into biological responses, allows cells to respond and adapt to their dynamic environment<sup>32</sup>. Although the molecular processes underlying cellular mechanotransduction have yet to be completely elucidated, it is generally accepted that this process is mediated by adhesion sites and the cytoskeleton<sup>25,32</sup>. The analysis of cellular biomechanics allows determination of the effects of the mechanical cues present in the extracellular environment upon cellular gene expression, mRNA and protein production, extracellular matrix interactions and the molecular signaling pathways which regulate these responses<sup>33</sup>.

### 1.4.1 Cellular adhesion formation

Adhesions molecules embedded within the membrane of cells, linking the intra- and extracellular environment, are responsible for cell mechanotransduction. For example, platelets utilize platelet endothelial cell adhesion molecule (PECAM), vascular endothelial cells utilize cadherin, and fibroblasts interact directly with the ECM through integrins, actin-associated molecules (tensin, filamin, talin,  $\alpha$ -actin) and adaptor proteins<sup>25,34</sup>. Of interest to our research, for fibroblasts, matrix producing cells which are key to tissue homeostasis and implant integration, adhesion sites have been investigated extensively. Integrins are dynamic structures within adhesions composed of both  $\alpha$  and  $\beta$  subunits, capable of alteration with maturity<sup>35</sup>. Initially, Rac1 stimulates an intermediate adhesion complex, with a 200 nm diameter, observed within the lamellipodia composed of high tyrosine phosphorylation levels, integrin  $\beta$ 3, paxillin and talin, with low levels of vinculin and FAK<sup>36-38</sup>. These small adhesion complexes exert a local force of 1-3 nN/ $\mu\text{m}^2$ <sup>39</sup>. Focal adhesions, stimulated by RhoA, are matured intermediate adhesion complexes characterized by a recruitment of zyxin, integrin  $\alpha$ v $\beta$ 3, talin, vinculin, increased tyrosine

phosphorylation, and increased adhesion area (3 - 10  $\mu\text{m}$ ) at the terminus of actin stress fibers due to an increased local force ( $\sim 5 \text{ nN}/\mu\text{m}^2$ )<sup>39-42</sup>. Underlying the cell body, fibrillar adhesions are elongated along the fibronectin matrix in association with  $\alpha 5\beta 1$  integrin and tensin in response to experienced mechanical stress<sup>43-45</sup>. During rapid migration, cells avoid well-formed adhesions and establish diffusely organized adhesions, relatively close to the substratum (30 nm)<sup>46</sup>. Many tyrosine, serine, or threonine-specific protein kinases and phosphatases, Rho-family GTPases, function as intra-adhesion local and global cell regulators of many cellular processes including adhesion, proliferation, migration, and differentiation by activating intracellular signalling pathways<sup>25</sup>. Among the most important signaling pathways activated by adhesion mechanotransduction are the Rho, ROCK, and Rac signaling cascades influencing actin stabilization, cell contraction, and adhesion formation and maturation<sup>32</sup>.

The cell cytoskeleton, composed of tubulin microtubules, intermediate filaments and actin microfilaments, serves both a structure and signaling function within a cell. The cell cytoskeleton plays a vital role in mechanochemical transduction by establishing mechanical linkages, adhesions, between the extracellular matrix, cell membrane and nucleus, mediating structural force balance and providing a means for response through actin-myosin complex cell contractility<sup>47,48</sup>. *In vivo*, the mechanical properties of the extracellular environment varies through extracellular matrix protein deposition and degradation, cell migration and blood flow<sup>49</sup>. Substratum physical dimensionality (topography), mechanical properties (elastic moduli) and heterogeneity modulate many biological activities including adhesion formation, gene expression, cell morphology, migration, and proliferation/survival in a cell-type specific manner<sup>25,50,51</sup>. To date, to completely understand the function of the various components involved in mechanotransduction, it has been necessary to isolate each extracellular stimulus, and evaluate the cellular response to them through a reductionist approach. The ultimate goal of this thesis is to develop a novel multi-stimuli cell culture device for the simultaneous analysis of surface topography and substratum modulus.

## 1.5 A mechanism of migration: Contact guidance

Contact guidance is the influence of topographies found in the cellular microenvironment upon cell behavior, including morphology, orientation, and migration (Leland Villard 2020). The topography of the extracellular environment refers to the size, shape and organization of structural elements surrounding cells, including the ECM and neighboring cells. ECM structures can range from randomly organized elements to highly aligned environments composed of organized collagen fibers <sup>52</sup>.

Contact guidance was first reported in 1912 when chicken embryo cells were seen to require a migratory support <sup>53</sup>. When providing a linear arrangement, the chicken embryo cells were aligned and underwent directed migration <sup>53</sup>. In 1934, contact guidance was again described within axons of nerve cells orienting to parallel grooves formed by coagulated blood brushed along a coverslip <sup>54</sup>. Since these initial findings, contact guidance has been observed in various cell types using structured substratum that mimic native tissue topographies or present artificial conditions, revealing the profound effects of topography on cellular behavior <sup>52</sup>. Currently, there are three main working theories surrounding the mechanism of contact guidance <sup>52</sup>.

The first of these theories is known as the focal adhesion restriction theory and was postulated in 1979 by Ohara and Buck following a corresponding earlier hypothesis by Dunn and Health in 1973 <sup>55,56</sup>. The focal adhesion restriction theory states that when cells encounter a continuous unidirectional surface, the topographical cues restrict the formation and distribution of focal adhesions <sup>52,55</sup>. As a result, the adhesions can only elongate and mature in one direction, such as the direction of the continuous topographic ridges, restricted by the width of the ridge and therefore limiting the adhesion site's growth and maturation <sup>52</sup>. This also leads to the reorganization of the cytoskeleton and alignment of the cell along the direction of the lines <sup>55</sup>.

The Curtis and Clark theory from 1990 works on the property of discontinuity within the substratum <sup>52,57</sup>. Through their review of data, they theorized cells respond to discontinuity in topography by actin condensations or nucleation leading to adhesion formation upon



edges of structures<sup>57</sup>. As the magnitude of the discontinuities increase to equal or greater to that of the cell, cells orient with respect to the discontinuities<sup>57</sup>.

Lastly, the curvature hypothesis proposes that nanotopography, specifically the nanoscale structures present on surfaces, can influence cellular processes by inducing local changes in membrane curvature<sup>52,58</sup>. These curvatures can activate intracellular signaling pathways related to processes like endocytosis, filopodia generation, adhesion, differentiation, and rearrangement of the actin cytoskeleton<sup>52,58</sup>. Additionally, nanotopography can also impact the shape of the nuclear envelope, potentially influencing nuclear mechanotransduction and epigenetic control mechanisms associated with chromatin organization<sup>58</sup>.

## 1.6 Controlling environmental parameters to regulate cell behaviour

The physical and mechanical cellular microenvironment including elastic moduli and topography are known to strongly influence cellular behaviour<sup>47,57,59,60</sup>. Ultimately, how the physical and mechanical cellular microenvironment can influence these cellular behaviours, among many others, may provide a means of controlling specific cellular behaviour through material manufacturing.

### 1.6.1 Elastic modulus

The elastic modulus, also known as the Young's modulus, is a characteristic indicative of material stiffness. Stiffness is measured by the tensile stress over the tensile strain, prior to the material yield point. The greater the stiffness – the harder the material is to deform, the higher the elastic modulus. Many aspects of cell behaviour and structure, and human health are affected by the transmission of substratum mechanical load, imposed by the substratum's elastic modulus, through cell adhesion complexes<sup>47</sup>. The tissues of the human body possess a broad variety of elastic moduli with which cells must interact. Healthy skin

lies upon soft tissue of elastic moduli  $\sim 100 - 400$  kPa, while gingiva lies upon alveolar bone of an elastic modulus of  $12.7$  GPa<sup>61-65</sup>. While interacting with other cells, cells contend with elastic moduli between  $10 - 10\,000$  Pa<sup>47,66</sup>. In the process of wound healing, a fibrin clot possesses a Young's modulus of  $10 - 1\,000$  Pa, and within a rat model, cells contend with highly compliant granulation tissue, with an elastic modulus of  $18.5$  kPa, and scar tissue, exhibiting an elastic modulus  $\sim 80$  kPa<sup>14,62,67,68</sup>. In a process known as durotaxis, cells have a propensity to migrate toward stiffer substratum<sup>49</sup>. With increased elastic modulus, cell morphology becomes broader and flatter, and growth is most optimal when the substratum elasticity matched to the cells' intrinsic elasticity<sup>69</sup>. Additionally, through haptotaxis, cells migrate and attach to substrata with optimal adhesive properties which are also influenced by the substratum's surface elastic modulus<sup>60</sup>. The harnessing of the intrinsic cell properties and behaviours upon biomaterials with the corresponding physical and mechanical characteristics poses a unique field of research to optimize biomaterial application.

## 1.6.2 Topography

Through contact guidance, whereby cells mechanosense and utilize substratum topographic cues of orientation and shape, cell behaviour such as migration and adhesion formation are influenced<sup>60</sup>. Contact guidance is essential in development, pathological processes, repair and regenerative processes as observed within tissue healing<sup>57,59,70</sup>. Cells utilize contact guidance along patterns of fibrils or grooves in integrin-dependent migration within the extracellular matrix<sup>71</sup>. Ligand spacing of  $\sim 60 - 140$  nm is required for regular focal adhesion and stress fiber formation, while  $440$  nm of peptide spacing is required for  $\alpha v \beta 3$  mediated cell spreading within human foreskin fibroblasts<sup>40,72,73</sup>. Filopodia extensions and focal adhesions have been implicated in the process of contact guidance on nanometric surfaces<sup>74</sup>. Utilizing unique, well defined topographical substrata, as depicted in Figure 1-2, researchers can investigate the influence of substratum topography upon cell physiology and structure in a controlled environment. However, due to the complex nature

of the chemical and physical extra and intracellular environments, the exact process and mechanism have yet to be explained<sup>60,75</sup>.

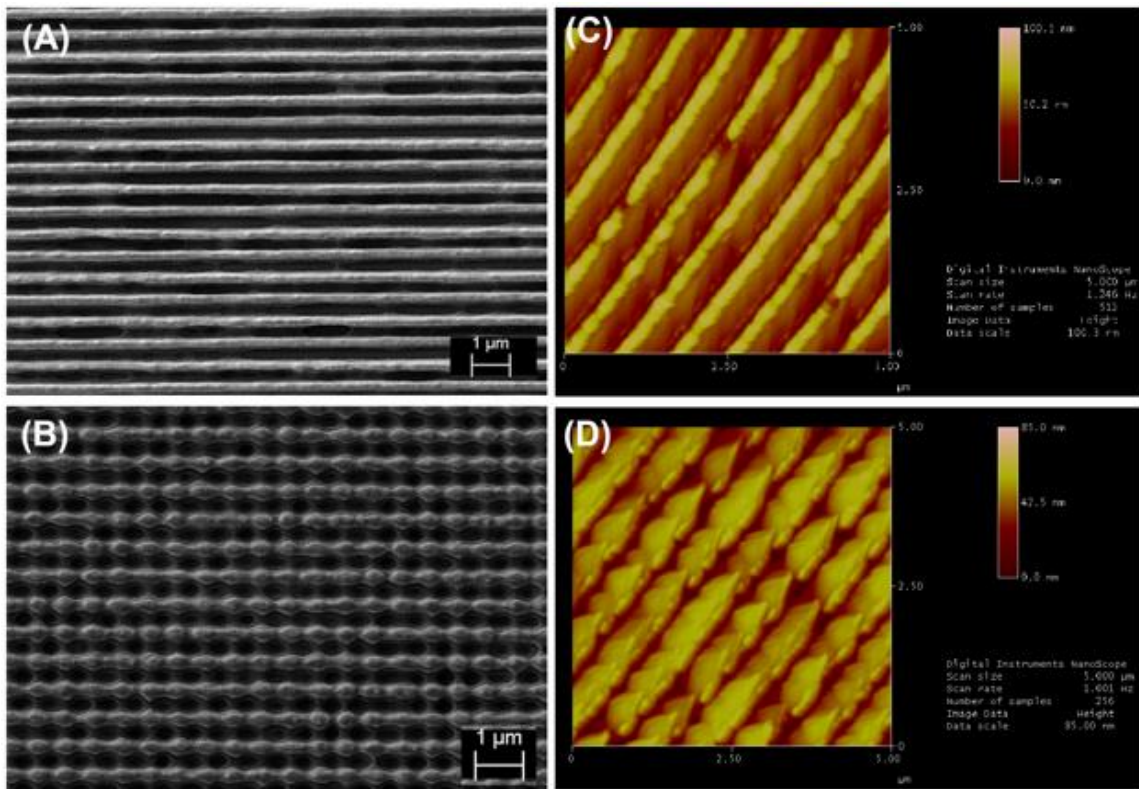


**Figure 1-2: Scanning electron microscopy images of (A) nanogrooves, and (B) discontinuous nanogroove dot topographies employed in topographical studies of cell physiology.**

Atomic force microscopy indicating the pitch, distance from the beginning of one ridge to the next, and height, the depth of the groove, of the nanogroove and discontinuous nanogroove dot topographies <sup>74</sup>.

## 1.7 Thesis Overview

By utilizing a reductionist approach, I have worked to understand the mechanisms underlying human dermal (HDF) and gingival (HGF) fibroblast adhesion patterns on topography and various elastic moduli tissue culture plates and their relation to physiological behaviours associated with fibrosis. The mechanical stimuli of surface topography and elastic modulus were investigated independently and later combined to allude the mechanosensory mechanisms of dermal and gingival fibroblasts of these complex stimuli *in vivo*.

I hypothesized that topographic features, with submicron periodicity, would inhibit increased cell contraction and excessive extracellular matrix deposition by altering adhesion structure on materials with a high elastic modulus.

The effect of topography upon human dermal and gingival fibroblast adhesion composition and behaviour was first investigated upon silica submicron grooved surfaces. Focal and fibrillar adhesion formation were evaluated for directionality, quantity, and area. F-actin cytoskeletal elements were evaluated under the same conditions for directionality. Next, fibronectin deposition and organization were evaluated. Finally, the role of integrin  $\alpha\beta3$  and integrin  $\beta1$  in contact guidance was quantified.

In the second chapter, I quantified the effect of substratum elastic modulus upon human dermal and gingival fibroblast adhesion composition and behaviour. Initially, HDF and HGF proliferation and adhesion was quantified upon the variation of elastic modulus of the cell culture surfaces. The adhesion sites were analyzed for composition, quantity, and stability. The ability for HDF and HGF to differentiate into myofibroblasts and deposit extracellular matrix upon various elastic modulus surfaces was next evaluated. Finally, how the culturing of HDF and HGF upon various elastic modulus surfaces impacts their intracellular signalling pathways was investigated.

In the third chapter, the fabrication of tunable elastic modulus silicone cell substrata containing submicron nanogrooves was outlined. The fabrication process was evaluated for reproducibility, consistency, and accuracy of the topographic details. The elastic

modulus and surface wettability was defined. Finally, cell viability upon the newly fabricated elastic modulus varied topographic surface was quantified.

## 1.8 References

- (1) Ghosh, S.; Abanteriba, S. Status of Surface Modification Techniques for Artificial Hip Implants. *Sci Technol Adv Mater* **2016**, *17* (1), 715–735.  
<https://doi.org/10.1080/14686996.2016.1240575>.
- (2) Gupta, S.; Dahiya, V.; Shukla, P. Surface Topography of Dental Implants: A Review. *Journal of Dental Implants* **2014**, *4* (1), 66. <https://doi.org/10.4103/0974-6781.131009>.
- (3) Kim, S. S.; Wen, W.; Prowse, P.; Hamilton, D. W. Regulation of Matrix Remodelling Phenotype in Gingival Fibroblasts by Substratum Topography. *J Cell Mol Med* **2015**, *19* (6), 1183–1196. <https://doi.org/10.1111/jcmm.12451>.
- (4) Gurtner, G. C.; Werner, S.; Barrando, Y.; Longaker, M. T. Wound Repair and Regeneration. *Nature* **2008**, *453*, 314–321. <https://doi.org/10.1159/000339613>.
- (5) Fan, C.; Dong, Y.; Xie, Y.; Su, Y.; Zhang, X.; Leavesley, D.; Upton, Z. Shikonin Reduces TGF-B1-Induced Collagen Production and Contraction in Hypertrophic Scar-Derived Human Skin Fibroblasts. *Int J Mol Med* **2015**, 985–991.  
<https://doi.org/10.3892/ijmm.2015.2299>.
- (6) Sriram, G.; Bigliardi, P. L.; Bigliardi-Qi, M. Fibroblast Heterogeneity and Its Implications for Engineering Organotypic Skin Models in Vitro. *Eur J Cell Biol* **2015**, *94* (11), 483–512. <https://doi.org/10.1016/j.ejcb.2015.08.001>.
- (7) Yang, S.; Plotnikov, S. V. Mechanosensitive Regulation of Fibrosis. *Cells*. MDPI May 1, 2021. <https://doi.org/10.3390/cells10050994>.
- (8) Leask, A. The Hard Problem: Mechanotransduction Perpetuates the Myofibroblast Phenotype in Scleroderma Fibrosis. *Wound Repair Regen* **2021**, *29* (4), 582–587.  
<https://doi.org/10.1111/wrr.12889>.
- (9) Rodrigues, M.; Kosaric, N.; Bonham, C. A.; Gurtner, G. C. Wound Healing: A Cellular Perspective. *Physiol Rev* **2019**, *99* (1), 665–706.  
<https://doi.org/10.1152/physrev.00067.2017>.



- (10) Zhao, T.; Zhao, W.; Chen, Y.; Li, V. S.; Meng, W.; Sun, Y. Platelet-Derived Growth Factor-D Promotes Fibrogenesis of Cardiac Fibroblasts. *Am J Physiol Heart Circ Physiol* **2013**, *304* (12), H1719-26. <https://doi.org/10.1152/ajpheart.00130.2013>.
- (11) Arno, A. I.; Gauglitz, G. G.; Barret, J. P.; Jeschke, M. G. Up-to-Date Approach to Manage Keloids and Hypertrophic Scars: A Useful Guide. *Burns* **2014**, *40* (7), 1255–1266. <https://doi.org/10.1038/jid.2014.371>.
- (12) Cialdai, F.; Risaliti, C.; Monici, M. Role of Fibroblasts in Wound Healing and Tissue Remodeling on Earth and in Space. *Front Bioeng Biotechnol* **2022**, *10*, 958381. <https://doi.org/10.3389/fbioe.2022.958381>.
- (13) Correa-Gallegos, D.; Jiang, D.; Rinkevich, Y. Fibroblasts as Confederates of the Immune System. *Immunol Rev* **2021**, *302* (1), 147–162. <https://doi.org/10.1111/imr.12972>.
- (14) Van De Water, L.; Varney, S.; Tomasek, J. J. Mechanoregulation of the Myofibroblast in Wound Contraction, Scarring, and Fibrosis: Opportunities for New Therapeutic Intervention. *Adv Wound Care (New Rochelle)* **2013**, *2* (4), 122–141. <https://doi.org/10.1089/wound.2012.0393>.
- (15) Darby, I. A.; Hewitson, T. D. Fibroblast Differentiation in Wound Healing and Fibrosis. *Int Rev Cytol* **2007**, *257*, 143–179.
- (16) Bainbridge, P. Wound Healing and the Role of Fibroblasts. *J Wound Care* **2013**, *22* (8), 407–408, 410–412. <https://doi.org/10.12968/jowc.2013.22.8.407>.
- (17) Liu, B. H.; Chen, L.; Li, S. R.; Wang, Z. X.; Cheng, W. G. Smac/DIABLO Regulates the Apoptosis of Hypertrophic Scar Fibroblasts. *Int J Mol Med* **2013**, *32* (3), 615–622. <https://doi.org/10.3892/ijmm.2013.1442>.
- (18) Sawant, M.; Hinz, B.; Schönborn, K.; Zeinert, I.; Eckes, B.; Krieg, T.; Schuster, R. A Story of Fibers and Stress: Matrix-Embedded Signals for Fibroblast Activation in the Skin. *Wound Repair Regen* **2021**, *29* (4), 515–530. <https://doi.org/10.1111/wrr.12950>.

- (19) Arif, S.; Attiogbe, E.; Moulin, V. J. Granulation Tissue Myofibroblasts during Normal and Pathological Skin Healing: The Interaction between Their Secretome and the Microenvironment. *Wound Repair Regen* **2021**, *29* (4), 563–572.  
<https://doi.org/10.1111/wrr.12919>.
- (20) Hinz, B.; Lagares, D. Evasion of Apoptosis by Myofibroblasts: A Hallmark of Fibrotic Diseases. *Nat Rev Rheumatol* **2020**, *16* (1), 11–31. <https://doi.org/10.1038/s41584-019-0324-5>.
- (21) Thulabandu, V.; Chen, D.; Atit, R. P. Dermal Fibroblast in Cutaneous Development and Healing. *Wiley Interdisciplinary Reviews: Developmental Biology*. John Wiley and Sons Inc. March 1, 2018. <https://doi.org/10.1002/wdev.307>.
- (22) Fournier, B. P. J.; Larjava, H.; Häkkinen, L. Gingiva as a Source of Stem Cells with Therapeutic Potential. *Stem Cells Dev* **2013**, *22* (24), 3157–3177.  
<https://doi.org/10.1089/scd.2013.0015>.
- (23) Guo, F.; Carter, D. E.; Mukhopadhyay, A.; Leask, A. Gingival Fibroblasts Display Reduced Adhesion and Spreading on Extracellular Matrix: A Possible Basis for Scarless Tissue Repair? *PLoS One* **2011**, *6* (11), 1–9.  
<https://doi.org/10.1371/journal.pone.0027097>.
- (24) Warrick, J. W.; Murphy, W. L.; Beebe, D. J. Screening the Cellular Microenvironment: A Role for Microfluidics. *IEEE Rev Biomed Eng* **2008**, *1* (1), 75–93.  
<https://doi.org/10.2217/FON.09.6.Dendritic>.
- (25) Geiger, B.; Yamada, K. M. Molecular Architecture and Function of Matrix Adhesions. *Cold Spring Harb Perspect Biol* **2011**, 1–22.  
<https://doi.org/10.1101/cshperspect.a005033>.
- (26) Turley, E. A.; Noble, P. W.; Bourguignon, L. Y. W. Signaling Properties of Hyaluronan Receptors. *Journal of Biological Chemistry* **2002**, *277* (7), 4589–4592.  
<https://doi.org/10.1074/jbc.R100038200>.

- (27) Puré, E.; Assoian, R. K. NIH Public Access. **2010**, *21* (5), 651–655.  
<https://doi.org/10.1016/j.cellsig.2009.01.024>.Rheostatic.
- (28) Heino, J.; Huhtala, M.; Käpylä, J.; Johnson, M. S. Evolution of Collagen-Based Adhesion Systems. *International Journal of Biochemistry and Cell Biology* **2009**, *41* (2), 341–348.  
<https://doi.org/10.1016/j.biocel.2008.08.021>.
- (29) Khalili, A. A.; Ahmad, M. R. A Review of Cell Adhesion Studies for Biomedical and Biological Applications. *International Journal of Molecular Sciences*. 2015.  
<https://doi.org/10.3390/ijms160818149>.
- (30) Bose, S.; Robertson, S. F.; Bandyopadhyay, A. Surface Modification of Biomaterials and Biomedical Devices Using Additive Manufacturing. *Acta Biomater* **2018**, *66*, 6–22.  
<https://doi.org/10.1016/j.actbio.2017.11.003>.
- (31) Pacelli, S.; Manoharan, V.; Desalvo, A.; Lomis, N.; Johda, K. S.; Prakash, S.; Paul, A. Tailoring Biomaterial Surface Properties to Modulate Host- Implant Interactions: Implication in Cardiovascular and Bone Therapy. *J Mater Chem B* **2016**, *4* (9), 1586–1599. <https://doi.org/10.4172/2157-7633.1000305>.Improved.
- (32) Vinarský, V.; Pagliari, S.; Forte, G.; Martino, F.; Perestrelo, A. R. Cellular Mechanotransduction: From Tension to Function. *Front Physiol* **2018**, *9* (July), 1–21.  
<https://doi.org/10.3389/fphys.2018.00824>.
- (33) Herzog, W. Molecular and Cellular Biomechanics. In *Encyclopedia of Neuroscience*; Binder, M. D., Hirokawa, N., Windhorst, U., Eds.; Springer: Berlin, Heidelberg, 2009; pp 2389–2393. [https://doi.org/10.1007/978-3-540-29678-2\\_3262](https://doi.org/10.1007/978-3-540-29678-2_3262).
- (34) Muhamed, I.; Chowdhury, F.; Maruthamuthu, V. Biophysical Tools to Study Cellular Mechanotransduction. *Bioengineering* **2017**, *4* (4), 12.  
<https://doi.org/10.3390/bioengineering4010012>.
- (35) Hynes, R. O.; Naba, A. Overview of the Matrisome-An Inventory of Extracellular Matrix Constituents and Functions. *Cold Spring Harb Perspect Biol* **2012**, *4* (1), 1–16.  
<https://doi.org/10.1101/cshperspect.a004903>.

- (36) Nobes, C. D.; Hall, A. Rho, Rac, and Cdc42 GTPases Regulate the Assembly of Multimolecular Focal Complexes Associated with Actin Stress Fibers, Lamellipodia, and Filopodia. *Cell* **1995**, *81* (1), 53–62. [https://doi.org/10.1016/0092-8674\(95\)90370-4](https://doi.org/10.1016/0092-8674(95)90370-4).
- (37) Rottner, K.; Hall, A.; Small, J. V. Interplay between Rac and Rho in the Control of Substrate Contact Dynamics. *Current Biology* **1999**, *9* (12), 640–648. [https://doi.org/10.1016/S0960-9822\(99\)80286-3](https://doi.org/10.1016/S0960-9822(99)80286-3).
- (38) Zaidel-Bar, R.; Ballestrem, C.; Kam, Z.; Geiger, B. Early Molecular Events in the Assembly of Matrix Adhesions at the Leading Edge of Migrating Cells. *J Cell Sci* **2003**, *116*, 4605–4613. <https://doi.org/10.1242/jcs.00792>.
- (39) Marquis, M.-E.; Lord, E.; Bergeron, E.; Drevelle, O.; Park, H.; Cabana, F.; Senta, H.; Faucheux, N. Bone Cells-Biomaterials Interactions. *Frontiers in Bioscience* **2009**, *14*, 1023–1067. <https://doi.org/10.2741/3293>.
- (40) Geiger, B.; Spatz, J. P.; Bershadsky, A. D. Environmental Sensing through Focal Adhesions. *Nat Rev Mol Cell Biol* **2009**, *10* (1), 21–33. <https://doi.org/10.1038/nrm2593>.
- (41) Balaban, N. Q.; Schwarz, U. S.; Rivelino, D.; Goichberg, P.; Tzur, G.; Sabanay, I.; Mahalu, D.; Safran, S.; Bershadsky, A.; Addadi, L.; Geiger, B. Force and Focal Adhesion Assembly: A Close Relationship Studied Using Elastic Micropatterned Substrates. *Nat Cell Biol* **2001**, *3* (5), 466–472. <https://doi.org/10.1038/35074532> [pii].
- (42) Prager-Khoutorsky, M.; Lichtenstein, A.; Krishnan, R.; Rajendran, K.; Mayo, A.; Kam, Z.; Geiger, B.; Bershadsky, A. D. Fibroblast Polarization Is a Matrix-Rigidity-Dependent Process Controlled by Focal Adhesion Mechanosensing. *Nat Cell Biol* **2011**, *13* (12), 1457–1465. <https://doi.org/10.1038/ncb2370>.
- (43) Chen, W. T.; Hasegawa, T.; Hasegawa, C.; Weinstock, C.; Yamada, K. M. Development of Cell Surface Linkage Complexes in Cultivated Fibroblasts. *Journal of Cell Biology* **1985**, *100*, 1103–1114.
- (44) Zamir, E.; Katz, M.; Posen, Y.; Erez, N.; Yamada, K. M.; Katz, B.-Z.; Lin, S.; Lin, D. C.; Bershadsky, A.; Kam, Z.; Geiger, B. Dynamics and Segregation of Cell–Matrix

Adhesions in Cultured Fibroblasts. *Nat Cell Biol* **2000**, 2 (4), 191–196.  
<https://doi.org/10.1038/35008607>.

- (45) Zhong, C.; Chrzanowska-Wodnicka, M.; Brown, J.; Shaub, A.; Belkin, A. M.; Burridge, K. Rho-Mediated Contractility Exposes a Cryptic Site in Fibronectin and Induces Fibronectin Matrix Assembly. *Journal of Cell Biology* **1998**, 141 (2), 539–551.  
<https://doi.org/10.1083/jcb.141.2.539>.
- (46) Couchman, J. R.; Rees, D. a. The Behaviour of Fibroblasts Migrating from Chick Heart Explants: Changes in Adhesion, Locomotion and Growth, and in the Distribution of Actomyosin and Fibronectin. *J Cell Sci* **1979**, 39, 149–165.
- (47) Bao, G.; Suresh, S. Cell and Molecular Mechanics of Biological Materials. *Nat Mater* **2003**, 2 (11), 715–725.
- (48) Chicurel, M. E.; Chen, C. S.; Ingber, D. E. Cellular Control Lies in the Balance of Forces. *Curr Opin Cell Biol* **1998**, 10, 232–239.
- (49) Pelham, R. J.; Yu-Li, W. Cell Locomotion and Focal Adhesions Are Regulated by Substrate Flexibility. *Proc Natl Acad Sci U S A* **1997**, 94, 13661–13665.  
<https://doi.org/10.1073/pnas.94.25.13661>.
- (50) Schwartz, M. A. Integrins and Extracellular Matrix in Mechanotransduction. *Cold Spring Harb Perspect Biol* **2010**, 2 (12), 1–13.  
<https://doi.org/http://dx.doi.org/10.2147/CHC.S21829>.
- (51) Yeung, T.; Georges, P. C.; Flanagan, L. A.; Marg, B.; Ortiz, M.; Funaki, M.; Zahir, N.; Ming, W.; Weaver, V.; Janmey, P. A. Effects of Substrate Stiffness on Cell Morphology, Cytoskeletal Structure, and Adhesion. *Cell Motil Cytoskeleton* **2005**, 60 (1), 24–34.  
<https://doi.org/10.1002/cm.20041>.
- (52) Leclech, C.; Villard, C. Cellular and Subcellular Contact Guidance on Microfabricated Substrates. *Frontiers in Bioengineering and Biotechnology*. Frontiers Media S.A. October 22, 2020. <https://doi.org/10.3389/fbioe.2020.551505>.

- (53) Harrison, R. G. The Cultivation of Tissues in Extraneous Media as a Method of Morpho-Genetic Study. *Anat Rec* **1912**, *6* (4), 181–193.
- (54) Weiss, P. In Vitro Experiments on the Factors Determining the Course of the Outgrowing Nerve Fiber. *Experimental Zoology* **1934**, *68* (3), 393–448.
- (55) Ohara, P. T.; Buck, R. C. *CONTACT GUIDANCE IN VITRO A Light, Transmission, and Scanning Electron Microscopic Study*; 1979; Vol. 121.
- (56) Dunn, G. A.; Heath, J. P. *A NEW HYPOTHESIS OF CONTACT GUIDANCE IN TISSUE CELLS*; 1976; Vol. 101.
- (57) Curtis, A. S. G.; Clark, P. The Effects of Topographic and Mechanical Properties of Materials on Cell Behaviour. *Critical Reviews in Biocompatibility* **1990**, *5*, 343–362.
- (58) Lou, H. Y.; Zhao, W.; Zeng, Y.; Cui, B. The Role of Membrane Curvature in Nanoscale Topography-Induced Intracellular Signaling. *Acc Chem Res* **2018**, *51* (5), 1046–1053. <https://doi.org/10.1021/acs.accounts.7b00594>.
- (59) Britland, S.; Morgan, H.; Wojniak-Stodart, B.; Riehle, M.; Curtis, a; Wilkinson, C. Synergistic and Hierarchical Adhesive and Topographic Guidance of BHK Cells. *Exp Cell Res* **1996**, *228* (228), 313–325. <https://doi.org/10.1006/excr.1996.0331>.
- (60) Brunette, D. M.; Chehroudi, B. The Effects of the Surface Topography of Micromachined Titanium Substrata on Cell Behavior in Vitro and in Vivo. *J Biomech Eng* **1999**, *121*, 49–57.
- (61) Schwartz-Dabney, C. L.; Dechow, P. C. Variations in Cortical Material Properties throughout the Human Dentate Mandible. *Am J Phys Anthropol* **2003**, *120* (3), 252–277. <https://doi.org/10.1002/ajpa.10121>.
- (62) Clark, J. a.; Cheng, J. C. Y.; Leung, K. S. Mechanical Properties of Normal Skin and Hypertrophic Scars. *Burns* **1996**, *22* (6), 443–446. [https://doi.org/10.1016/0305-4179\(96\)00038-1](https://doi.org/10.1016/0305-4179(96)00038-1).

- (63) Solon, J.; Levental, I.; Sengupta, K.; Georges, P. C.; Janmey, P. A. Fibroblast Adaptation and Stiffness Matching to Soft Elastic Substrates. *Biophys J* **2007**, *93* (12), 4453–4461. <https://doi.org/10.1529/biophysj.106.101386>.
- (64) Levental, I.; Georges, P. C.; Janmey, P. A. Soft Biological Materials and Their Impact on Cell Function. *Soft Matter* **2007**, *3* (July 2006), 299–306. <https://doi.org/10.1039/b610522j>.
- (65) Garland, S. P.; McKee, C. T.; Chang, Y. R.; Raghunathan, V. K.; Russell, P.; Murphy, C. J. A Cell Culture Substrate with Biologically Relevant Size-Scale Topography and Compliance of the Basement Membrane. *Langmuir* **2014**, *30* (8), 2101–2108. <https://doi.org/10.1021/la403590v>.
- (66) Wakatsuki, T.; Kolodney, M. S.; Zahalak, G. I.; Elson, E. L. Cell Mechanics Studied by a Reconstituted Model Tissue. *Biophys J* **2000**, *79* (5), 2353–2368. [https://doi.org/10.1016/S0006-3495\(00\)76481-2](https://doi.org/10.1016/S0006-3495(00)76481-2).
- (67) Corr, D. T.; Hart, D. A. Biomechanics of Scar Tissue and Uninjured Skin. *Adv Wound Care (New Rochelle)* **2013**, *2* (2), 37–43. <https://doi.org/10.1089/wound.2011.0321>.
- (68) Elliott, C. G.; Wang, J.; Guo, X.; Xu, S.; Eastwood, M.; Guan, J.; Leask, A.; Conway, S. J.; Hamilton, D. W. Periostin Modulates Myofibroblast Differentiation during Full-Thickness Cutaneous Wound Repair. *J Cell Sci* **2011**, *125* (Pt 1), 121–132. <https://doi.org/10.1242/jcs.087841>.
- (69) Discher, D. E.; Janmey, P.; Wang, Y.-L. Tissue Cells Feel and Respond to the Stiffness of Their Substrate. *Science* **2005**, *310* (5751), 1139–1143. <https://doi.org/10.1126/science.1116995>.
- (70) Brunette, D. M. The Effects of Surface Topography on the Behaviour of Cells on Implants. *International Journal of Oral and Maxillofacial Implantology* **1988**, *3*, 231–246.
- (71) Doyle, A. D.; Carvajal, N.; Jin, A.; Matsumoto, K.; Yamada, K. M. Local 3D Matrix Microenvironment Regulates Cell Migration through Spatiotemporal Dynamics of

Contractility-Dependent Adhesions. *Nat Commun* **2015**, *6*, 8720.  
<https://doi.org/10.1038/ncomms9720>.

- (72) Cavalcanti-adam, E. A.; Volberg, T.; Micoulet, A.; Kessler, H.; Geiger, B.; Spatz, J. P. Cell Spreading and Focal Adhesion Dynamics Are Regulated by Spacing of Integrin Ligands. **2007**, *92* (April), 2964–2974. <https://doi.org/10.1529/biophysj.106.089730>.
- (73) Massia, S. P.; Hubbell, J. A. An RGD Spacing of 440 Nm Is Sufficient for Integrin  $\text{Av}\beta 3$ -Mediated Fibroblast Spreading and 140 Nm for Focal Contact and Stress Fiber Formation. *Journal of Cell Biology* **1991**, *114* (5), 1089–1100.
- (74) Hamilton, D. W.; Oates, C. J.; Hasanzadeh, A.; Mittler, S. Migration of Periodontal Ligament Fibroblasts on Nanometric Topographical Patterns: Influence of Filopodia and Focal Adhesions on Contact Guidance. *PLoS One* **2010**, *5* (12).  
<https://doi.org/10.1371/journal.pone.0015129>.
- (75) Hamilton, D. W.; Brunette, D. M. “Gap Guidance” of Fibroblasts and Epithelial Cells by Discontinuous Edged Surfaces. *Exp Cell Res* **2005**, *309* (2), 429–437.  
<https://doi.org/10.1016/j.yexcr.2005.06.015>.



## 2 Quantification and comparison of human dermal and gingival fibroblast behaviours, associated with fibrosis, upon materials of various topographies.<sup>1</sup>

### 2.1 Introduction

Topographic surfaces have been demonstrated to affect human fibroblast physiology through contact guidance. Adhesion formation, migration, morphology and matrix remodeling all are influenced by topographic cues from their substratum<sup>1,2</sup>. Human dermal fibroblasts demonstrate significant increase in fibronectin secretion, guided migration, decreased planar cell surface area, and decreased MMP protein expression upon topographic substrates compared to surfaces lacking a distinct topography<sup>3,4</sup>. However, little research currently presents the effects of topographic substrates upon human gingival fibroblast physiology<sup>1</sup>.

The dynamic nature of the extracellular matrix, specifically within the wound healing environment, presents cells with various topographic cues with which they must contend. The addition of a substratum topography is hypothesized to decrease fibrosis associated behaviours; a decrease in cellular adhesion, proliferation, extracellular matrix production and cell contractility will be observed. Human dermal and gingival fibroblasts are hypothesized to exhibit differential responses to substratum topography; human gingival fibroblasts will exhibit less sensitivity, through a minimal effect of substratum topography upon the investigated behaviours, as compared to human dermal fibroblast populations. In this aim, I will study adhesion assembly, cytoskeleton structure, extracellular matrix excretion, proliferation and cytokine production of human dermal and gingival fibroblasts on nanoscopic topographies. Comparative studies between human dermal and gingival

---

<sup>1</sup> This chapter is published in ACS Applied Materials & Interfaces: Brooks S, Mittler S, Hamilton DW.

Contact Guidance of Connective Tissue Fibroblasts on Submicrometer Anisotropic Topographical Cues Is Dependent on Tissue of Origin,  $\beta$ 1 Integrins, and Tensin-1 Recruitment, 2023; 15 (16), 19817-19832, DOI: 10.1021/acsami.2c22381.

fibroblasts may shed light upon mechanistic differences between scar formation of dermal fibroblasts and the unique regenerative wound healing ability of human gingival fibroblasts, not previously established.

## 2.2 Materials and Methods

### 2.2.1 Dermal and gingival fibroblast isolation and culture

In accordance with the guidelines of the University's Research Ethics Board for Health Sciences Research (Appendix B), *in vitro* studies were performed utilizing human dermal fibroblasts (HDF) populations isolated from skin tissue under informed consent from patients undergoing elective limb amputation. Human gingival fibroblasts (HGF) were isolated from tissue retrieved under informed patient consent during elective periodontal procedures in the Oral Surgery Clinic at the Schulich School of Medicine and Dentistry, University of Western Ontario. Human dermal and gingival fibroblasts populations, each from 3 different patients, were maintained under passage 6 in high glucose (4.5 g/L) Dulbecco's Modified Eagle Medium (DMEM; Thermo Fisher Scientific, Burlington, ON, Canada) supplemented with 10% fetal bovine serum (FBS) (Gibco Life Technologies, Burlington, ON, Canada) and 1% antibiotics and antimycotic (AA) solution (Gibco Life Technologies, Burlington, ON, Canada) at 37 °C, 5% CO<sub>2</sub>. Media is changed every 2-3 days.

### 2.2.2 Fabrication of topographical cues

The dynamic nature of the extracellular matrix, specifically within the wound healing environment, presents cells with various topographic cues with which they must interact<sup>5</sup>. Many of the features cells encounter in the ECM are in the range of nanometers to micrometers in size<sup>5</sup>. In this study, I utilized 2 separate glass topographical surfaces: continuous nanogrooves, and symmetrical nanodots, imparting line, and dot topographical details, fabricated using HeCd laser nanolithography by the Mittler Lab (Figure 2a) (Ertorer et al. 2013). Each topographic pattern had a periodicity of 600 nm, 900 nm, and 1200 nm,

with a depth of ~ 100 nm (Figure 2b). Replicates were fabricated in polystyrene according to a previously established protocol containing 100 g polystyrene and 50 mL chloroform.

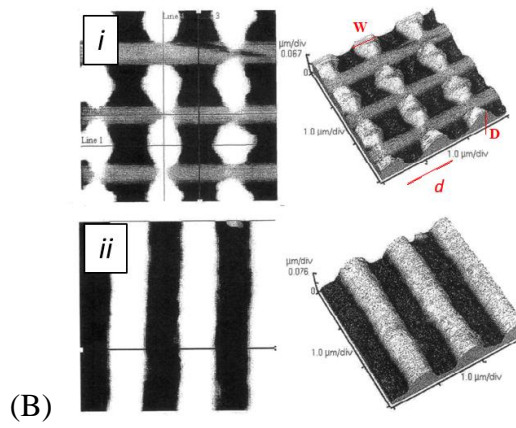
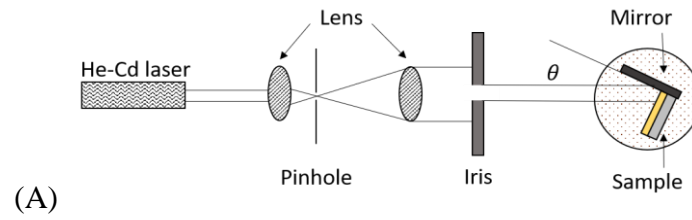


**Figure 2-1: Schematic of submicron topographical silicon surface fabrication**

(A) Experimental set up of the Lloyd's mirror interferometer<sup>6</sup>, to fabricate grating patterns in photoresist upon fused silica samples. The periodicity ( $d$ ) of the grating is calculated by the wavelength of the incident beam ( $\lambda_{\text{HeCd}}$ ) and the angle of the sample to the optical axis ( $\theta$ ):

$$d = \frac{\lambda_{\text{HeCd}}}{2 \sin \theta}$$

The nanodots are made by a second exposure after rotating the sample by 90° on the sample mount. Further photoresist developing and backing steps as well as ion-milling will lead to the pattern physically imprinted into the fused silica substrate surface.

(B) Scanning electron microscopy and atomic force microscopy images depicting the topographic surface characteristics of *i.* nanodots, and *ii.* nanogrooves. Whereby the width of the structures ( $W$ ) is constant, the depth ( $D$ ) is ~100 nm, and the periodicity ( $d$ ) is 600 nm, 900 nm or 1200 nm.

### 2.2.3 Atomic force microscopy

Atomic force microscopy was performed by Dr. Heng-Yong Nie at Surface Science Western using a Park Systems XE-100. The surface morphology was imaged with the dynamic force mode using a silicon cantilever having a nominal spring constant of 40 N/m and resonant frequency of 325 kHz. The radius of the apex of the AFM tip at the free end of the cantilever was nominally 8 nm. The AFM images were obtained in air at 256 x 256 pixels.

### 2.2.4 Sessile Drop Goniometry

Sessile drop goniometry was performed by Dr. Heng-Yong Nie at Surface Science Western using a DSA30E Drop Shape Analyzer (KRÜSS). 2  $\mu$ L ultra pure water was used to measure the contact angle upon all surfaces.

### 2.2.5 Submicron topographic substrate cell culture

All topographies were sterilized with argon plasma prior to cell seeding. HGFs and HDFs were removed from their growth surfaces using trypsin (0.5%) (Gibco). Cells were seeded on each of the surfaces at a density of 5000 cells/cm<sup>2</sup>, allowed to adhere for 30 min, and flooded with DMEM containing 10% FBS and 1% AA. The cells were maintained in a humidified environment at 37 °C, 5% CO<sub>2</sub>. To examine the effect of integrin  $\alpha$ v $\beta$ 3 and integrin  $\beta$ 1 upon HGF and HDF adhesion and alignment, inhibitory antibodies against anti-integrin  $\alpha$ v $\beta$ 3 (MAB1976Z; Millipore Sigma, Oakville, ON, Canada), anti-integrin  $\beta$ 1 (MAB2253; Millipore Sigma) and control IgG were added to independent cell suspensions at 25  $\mu$ g/mL. The suspensions were incubated at 37 °C, with gentle agitation, for 30 min prior to seeding as described above.

## 2.2.6 Immunocytochemistry of adhesion formation and extracellular matrix deposition analysis

Cells were fixed with 4% paraformaldehyde for 5 min, rinsed in 1X phosphate buffered saline, incubated within 0.1% Triton X-100 (0694; VWR, Mississauga, ON) solution for 5 min, rinsed, and blocked by a 1% bovine serum albumin solution (Millipore Sigma) for 30 min. Focal adhesions were visualized using antibodies specific for vinculin (MAB3574; Millipore Sigma) and integrin  $\alpha$ v $\beta$ 3 (MAB1976Z; Millipore Sigma). Fibrillar adhesions were identified using specific antibodies to tensin-1 (NBP1-84129; Novus biologicals, Toronto, ON), integrin  $\beta$ 1 (MAB17781; R&D Systems, Minneapolis, MN) and integrin  $\alpha$ 5 (ab150361; Abcam, Waltham, MA). Extracellular matrix deposition was identified using antibodies to fibronectin (ab1954; Abcam, Waltham, MA). F-actin was labelled with rhodamine conjugated phalloidin (R415; Life Technologies, Grand Island, New York), and nuclei counterstained with Hoechst (H3560; Invitrogen, Burlington, ON). Images were taken on a Carl Zeiss Axio Imager M2m microscope (Zeiss Microscopes, North York, ON) under reverse osmosis water immersion and processed using Zen Pro software.

## 2.2.7 Focal and fibrillar adhesion quantification

Immunofluorescent images of HDF and HGF cell populations on each experimental surface were imported into ImageJ. For each stain, a threshold (maximum pixel intensity for each individual dye) was applied to segment regions of interest and the area calculated with data points imported into Graphpad Software v.5 (Graphpad Software, La Jolla, CA, USA) for analysis. Overall planar cell area was measured from tracing the borders of F-actin labeling. Cell circularity was also determined with F-actin labelling and applying the circularity formula  $[4\pi(\text{area}/\text{perimeter}^2)]$ , whereby a value of 1.0 indicates a perfect circle and approaches 0.0 with increasingly elongated structures. Focal adhesion site area was determined using vinculin labeling, and fibrillar adhesion site area by tensin-1 labeling. These focal and fibrillar adhesion sites were identified within the cell boundary and total number and area were normalized to the planar cell area. Directionality of focal and fibrillar adhesion protein complexes, as well as F-actin cytoskeletal organization was determined

through Fourier transform analysis of pixelated segments within each cell, or the image frame in the case of fibronectin (Directionality plug in; Fiji; Ashburn, VA, USA). These segments are mapped on a coordinate system and directionality determined based upon similar frequency in a direction indicated upon the coordinate system from  $-90^{\circ}$  to  $90^{\circ}$  in  $2^{\circ}$  bins. These bins were joined to  $10^{\circ}$  separation for statistical analysis. The same procedure was repeated for experiments where cells were treated with blocking antibodies for integrin  $\alpha v\beta 3$ , integrin  $\beta 1$  and control IgG.

### 2.2.8 Statistical Analysis

In all experiments, 3 separate lines of HDFs and HGFs isolated from different individuals were used. The quantification of adhesion sites for quantity and size was made from a minimum of 10 cells per experiment from 3 different lines. Results were entered into Graphpad for one-way ANOVA, followed by a Bonferroni correction. Directionality quantification of adhesion sites, and the F-actin cytoskeletal element was performed upon 10 cells from 3 independent cell lines of both HDF and HGF cell populations. Fibronectin deposition directionality was quantified upon 3 surface images obtained from 3 independent cell lines of both HDF and HGF cell populations. The Komolgorov-Smirnov test was used to identify statistical significance of directionality between control conditions and experimental conditions. The quantification of cell area and circularity was made from 10 cells, repeated for 3 independent cell lines of both HDF and HGF cell populations for each time point and condition. Results were entered into Graphpad Software v.5 for Two-way ANOVA, followed by a Bonferroni correction. For all statistical analyses,  $P \leq 0.05$  was considered significant.



## 2.3 Results

### 2.3.1 Submicron repeating grooves induce alignment of vinculin, tensin-1 and F-actin in HDFs and HGFs without altering adhesion site quantity or area

To investigate the influence of submicron repeating grooved topographies upon focal adhesion, fibrillar adhesion and cytoskeletal formation and organization, HDF and HGF were labeled for vinculin, tensin-1, and F-actin with orientation calculated relative to the long axis of the groove. All grooved surfaces imparted linear directionality to HDF and HGF morphology as assessed through alignment of vinculin and F-actin relative to cells cultured on smooth control surfaces (Figure 2-2). 900 nm periodicity grooves were observed to exert the strongest directional cue with respect to orientation of vinculin, tensin-1 and F-actin in both HDF and HGF (Figure 2-3). Quantification of alignment using Fourier transform analysis demonstrated that all of the tested groove dimensions influenced alignment of vinculin, tensin-1 (Figure 2-4) and F-actin dependent on the groove periodicity and cell type (Figure 2-5). In HGFs, vinculin was significantly aligned on all tested periodicities compared to smooth controls ( $p < 0.05$ , Kolmogorov-Smirnov test), tensin-1 adhesion sites only significantly aligned on 600 and 900 nm ( $p < 0.05$ , Kolmogorov-Smirnov test), and F-actin aligned on 600 and 1200 nm ( $p < 0.05$ , Kolmogorov-Smirnov test). In HDFs, vinculin was only significantly aligned on 900 nm periodicity ( $p < 0.05$ , Kolmogorov-Smirnov test), tensin-1 sites and F-actin significantly oriented on 600 and 900 nm periodicities ( $p < 0.05$ , Kolmogorov-Smirnov test). Quantification of vinculin containing focal adhesions and tensin-1 containing fibrillar adhesion site quantity and area normalized to individual HGF and HDF area (Table 2-1 and Table 2-2) indicated minimal change in size across the investigated topographies when compared to the smooth control ( $p < 0.05$ , ANOVA, Bonferroni correction).

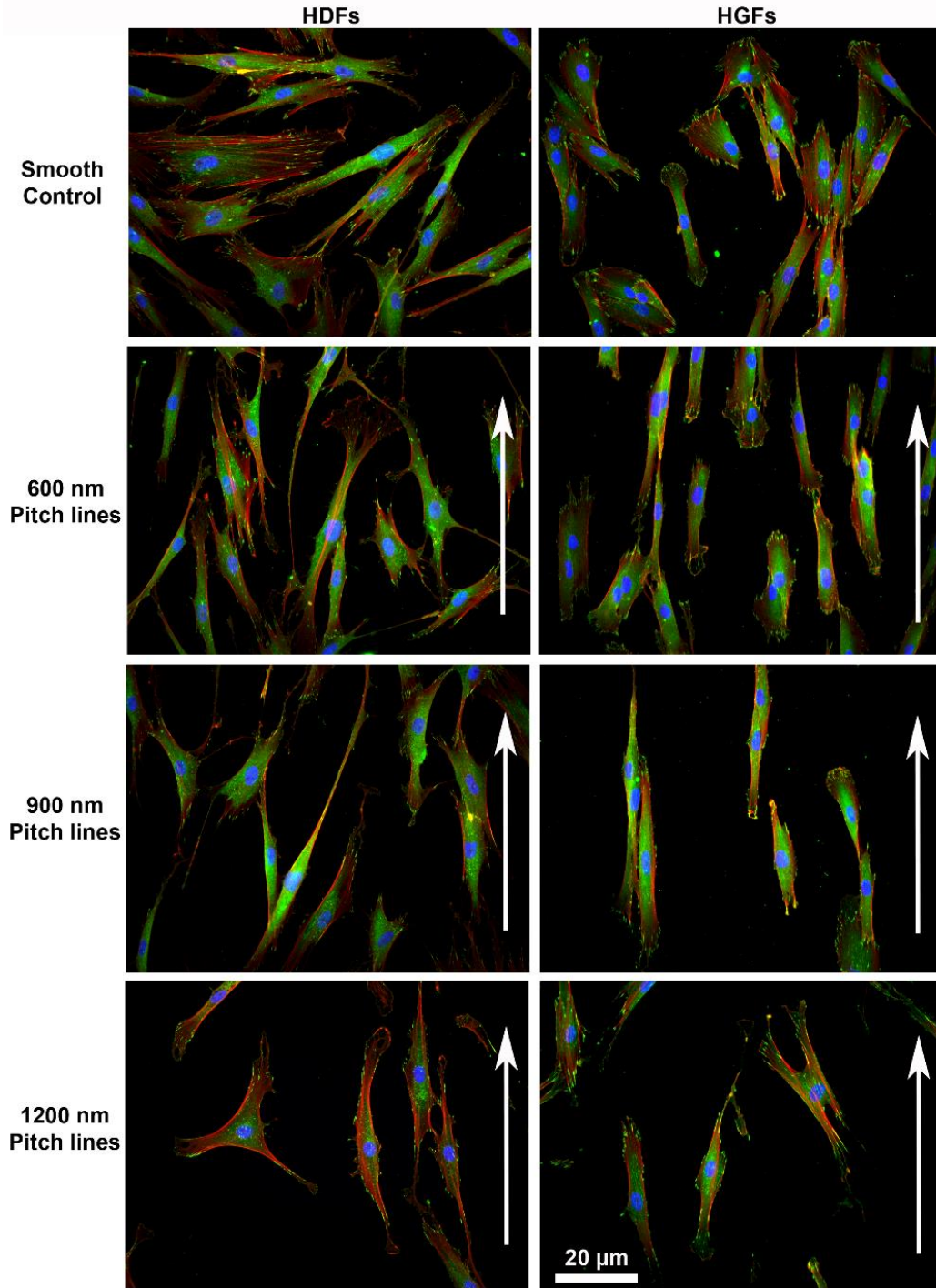


**Figure 2-2: HDFs and HGFs orient with respect to the long axis of the groove topographies.**

HDF and HGF cell populations were cultured for 24 h upon smooth and groove surfaces with periodicities of 600 nm, 900 nm, and 1200 nm. Vinculin (green), F-Actin (red) and nuclei (blue) are identified through immunofluorescent staining. The direction of the underlying nanogroove long axis is indicated with white arrows.

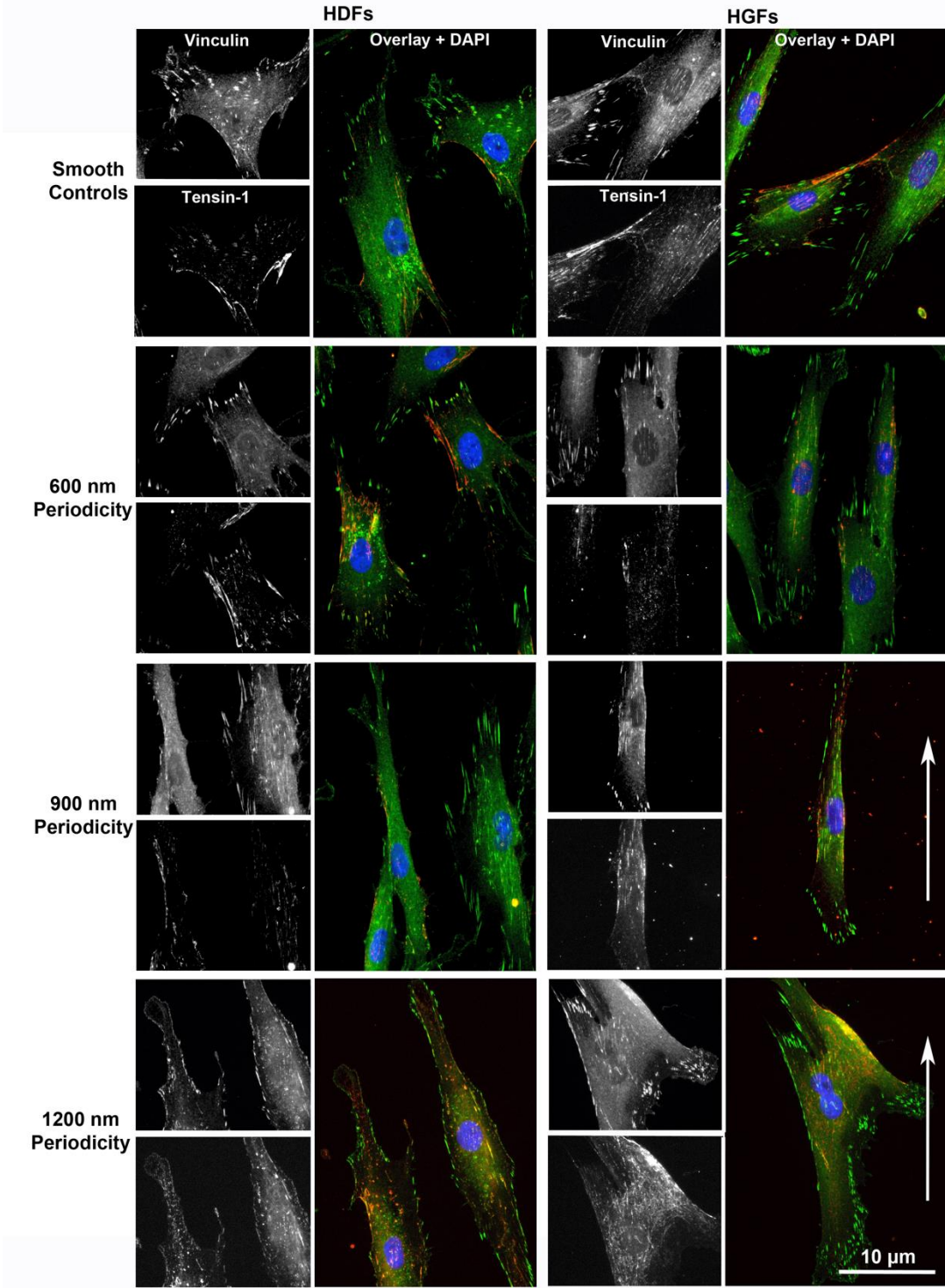


**Figure 2-3: Nanogrooves effect adhesion site and intracellular cytoskeletal protein expression of HGFs and HDFs.**

Immunofluorescent staining of vinculin (green), tensin-1 (red) and nuclei (blue) in HDF and HGF populations following a 24 h timepoint upon smooth and groove surfaces. The direction of the underlying nanogroove long axis is indicated with white arrows.

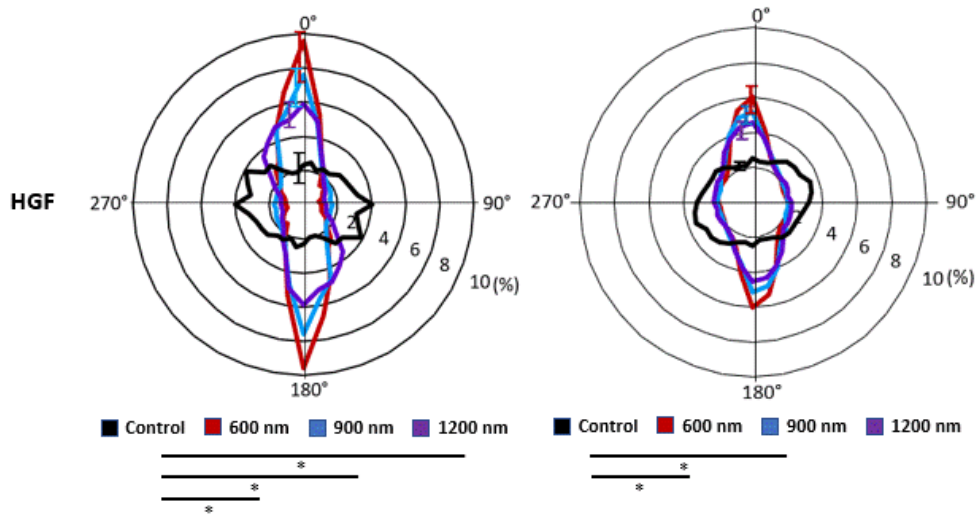
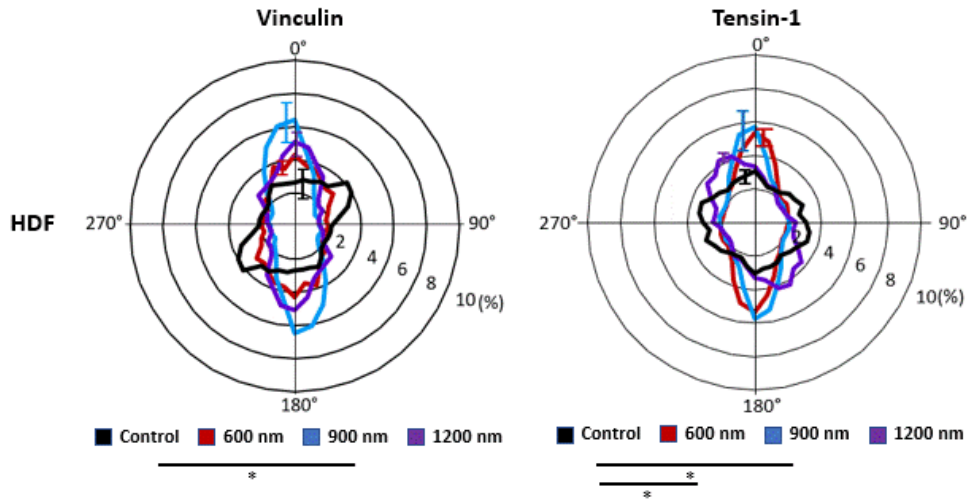


**Figure 2-4: Submicron grooves orient HGF and HDF adhesion proteins.**

Directionality of vinculin and tensin-1 in (a) HDF and (b) HGF fibroblasts at 24 h post-seeding. Mean values established through Fourier transform analysis are displayed in 10° increments ranging from 0° to 360°. The greatest standard deviation at any point of the distribution is displayed. Data were analyzed using the Kolmogorov-Smirnov test of the smooth controls and each experimental surface for both HDF and HGF populations (N = 3; \*P < 0.05).

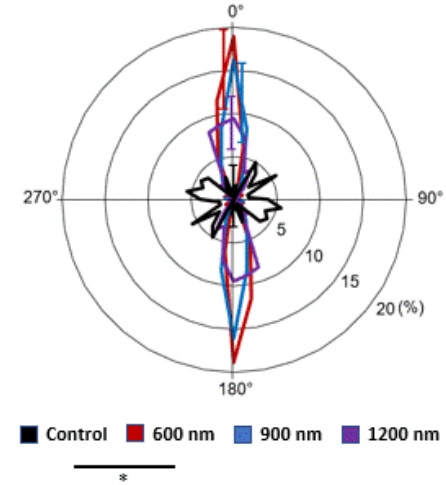
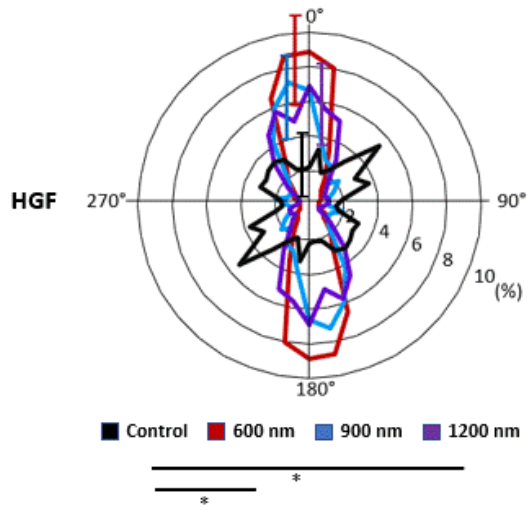
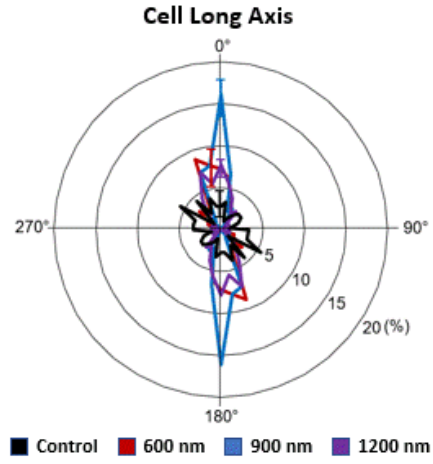
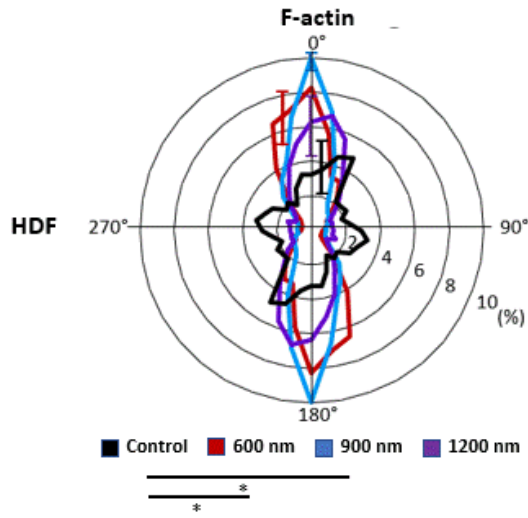




**Figure 2-5: Submicron grooves orient HGF and HDF cytoskeletal proteins.**

Directionality of F-actin and the cellular long axis in (a) HDF and (b) HGF fibroblasts at 24 h post-seeding. Mean values established through Fourier transform analysis are displayed in  $10^\circ$  increments ranging from  $0^\circ$  to  $360^\circ$ . The greatest standard deviation at any point of the distribution is displayed. Data were analyzed using the Kolmogorov-Smirnov test of the smooth controls and each experimental surface for both HDF and HGF populations (N = 3; \*P < 0.05).

**Table 2-1: Average quantity and area of vinculin containing focal adhesions**

Topography	Cell Population	Average Number of Adhesions (per $\mu\text{m}^2$ )	Average Adhesion Area ( $\mu\text{m}^2$ )
Smooth Control	HDF	$0.033 \pm 0.012$	$2.423 \pm 0.998$
	HGF	$0.022 \pm 0.008$	$2.140 \pm 1.106$
600 nm Groove	HDF	$0.032 \pm 0.009$	$1.866 \pm 0.709$
	HGF	$0.026 \pm 0.014$	$2.178 \pm 1.204$
900 nm Groove	HDF	$0.039 \pm 0.009$	$2.165 \pm 1.101$
	HGF	$0.027 \pm 0.009$	$1.594 \pm 0.586$
1200 nm Groove	HDF	$0.039 \pm 0.011$	$2.267 \pm 0.753$
	HGF	$0.026 \pm 0.006$	$1.738 \pm 0.688$

Note: Data was analyzed using one way-ANOVA of the smooth controls and each experimental surface for both HDF and HGF populations (N = 3; n = 10; \*P < 0.05).

**Table 2-2: Average quantity and area of tensin-1 containing fibrillar adhesions**

Topography	Cell Population	Average Number of Adhesions (per $\mu\text{m}^2$ )	Average Adhesion Area ( $\mu\text{m}^2$ )
Flat Control	HDF	$0.036 \pm 0.013$	$1.905 \pm 1.084$
	HGF	$0.024 \pm 0.012$	$1.707 \pm 0.626$
600 nm Groove	HDF	$0.044 \pm 0.016$	$1.343 \pm 0.637$
	HGF	$0.031 \pm 0.016$	$1.323 \pm 0.803$
900 nm Groove	HDF	$0.045 \pm 0.014$	$1.138 \pm 0.664$ *
	HGF	$0.031 \pm 0.014$	$1.325 \pm 1.280$
1200 nm Groove	HDF	$0.040 \pm 0.016$	$1.750 \pm 1.305$
	HGF	$0.027 \pm 0.017$	$1.340 \pm 0.586$

Note: Data was analyzed using one way-ANOVA of the smooth controls and each experimental surface for both HDF and HGF populations (N = 3; n = 10; \*P < 0.05).

### 2.3.2 Fibronectin deposition and organization

As fibronectin deposition requires formation of fibrillar adhesion, I next assessed HDF and HGF fibronectin organization at 24 h post-seeding on all tested surfaces (Figure 2-6). In general, HGFs secreted higher amounts of fibronectin on smooth control surfaces than HDFs. On grooves with 600 nm, 900 nm and 1200 nm periodicities, both HDFs and HGFs show reduced fibronectin fibril formation compared to both cell types cultured on smooth control surfaces, with a more punctate appearance evident. As fibronectin fibrillogenesis is associated with  $\alpha5\beta1$  integrins, using antibodies specific for  $\alpha5$  and  $\beta1$  I assessed their co-localization and assembly in heterodimers (Figure 2-7). On smooth surfaces, HDF and HGF integrin  $\alpha5$  and  $\beta1$  colocalize in long plaque-like adhesion sites, but on all experimental grooved surfaces although the subunits co-localize, adhesion size was diminished.

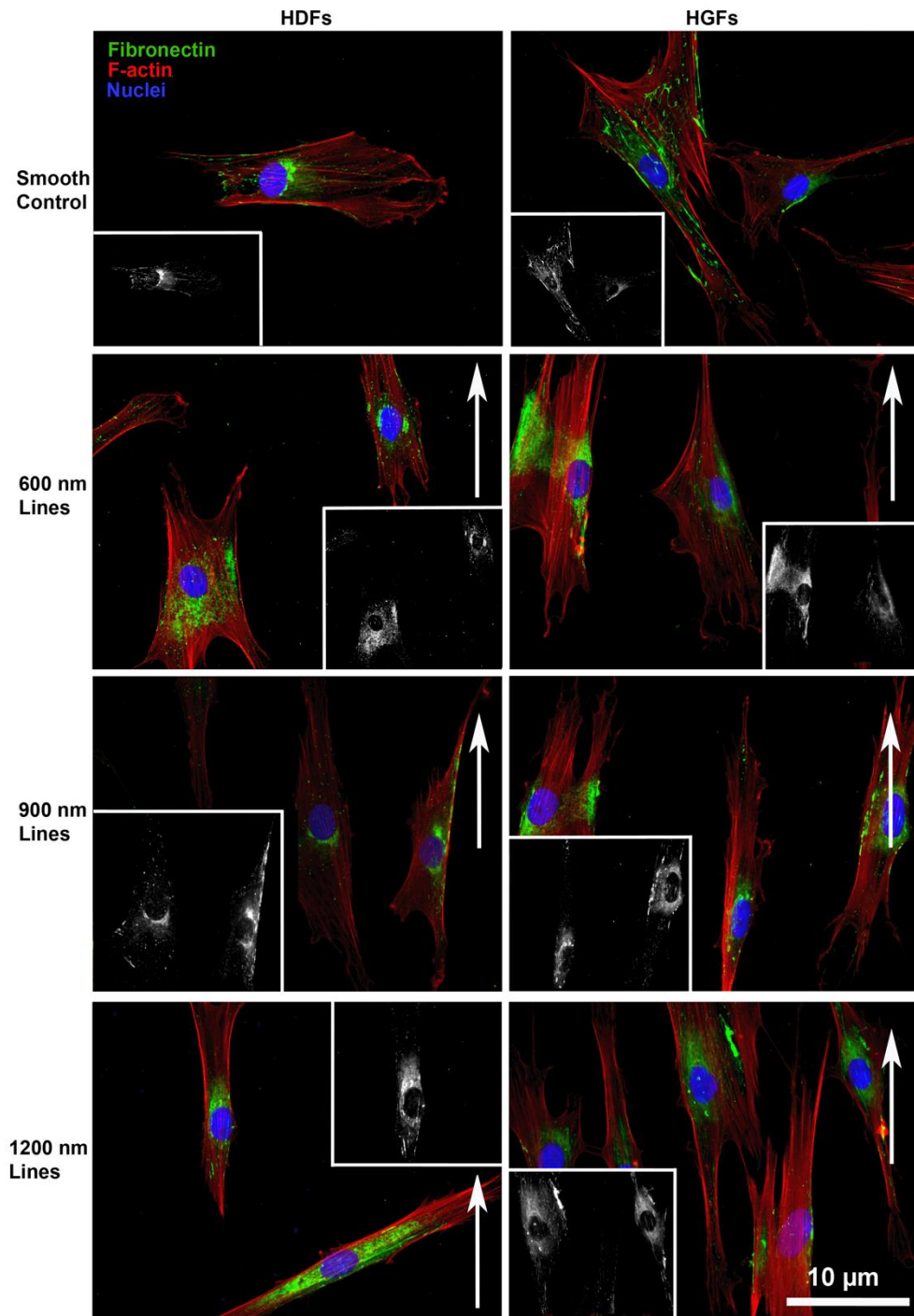


**Figure 2-6: HDF and HGF fibronectin fibril assembly is disrupted by anisotropic repeating groove topographies.**

Representative images of immunofluorescent staining of fibronectin (green), F-Actin (red) and Nuclei (blue) within HDF and HGF populations following a 24 h timepoint upon the smooth and groove surfaces. The direction of the underlying nanogroove long axis is indicated with white arrows.

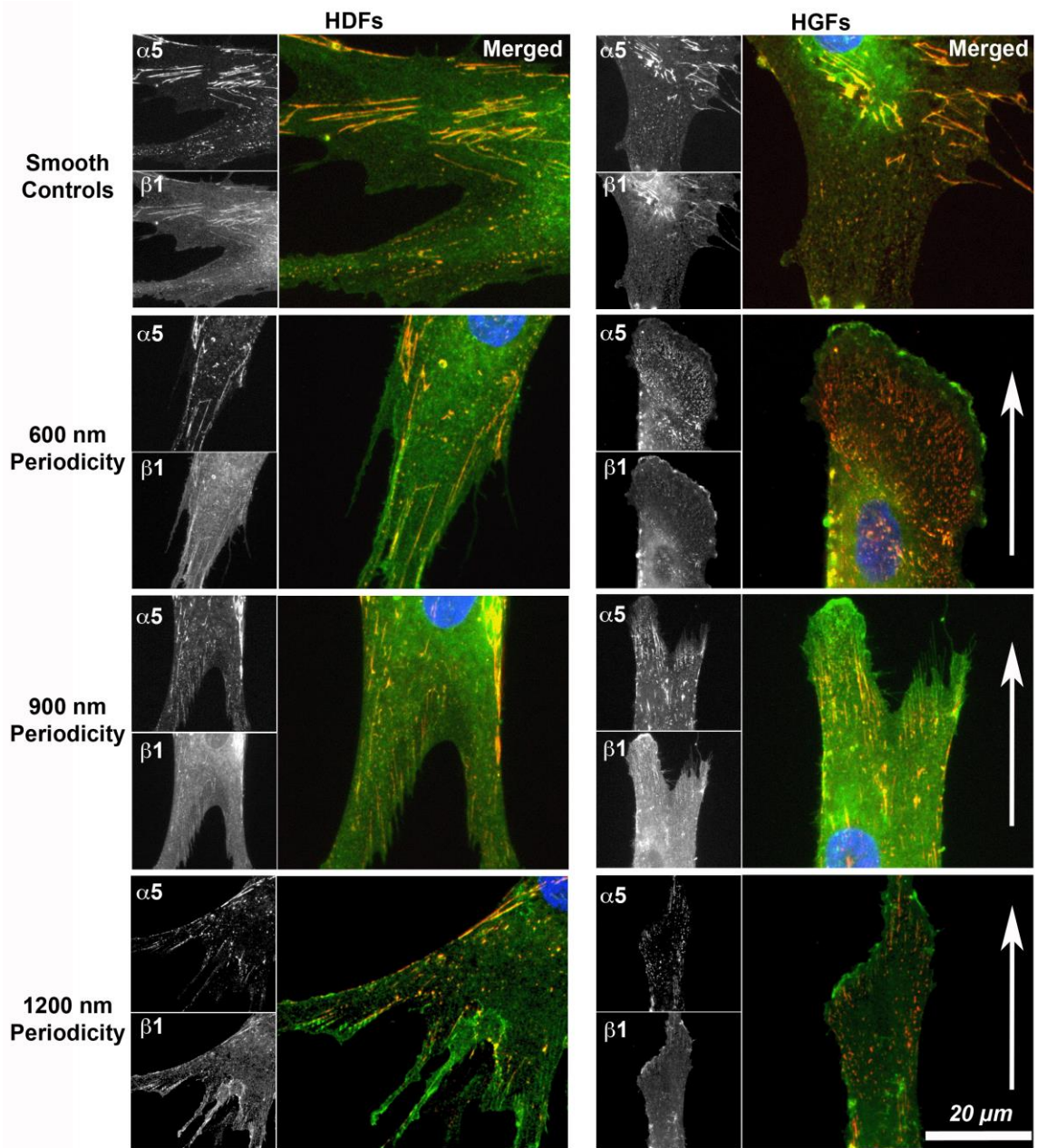


**Figure 2-7: Association of  $\alpha 5$  and  $\beta 1$  integrin dimers are disrupted on anisotropic repeating groove topographies.**

Representative images of immunofluorescent staining of integrin  $\beta 1$  (green), integrin  $\alpha 5$  (red) and Nuclei (blue) within HDF and HGF populations following a 24 h timepoint upon the smooth and groove surfaces to evaluate the colocalization of the integrin dimers. The direction of the underlying nanogroove long axis is indicated with white arrows.



### 2.3.3 Inhibition of integrin $\alpha\beta3$ and integrin $\beta1$ influence HDF and HGF spreading

As integrin  $\alpha\beta3$  containing adhesions are associated with initial adhesion and  $\beta1$  integrin with more mature fibrillar adhesions, I examined the influence of their inhibition on early spreading events of HDFs and HGFs (Figure 2-8). Assessment of cell spreading through vinculin and F-actin labelling of HDF and HGF on the 900 nm periodicity groove surface showed altered spreading in both cell populations. Inhibition of both  $\alpha\beta3$  and  $\beta1$  integrins in HDFs resulted in filopodia extensions around the entire cell edges at 1-hour post-seeding (Figure 2-8A). In contrast, HGFs remained spherical with both  $\alpha\beta3$  and  $\beta1$  integrin inhibition, similar to the morphology of IgG treated control groups at 1 h. At 6 hours post-seeding, both HGFs and HDFs exhibited increased spreading, but qualitatively no increased directionality of the cell long axis to the groove long axis was observed. This was particularly evident in HGFs (Figure 2-8B). Quantification of average cell area demonstrated no significant change in HDFs between the treatment groups (Figure 2-9A), but circularity was significantly reduced by both  $\alpha\beta3$  and  $\beta1$  integrin inhibition at 1 and 3 h, but not 6-hours post-seeding (Figure 2-9B). Integrin  $\alpha\beta3$  and integrin  $\beta1$  inhibition in HGFs had no effect on cell area or circularity at 1-hour post seeding (Figure 2-9C&D). Inhibition of integrin  $\alpha\beta3$  in HGFs did not significantly alter average cell area at 6-h post-seeding in 2 of 3 cell lines tested (Figure 2-9C). However, the average circularity of integrin  $\alpha\beta3$  inhibited HGFs was significantly different from the IgG control in 2 tested cell lines at 6-h post seeding (Figure 2-9C).

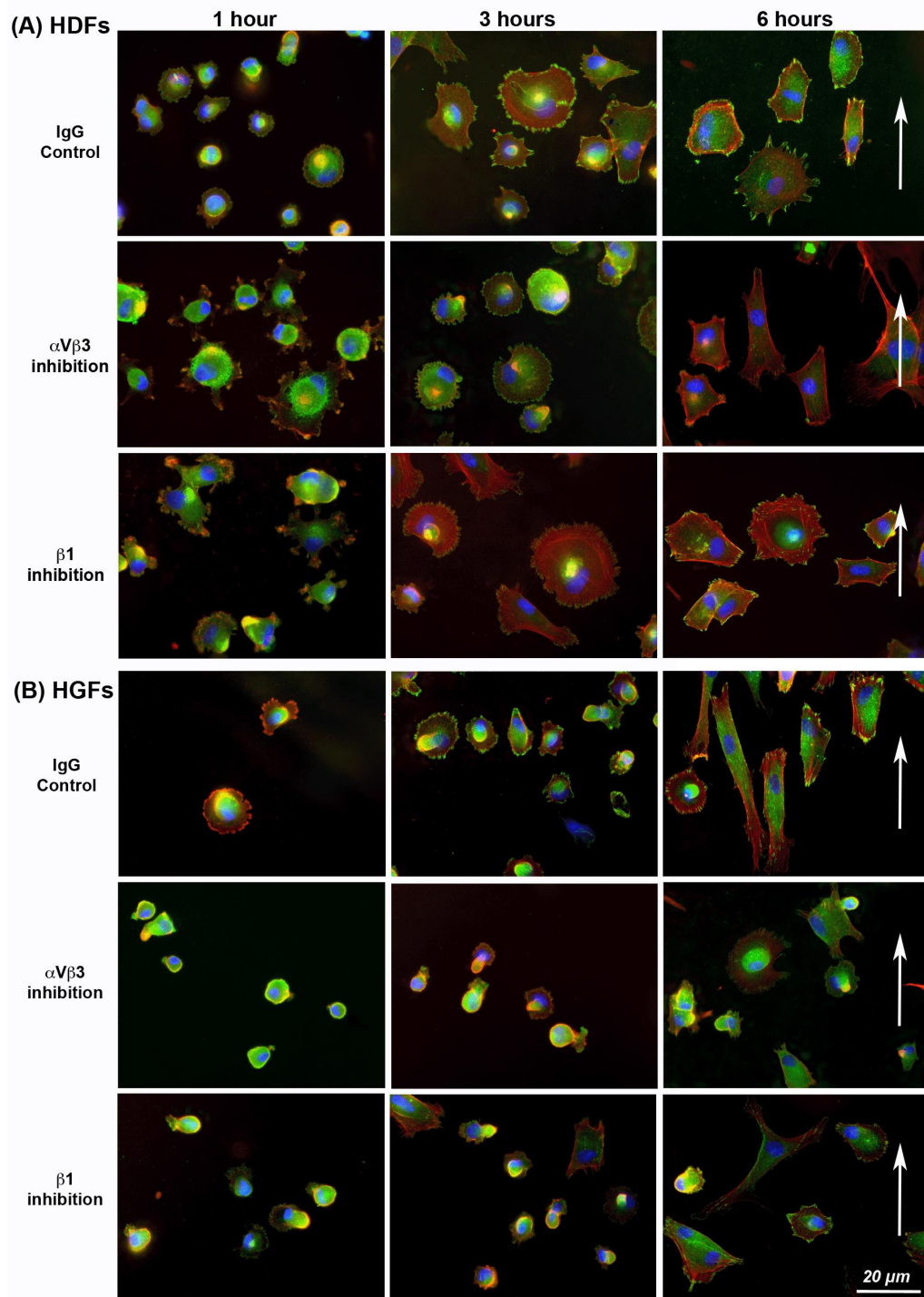


**Figure 2-8: Inhibition of integrin  $\alpha\text{v}\beta\text{3}$  and integrin  $\beta\text{1}$  has a differential effect upon HGF and HDF spreading.**

Representative images from immunofluorescent staining of (A) HDF and (B) HGF vinculin (green), F-actin (red) and nuclei (blue) following 1, 3 and 6 h upon a 900 nm periodicity groove surface with functional inhibition of integrin  $\alpha\text{v}\beta\text{3}$  and integrin  $\beta\text{1}$  and a IgG control treatment. The direction of the underlying nanogroove long axis is indicated by white arrows. Scale bar: 20  $\mu\text{m}$ .

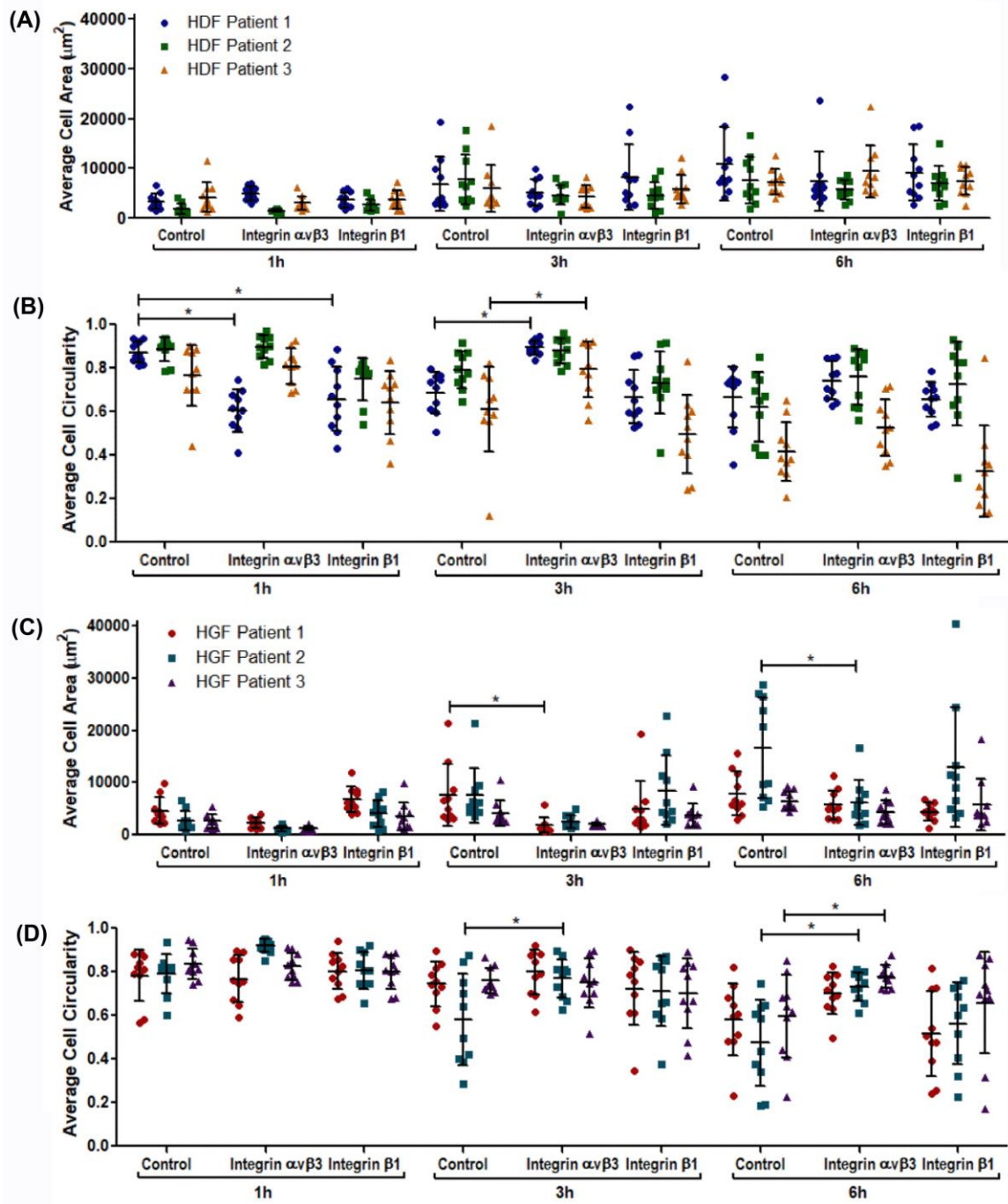


**Figure 2-9: HDF and HGF cell area and circularity are affected by  $\alpha\beta3$  and integrin  $\beta1$  blocking antibodies.**

The average HDF (A) and HGF (C) area and HDF (B) and HGF (D) circularity in the presence of integrin  $\alpha\beta3$  and  $\beta1$  blocking antibodies at 1, 3 and 6 h were quantified. Data is expressed as mean  $\pm$  standard deviation. Data was analyzed using two-way ANOVA, followed by Bonferroni post-tests. (N = 3; \*P < 0.05).

#### 2.3.4 Inhibition of integrin $\alpha\beta3$ and integrin $\beta1$ reduce HDF orientation/alignment, but not in HGFs at 24 h post seeding

HGFs and HDFs were cultured on smooth surfaces or 900 nm grooves with integrin  $\alpha\beta3$  or integrin  $\beta1$  inhibited (Figure 2-10). F-actin labelling demonstrated qualitatively that inhibition of integrin  $\beta1$  and  $\alpha\beta3$  had a larger influence on HDF directionality than HGFs on 900 nm grooves (Figure 2-10A). Fourier transform analysis demonstrated a significant reduction in linear orientation of the cells' long axis within HDFs when integrin  $\beta1$  ( $p < 0.05$ ), but not  $\alpha\beta3$  ( $p > 0.05$ ), was inhibited compared to IgG controls (Figure 2-10B). In contrast, inhibition of  $\beta1$  and  $\alpha\beta3$  integrins had no effect on linear orientation of HGFs versus IgG controls ( $p > 0.05$ ) (Figure 2-10C). Assessment of vinculin (focal adhesions), and tensin-1 (fibrillar adhesions) demonstrated that in HDFs, both  $\alpha\beta3$  and integrin  $\beta1$  inhibition attenuated fibrillar adhesion formation at 24 h post seeding (Figure 2-11A). In contrast, in HGFs  $\alpha\beta3$  and integrin  $\beta1$  inhibition had no effect on fibrillar or focal adhesion formation (Figure 2-11B). Inhibition of integrin  $\beta1$  in HDFs and HGFs cultured on 900 nm periodicity grooves demonstrated difference in tensin-1 localization (Figure 2-12). In HDFs, integrin  $\alpha\beta3$  is observed near the periphery of the cell, colocalized with tensin-1. In contrast, HGFs do not exhibit colocalized tensin-1 and integrin  $\alpha\beta3$ .

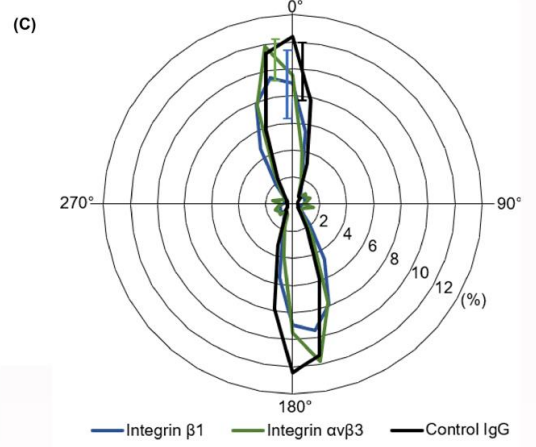
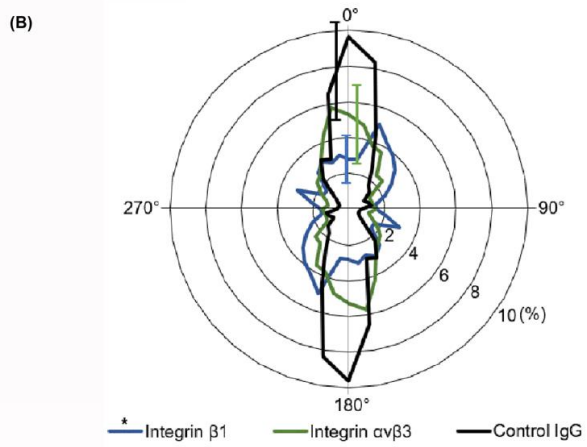
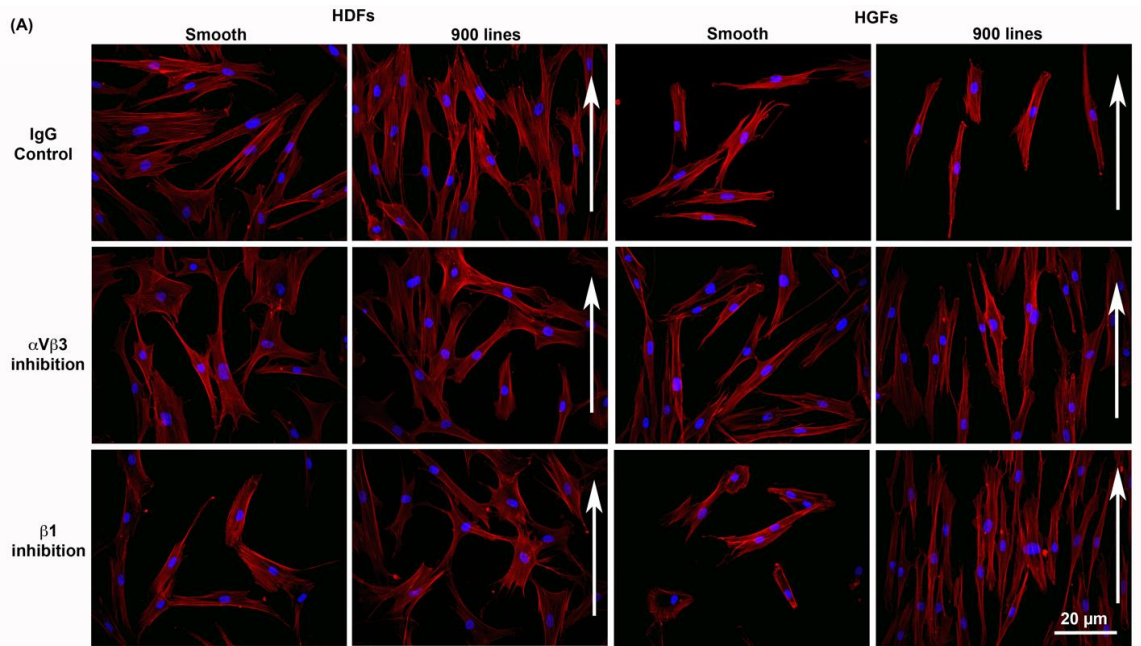


**Figure 2-10: Independent inhibition of integrin  $\alpha\beta3$  and integrin  $\beta1$  demonstrates contrast in alignment between HDF and HGF.**

(A) Immunofluorescent staining of F-actin in HDFs and HGFs at 24 h on a 900 nm periodicity groove surface with functional inhibition of integrin  $\alpha\beta3$  and integrin  $\beta1$  and an IgG control treatment. (B) Directionality of F-actin expression of integrin  $\alpha\beta3$  and integrin  $\beta1$  inhibited HDF and (C) HGF following a 24 h timepoint. Mean values are displayed in  $10^\circ$  increments ranging from 0 to  $360^\circ$ . The greatest standard deviation at any point of the distribution is displayed. Data was analyzed using the Komolgorov-Smirnov test between each experimental condition and the control IgG treatment for both HDF and HGF populations (N = 3; \*P < 0.05). The direction of the underlying nanogroove long axis is indicated by white arrows.



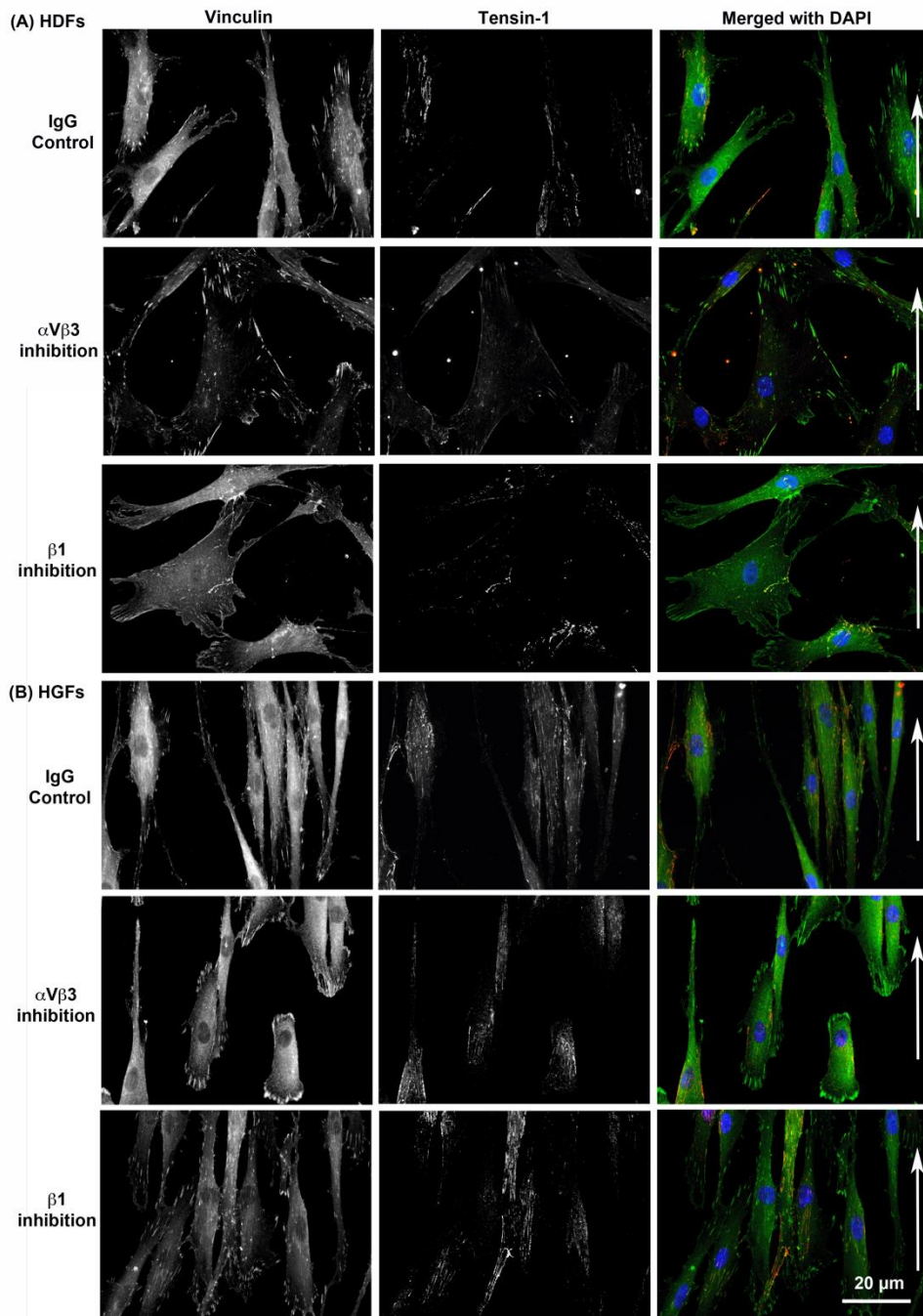


**Figure 2-11: Independent inhibition of integrin  $\alpha v \beta 3$  and integrin  $\beta 1$  demonstrates a functional disparity amongst HDF and HGF.**

Immunofluorescent staining of vinculin (green), tensin-1 (red), and nuclei (blue) within HDF and HGF populations, following a 24 h timepoint, upon a 900 nm periodicity nanogroove surface. The direction of the underlying nanogroove long axis is indicated by white arrows.

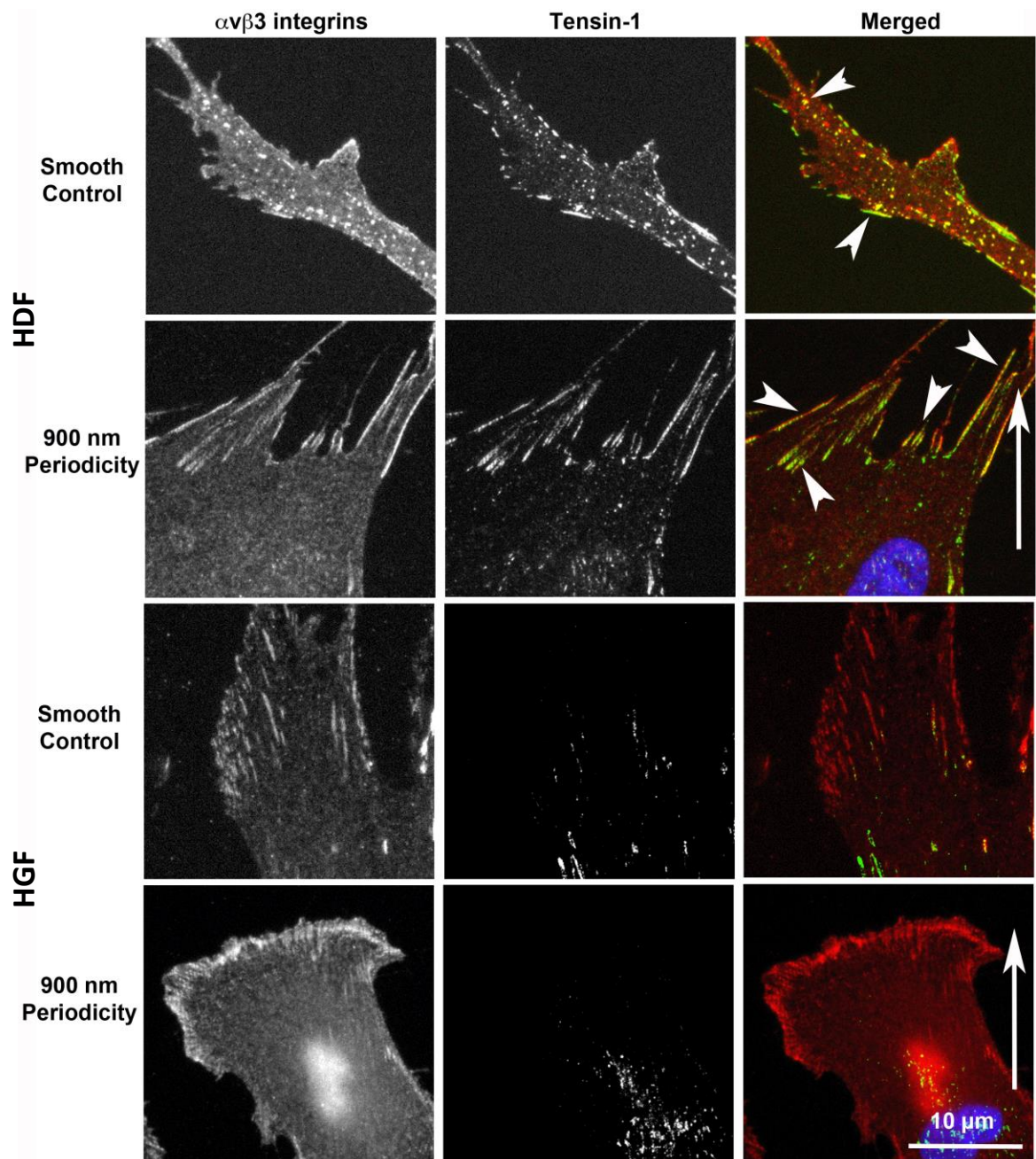


**Figure 2-12: Inhibition of integrin  $\beta 1$  results in tensin-1 recruitment to  $\alpha \nu \beta 3$  peripheral adhesion sites in HDFs, but not HGFs.**

Immunofluorescent staining of tensin-1 (green), integrin  $\alpha \nu \beta 3$  (red) and Nuclei (blue) within HDF and HGF populations following a 24 h timepoint with functional inhibition of integrin  $\beta 1$ . The white arrow heads indicate tensin-1 localization at peripheral sites of integrin  $\alpha \nu \beta 3$  expression within the HDF population. The direction of the underlying nanogroove long axis is indicated by white arrows.

## 2.4 Discussion

Topographic modification of biomaterials to control cell colonization and tissue integration has been a major research focus driven particularly by the evolution of devices such as dental implants <sup>7</sup>. It is known that cells respond to topographical cues through changes in adhesion, spreading, alignment and migration, which can subsequently enhance integration of biomaterials into host tissues <sup>1,8,9</sup>. Although topographic modifications for bone interfacing biomaterials have been determined and are used clinically with great success, slower progress has been made in optimal topographic modifications of biomaterials for enhancing repair of soft tissues such as skin and gingiva <sup>10</sup>. Despite residing in tissues with a similar histological architecture, fibroblasts originating from gingiva tissue are associated with a fetal-like wound healing phenotype compared to dermal fibroblasts, with gingiva exhibiting a propensity towards tissue regeneration rather than scar formation seen in skin <sup>11</sup>. In this study, using both gingival and dermal fibroblasts, I investigated the effect of sub-micron repeating groove topographies on adhesion formation, contact guidance, and fibronectin fibrillogenesis.

### 2.4.1 HGFs and HDFs exhibit morphological and adhesion alignment to sub-micron groove topographies.

In this study, I utilized sub-micron grooves with varying periodicity as in our previous studies determined that periodicity of structures exerted a significant influence in human periodontal ligament (PDL) fibroblasts, orienting adhesion formation and spreading as early as 30 minutes post-seeding <sup>12</sup>. In addition, cell orientation of PDL fibroblasts to the groove long axis was quantified, with guided migration also evident. Therefore, topographies in the range of 600-900 nm in periodicity and 50-100 nm in depth are sufficient to induce contact guidance by augmenting cellular components and responses rather than the entire cell itself being oriented on a microscale topography. I utilized these surfaces in this study to investigate the response of gingival and dermal fibroblasts. Both HGFs and HDFs aligned to all periodicities of grooves tested compared to smooth control surfaces. Qualitatively, elongation of the cells was most prominent on 600 and 900 nm

periodicities compared to 1200 nm, where cells exhibited more spreading perpendicular to the groove long axis. Previous studies have suggested that cell alignment on topographical cue is related to the likelihood of a cell forming stable adhesion sites<sup>13</sup>, with Curtis hypothesizing that cells form adhesions related to discontinuities such as groove/ridge boundaries<sup>14</sup>. It is conceivable that as the periodicity of the grooves increases to 1200 nm, adhesions sites are less restricted in angle of formation (relative to groove long axis) compared to 600 and 900 nm, which allows stable adhesion formation in a direction other than the groove long axis. We have previously shown in PDL cells that adhesion formation and elongation/orientation is driven primarily by adhesion formation in the presence of a continuous groove edge, and lateral adhesion and spreading is increased if the groove edge is discontinuous. As stable adhesion sites allow formation of the leading filopodia and cell spreading, directed migration would most likely occur in the same direction as the adhesion forms. Indeed, filopodia extensions and focal adhesions have been implicated in the process of contact guidance by us and others<sup>12,15,16</sup>.

One interesting finding of our study is when comparing the response of the two fibroblast populations, HGFs consistently formed fewer adhesion sites than HDFs. Previous studies have highlighted reduced expression of pro-adhesive mRNAs, adherence and spreading on type I collagen and fibronectin of HGF when compared to HDFs<sup>17</sup>. Our results demonstrate that on nanogrooves, HDFs and HGFs maintain this difference in adhesion formation, suggesting intrinsic difference within fibroblast response that are most likely due to the tissue of origin. Based on lineage tracing studies and cell separation<sup>18,19</sup>, it is becoming clear that embryonic origin of cells and the microenvironment of the tissue they reside in confer distinct properties to them, or "intrinsic" characteristics<sup>20</sup>. Intrinsic differences encompass gene expression, epigenetics, signaling molecules, transcription factors and adhesion<sup>20</sup>. Evidence has previously highlighted that cells align and adhere preferentially to nanogroove topographies of optimal dimensions, specific to the cell type and cell niche<sup>21</sup>. As stated previously, gingival tissue is associated with a scarless response in tissue repair compared to dermal healing<sup>11</sup>. Dermal fibroblasts upon activation exhibit an increase in focal adhesion number and size which correlates with increased cellular contractility and the differentiation of fibroblasts into myofibroblasts, subsequently establishing scar tissue<sup>22</sup>. We have previously shown in a rat model that gingival

fibroblasts do not transition into myofibroblasts during healing <sup>23,24</sup>, which supports our findings in this paper that it is likely due to these intrinsic differences in adhesion formation linked to tissue of origin.

Most research related to adhesion formation and contact guidance on topographical cues have focused on focal contacts and focal adhesions, with significantly less emphasis placed on fibrillar adhesions. Associated with recruitment of tensin-1 and  $\alpha 5\beta 1$  integrins <sup>25</sup>, fibrillar adhesions are also strongly implicated in the process of myofibroblast differentiation, fibronectin matrix deposition and crucially, mechanotransduction <sup>26-28</sup>. I show here that tensin-1 alignment with the groove long axis is most pronounced in both HDFs and HGFs on 600 and 900 nm periodicities. Furthermore, fibrillar adhesion sites in HGFs were smaller than those evident in HDFs. Interestingly, we have previously shown on micrometric topographies, HGFs form large and well developed fibrillar adhesions suggesting a clear difference in adhesion dynamics of HGFs on sub-micron topography <sup>29</sup>. However, it is also logical that in cells that show a propensity towards contractility and myofibroblast differentiation, that tensin-1 associated adhesion sites would be more pronounced as is seen in HDFs. Our previous work has shown that sub-micron random cues such as sand-blasted, acid etched topographies that limit available contact area for HGF adhesion formation reduce behaviours associated with fibrosis <sup>1</sup>.

#### 2.4.2 HDFs and HGFs require both integrin $\alpha v\beta 3$ and integrin $\beta 1$ adhesion sites for cell spreading and elongation up to 6 hours post-seeding.

As focal and fibrillar adhesions are associated with  $\alpha v\beta 3$  and  $\alpha 5\beta 1$  integrins respectively, I next investigated what influence their inhibition would have on contact guidance of HDFs and HGFs. Adhesions are considered to form in a hierarchical manner, with focal contacts least mature, followed by focal adhesions and finally formation of the supermature fibrillar adhesions <sup>30</sup>. While derivation of cell lines in which these integrins were genetically deleted would give a more direct measure of their involvement in contact guidance, in this study I utilized blocking antibodies. As both  $\alpha v\beta 3$  and  $\beta 1$  integrins are required for development, it would involve derivation of two separate conditional knockout mice lines to derive

appropriate cells. Furthermore, I wanted to make direct comparison between human dermal and gingival fibroblasts, and as inhibition of integrins are removed, it also allowed assessment of how long it took for cells to reorient to the grooves.

With regards to attachment and spreading, inhibition of integrin  $\alpha\beta3$  and integrin  $\beta1$  in both HGFs and HDFs had little significant impact on circularity or cell area compared to cells on control surfaces. However, assessment of cell morphology demonstrated differences between HGFs and HDFs, with HDFs in particular extending numerous filopodia when either integrin  $\alpha\beta3$  or integrin  $\beta1$  were blocked at 1-hour post-seeding. In contrast, HGFs remained spherical with no spreading evident. Both HGFs and HDFs showed increased spreading at 6 hours post-seeding, although orientation with groove long axis was minimal, particularly for HGFs. Perhaps not surprisingly, inhibition of  $\alpha\beta3$ , but not integrin  $\beta1$  reduces formation of vinculin containing adhesion even 6 hours post seeding in HDFs and HGFs. Integrin  $\alpha\beta3$  has been established as the primary integrin involved in focal adhesion complexes, and filopodia extensions, but is also a receptor for vitronectin and fibronectin<sup>31</sup>. Previous studies have shown that inhibition of integrin  $\alpha\beta3$  in oral squamous carcinoma cells eliminates directionality of cell migration on fibronectin-matrices<sup>32</sup>. Interestingly, it was also demonstrated that in the presence of DisBa-01 (RGD containing disintegrin), the size and number of paxillin associated adhesions increased in cancer cells of epithelial origin, but no differences were seen in fibroblasts. The inhibition of integrin  $\alpha\beta3$  should impede filopodia and lamellipodia stability, preventing activation of the mechanosensory pathways that would result in alignment of the cells to the groove long axis<sup>12,33</sup>. However, the disruption of integrin  $\beta1$  mediated adhesion demonstrates a clear need for fibrillar adhesions in contact guidance and initial alignment of cells to repeating grooves.

#### **2.4.3 Inhibition of integrin $\alpha\beta3$ and integrin $\beta1$ illustrates an essential role for $\beta1$ integrins in contact guidance of HDFs, but not HGFs.**

With an established short-term effect upon HGF and HDF adhesion and cell spreading as a result of integrin  $\alpha\beta3$  and integrin  $\beta1$  inhibition, I next investigated the influence of



integrin inhibition on cell orientation and adhesion formation at 24 hrs post-seeding. Assessment of cell alignment to the groove long axis through F-actin labeling revealed that inhibition of  $\beta 1$  integrins in HDFs attenuated orientation. Interestingly, I show that at 24 hrs post-inhibition, HDFs contain minimal fibrillar adhesions when either  $\alpha v\beta 3$ , or integrin  $\beta 1$  are inhibited and the cells do not align to the groove long axis. It provides further evidence of the hierarchical nature of adhesion formation in HDFs<sup>30</sup>, specifically with the observation that inhibition of  $\alpha v\beta 3$  prevents formation of mature fibrillar adhesions. However, the absence of tensin-1 associated fibrillar adhesions in HDFs when either  $\alpha v\beta 3$  and or  $\beta 1$  integrin establishes that  $\beta 1$  is required for alignment and contact guidance. Furthermore, it suggests that it is  $\beta 1$  integrins rather than their association with tensin-1 and fibrillar adhesions, that are required. Through antibody labeling, I show in control HDF cultures on 900 nm grooves that integrin  $\beta 1$  localizes to numerous punctate structures consistent with focal contacts or developing focal adhesions, rather than more mature fibrillar adhesions. This confirms an essential role for integrin  $\beta 1$  in cell response to submicron grooves independent of their localization with tensin-1. Of particular significance, it has been previously demonstrated that integrin  $\beta 1$  is required for matrix synthesis by dermal fibroblasts, where it is thought to be a primary mechanosensor<sup>34</sup>. As fibrotic encapsulation of materials including breast implants is a major clinical concern, understanding further the role of topography in recruitment of  $\beta 1$  integrins and its downstream effects could be of significance in biomaterial design<sup>35</sup>.

HDFs are known to be responsive to substratum stiffness, forming large fibrillar adhesions associated with recruitment of  $\beta 1$  integrins. In this study, grooves utilized are fabricated in fused silica which has a tensile strength in the mega-pascal range. It is conceivable that the material stiffness increases the requirement for integrin  $\beta 1$  engagement, and over-rides the orientation signals provided by the grooves. Of potential significance, we have shown previously that HGFs are resistant to forming large adhesions even on materials such as titanium, with a corresponding low level of myofibroblast transition evident<sup>1</sup>. Moreover, we also demonstrated substratum roughness induced nascent adhesion formation in HGFs which was associated with the upregulation of inflammatory and matrix remodeling genes. Further analysis of how topographical cues and substratum compliance combine to

influence cell phenotype will be of great importance, particularly for adhesion mediated events such as myofibroblast differentiation.

#### 2.4.4 HDFs recruit tensin-1 to focal adhesion in the absence of $\beta 1$ integrin adhesion sites

As previously described, fibrillar adhesions are classically defined by the presence of tensin-1 and integrin  $\alpha 5\beta 1$  largely localized in the centre of the cell. Through antibody labeling, I demonstrated in the presence of integrin  $\beta 1$  inhibition in HDFs, tensin-1 is recruited to and incorporated into the periphery of the cell, where it associates with integrin  $\alpha \nu\beta 3$  adhesion sites. Such a localization of tensin-1 into  $\alpha \nu\beta 3$  focal adhesions in dermal fibroblasts in response to  $\beta 1$  integrin inhibition suggests an attempt to increase contractility in the absence of mature fibrillar adhesions. I suggest that it is also the reason why at 24hrs post seeding HDFs lacking  $\beta 1$  adhesions do not align or exhibit contact guidance with respect to the groove long axis. Tensin-1 associated adhesions are stable and are known to slow migration which would account for HDFs not realigning with the groove long axis <sup>36</sup>. This alteration in tensin-1 recruitment upon inhibition of  $\beta 1$  integrins seen in dermal fibroblasts is not observed in HGFs, emphasizing an intrinsic difference in adhesion assembly on the same topographies. The recruitment of tensin-1 to sites of focal adhesions associated with vinculin, talin and integrin  $\alpha \nu\beta 3$  has been described previously <sup>37</sup>. These tensin-1 containing focal adhesions were found to have disrupted fibronectin fibrillogenesis unless bound to integrin  $\alpha 5\beta 1$  whereby fibronectin was deposited albeit with impaired fibril formation <sup>37</sup>. This observation is similar to our findings using submicron grooves as fibronectin fibril formation is attenuated when compared to cells on smooth controls. In essence, the addition of submicron grooves can replicate the disruption of integrin  $\beta 1$  complexes required for fibronectin fibrillogenesis in HDFs.

Interestingly, neither  $\alpha \nu\beta 3$  nor  $\beta 1$  inhibition, prevented alignment of HGFs on 900 nm periodicity grooves at 24 hours. However, in contrast to HDFs, in HGFs, tensin-1 labeling is somewhat similar to IgG controls, such that inhibition of  $\alpha \nu\beta 3$  and  $\beta 1$  integrins does not completely inhibit fibrillar adhesion formation at 24 hrs post seeding. It is conceivable that

HGFs are able to turnover integrins faster than HDFs, which would account for the presence of fibrillar adhesions particularly when integrin  $\beta 1$  is inhibited. However, it was also noted a significant difference in  $\beta 1$  localization in HGFs compared to HDFs, suggesting that they could be of less importance in adhesion-mediated events in gingival tissue. It does however emphasize that fibroblast populations from different tissues possess different properties and tissue specificity maybe important for the design of biomaterials for soft connective tissues such as skin or gingiva.

#### 2.4.5 Sub-micron grooves as an anti-fibrotic surface: Disruption of fibronectin fibril formation

Both integrin  $\alpha 5\beta 1$  and  $\alpha v\beta 3$  integrins are known to bind to fibronectin, with fibrillar adhesion in particular involved in fibronectin fibrillogenesis<sup>37</sup>. I show here through qualitative evaluation of HDFs and HGFs that the presence of submicron grooves disrupts fibronectin fibril formation. Upon the flat control surface, distinct fibrils of fibronectin can be seen under the cell. When cultured on the submicron grooves of all periodicities, immunofluorescence shows more punctate fibronectin organization, with fewer fibrils evident. This result is in agreement with previous studies which indicated a disruption in HGF fibronectin deposition upon roughened titanium surfaces relative to smooth controls<sup>1</sup>.

Biomaterials implanted within native tissues typically invoke a foreign body response, similar to the normal healing response, often resulting in the formation of fibrous or scar tissue around the biomaterial<sup>38,39</sup>. While recent studies have shown that changing the compliance of a material can reduce fibrotic tissue formation<sup>35</sup>, the potential of topographical modifications to reduce matrix production and myofibroblast differentiation on implanted materials is intriguing. This is particularly attractive as topographic modification of biomaterials is usually permanent and could avoid the need for changing the tensile strength of materials which could preclude their clinical utility. Future studies will assess how our submicron grooves influence capsule formation and fibrosis using in vivo models. Of encouragement, using a porcine model, it has been recently demonstrated

fibrotic capsule formation on pacemakers can be reduced by the addition of cellulose fabricated micrometric hexagonal topographic features <sup>40</sup>.

#### 2.4.6 Conclusions

Contact guidance is an important cell phenomenon that permits colonization and integration of biomaterials into host tissues. The results of this study demonstrate for the first time that  $\beta 1$  integrins are an important determinant of cell alignment to submicron grooves in dermal fibroblasts, and that fibroblasts isolated from gingiva and dermis exhibit different responses to the same topographies. The finding that fibroblasts with different tissue origins exhibit altered behaviour on the same topographies further highlights the specificity requirement in designing materials for augmenting tissue repair. In addition, our findings further highlight the difference in adhesion formation evident between dermal and gingival fibroblasts which point further at the role of  $\beta 1$  integrins and tensin-1 in the scarring phenotype of skin versus gingiva. Topographical modulation of integrin  $\beta 1$  and tensin-1 may provide new avenues of investigation for inhibiting fibrosis around implanted materials.

## 2.5 References

- (1) Kim, S. S.; Wen, W.; Prowse, P.; Hamilton, D. W. Regulation of Matrix Remodelling Phenotype in Gingival Fibroblasts by Substratum Topography. *J Cell Mol Med* **2015**, *19* (6), 1183–1196. <https://doi.org/10.1111/jcmm.12451>.
- (2) Brunette, D. M.; Chehroudi, B. The Effects of the Surface Topography of Micromachined Titanium Substrata on Cell Behavior in Vitro and in Vivo. *J Biomech Eng* **1999**, *121*, 49–57.
- (3) Mudera, V. C.; Pleass, R.; Eastwood, M.; Tarnuzzer, R.; Schultz, G.; Khaw, P. Molecular Responses of Human Dermal Fibroblasts to Dual Cues : Contact Guidance and Mechanical Load. *Cell Motil Cytoskeleton* **2000**, *45* (September 1999), 1–9.
- (4) Chou, L.; Firth, J. D.; Uitto, V.; Brunette, D. M. Substratum Surface Topography Alters Cell Shape and Regulates Fibronectin mRNA Level , mRNA Stability , Secretion and Assembly in Human Fibroblasts. *J Cell Sci* **1995**, *108*, 1563–1573.
- (5) Lee, I.; Kim, D.; Park, G. L.; Jeon, T. J.; Kim, S. M. Investigation of Wound Healing Process Guided by Nano-Scale Topographic Patterns Integrated within a Microfluidic System. *PLoS One* **2018**, *13* (7), 1–16. <https://doi.org/10.1371/journal.pone.0201418>.
- (6) Sun, Y.-L.; Mikolas, D.; Chang, E.-C.; Lin, P.-T.; Fu, C.-C. Lloyd's Mirror Interferometer Using a Single-Mode Fiber Spatial Filter. *Journal of Vacuum Science & Technology B, Nanotechnology and Microelectronics: Materials, Processing, Measurement, and Phenomena* **2013**, *31* (2), 021604. <https://doi.org/10.1116/1.4790660>.
- (7) Gupta, S.; Dahiya, V.; Shukla, P. Surface Topography of Dental Implants: A Review. *Journal of Dental Implants* **2014**, *4* (1), 66. <https://doi.org/10.4103/0974-6781.131009>.
- (8) Hamilton, D. W.; Chehroudi, B.; Brunette, D. M. Comparative Response of Epithelial Cells and Osteoblasts to Microfabricated Tapered Pit Topographies in Vitro and in Vivo. *Biomaterials* **2007**, *28* (14), 2281–2293. <https://doi.org/10.1016/j.biomaterials.2007.01.026>.

- (9) Prowse, P. D. H.; Elliott, C. G.; Hutter, J.; Hamilton, D. W. Inhibition of Rac and ROCK Signalling Influence Osteoblast Adhesion, Differentiation and Mineralization on Titanium Topographies. *PLoS One* **2013**, *8* (3), 17–26.  
<https://doi.org/10.1371/journal.pone.0058898>.
- (10) Devgan, S.; Sidhu, S. S. Evolution of Surface Modification Trends in Bone Related Biomaterials: A Review. *Mater Chem Phys* **2019**, *233*, 68–78.  
<https://doi.org/10.1016/j.matchemphys.2019.05.039>.
- (11) Fournier, B. P. J.; Larjava, H.; Häkkinen, L. Gingiva as a Source of Stem Cells with Therapeutic Potential. *Stem Cells Dev* **2013**, *22* (24), 3157–3177.  
<https://doi.org/10.1089/scd.2013.0015>.
- (12) Hamilton, D. W.; Oates, C. J.; Hasanzadeh, A.; Mittler, S. Migration of Periodontal Ligament Fibroblasts on Nanometric Topographical Patterns: Influence of Filopodia and Focal Adhesions on Contact Guidance. *PLoS One* **2010**, *5* (12).  
<https://doi.org/10.1371/journal.pone.0015129>.
- (13) Hamilton, D. W.; Brunette, D. M. “Gap Guidance” of Fibroblasts and Epithelial Cells by Discontinuous Edged Surfaces. *Exp Cell Res* **2005**, *309* (2), 429–437.  
<https://doi.org/10.1016/j.yexcr.2005.06.015>.
- (14) Curtis, A. S. G.; Clark, P. The Effects of Topographic and Mechanical Properties of Materials on Cell Behaviour. *Critical Reviews in Biocompatibility* **1990**, *5*, 343–362.
- (15) Klymov, A.; Bronkhorst, E. M.; Te Riet, J.; Jansen, J. A.; Walboomers, X. F. Bone Marrow-Derived Mesenchymal Cells Feature Selective Migration Behavior on Submicro- and Nano-Dimensional Multi-Patterned Substrates. *Acta Biomater* **2015**, *16* (1), 117–125.  
<https://doi.org/10.1016/j.actbio.2015.01.016>.
- (16) Prager-Khoutorsky, M.; Lichtenstein, A.; Krishnan, R.; Rajendran, K.; Mayo, A.; Kam, Z.; Geiger, B.; Bershadsky, A. D. Fibroblast Polarization Is a Matrix-Rigidity-Dependent Process Controlled by Focal Adhesion Mechanosensing. *Nat Cell Biol* **2011**, *13* (12), 1457–1465. <https://doi.org/10.1038/ncb2370>.

- (17) Guo, F.; Carter, D. E.; Mukhopadhyay, A.; Leask, A. Gingival Fibroblasts Display Reduced Adhesion and Spreading on Extracellular Matrix: A Possible Basis for Scarless Tissue Repair? *PLoS One* **2011**, *6* (11), 1–9.  
<https://doi.org/10.1371/journal.pone.0027097>.
- (18) Myung, P.; Andl, T.; Atit, R. The Origins of Skin Diversity: Lessons from Dermal Fibroblasts. *Development (Cambridge)*. Company of Biologists Ltd December 1, 2022.  
<https://doi.org/10.1242/dev.200298>.
- (19) Walker, J. T.; Flynn, L. E.; Hamilton, D. W. Lineage Tracing of Foxd1-Expressing Embryonic Progenitors to Assess the Role of Divergent Embryonic Lineages on Adult Dermal Fibroblast Function. *FASEB Bioadv* **2021**, *3* (7), 541–557.  
<https://doi.org/10.1096/fba.2020-00110>.
- (20) Picollet-D'hahan, N.; Dolega, M. E.; Freida, D.; Martin, D. K.; Gidrol, X. Deciphering Cell Intrinsic Properties: A Key Issue for Robust Organoid Production. *Trends in Biotechnology*. Elsevier Ltd November 1, 2017, pp 1035–1048.  
<https://doi.org/10.1016/j.tibtech.2017.08.003>.
- (21) Chung, K.; DeQuach, J. A.; Christman, K. L. Nanopatterned Interfaces for Controlling Cell Behavior. *Nano Life* **2010**, *01* (1-amp 2), 63–77.  
<https://doi.org/10.1142/s1793984410000055>.
- (22) Hinz, B. Formation and Function of the Myofibroblast during Tissue Repair. *Journal of Investigative Dermatology* **2007**, *127* (3), 526–537.  
<https://doi.org/10.1038/sj.jid.5700613>.
- (23) Nikoloudaki, G.; Creber, K.; Douglas, X.; Hamilton, W. Wound Healing and Fibrosis: A Contrasting Role for Periostin in Skin and the Oral Mucosa. **2020**.  
<https://doi.org/10.1152/ajpcell>.
- (24) Kim, S. S.; Nikoloudaki, G. E.; Michelsons, S.; Creber, K.; Hamilton, D. W. Fibronectin Synthesis, but Not  $\alpha$ -Smooth Muscle Expression, Is Regulated by Periostin in Gingival

- Healing through FAK/JNK Signaling. *Sci Rep* **2019**, 9 (1).  
<https://doi.org/10.1038/s41598-018-35805-6>.
- (25) Zamir, E.; Katz, M.; Posen, Y.; Erez, N.; Yamada, K. M.; Katz, B.-Z.; Lin, S.; Lin, D. C.; Bershadsky, A.; Kam, Z.; Geiger, B. Dynamics and Segregation of Cell– Matrix Adhesions in Cultured Fibroblasts. *Nat Cell Biol* **2000**, 2 (4), 191–196.  
<https://doi.org/10.1038/35008607>.
- (26) Bernau, K.; Torr, E. E.; Evans, M. D.; Aoki, J. K.; Ngam, C. R.; Sandbo, N. Tensin 1 Is Essential for Myofibroblast Differentiation and Extracellular Matrix Formation. *Am J Respir Cell Mol Biol* **2017**, 56 (4), 465–476. <https://doi.org/10.1165/rcmb.2016-0104OC>.
- (27) Pankov, R.; Cukierman, E.; Katz, B.-Z.; Matsumoto, K.; Lin, D. C.; Lin, S.; Hahn, C.; Yamada, K. M. *Integrin Dynamics and Matrix Assembly: Tensin-Dependent Translocation of  $\alpha 5 \beta 1$  Integrins Promotes Early Fibronectin Fibrillogenesis*; 2000; Vol. 148. <http://www.jcb.org>.
- (28) Chen, H.; Duncan, I. C.; Bozorgchami, H.; Lo, S. H. Tensin1 and a Previously Undocumented Family Member, Tensin2, Positively Regulate Cell Migration. *Proc Natl Acad Sci U S A* **2002**, 99 (2), 733–738.
- (29) Kokubu, E.; Hamilton, D. W.; Inoue, T.; Brunette, D. M. Modulation of Human Gingival Fibroblast Adhesion, Morphology, Tyrosine Phosphorylation, and ERK 1/2 Localization on Polished, Grooved and SLA Substratum Topographies. *J Biomed Mater Res A* **2009**, 91 (3), 663–670. <https://doi.org/10.1002/jbm.a.32273>.
- (30) Zaidel-Bar, R.; Cohen, M.; Addadi, L.; Geiger, B. Hierarchical Assembly of Cell-Matrix Adhesion Complexes. *Biochem Soc Trans* **2004**, 32 (Pt3), 416–420.  
<https://doi.org/10.1042/BST0320416>.
- (31) Patsenker, E.; Popov, Y.; Stickel, F.; Schneider, V.; Ledermann, M.; Sägeser, H.; Niedobitek, G.; Goodman, S. L.; Schuppan, D. Pharmacological Inhibition of Integrin  $\alpha v \beta 3$  Aggravates Experimental Liver Fibrosis and Suppresses Hepatic Angiogenesis. *Hepatology* **2009**, 50 (5), 1501–1511. <https://doi.org/10.1002/hep.23144>.



- (32) Montenegro, C. F.; Casali, B. C.; Lino, R. L. B.; Pachane, B. C.; Santos, P. K.; Horwitz, A. R.; Selistre-De-Araujo, H. S.; Lamers, M. L. Inhibition of Av $\beta$ 3 Integrin Induces Loss of Cell Directionality of Oral Squamous Carcinoma Cells (OSCC). *PLoS One* **2017**, *12* (4). <https://doi.org/10.1371/journal.pone.0176226>.
- (33) Wong, S.; Guo, W.-H.; Wang, Y.-L. Fibroblasts Probe Substrate Rigidity with Filopodia Extensions before Occupying an Area. *Proc Natl Acad Sci U S A* **2014**, *111* (48), 1–6. <https://doi.org/10.1073/pnas.1412285111>.
- (34) Leask, A. Integrin B1: A Mechanosignaling Sensor Essential for Connective Tissue Deposition by Fibroblasts. *Adv Wound Care (New Rochelle)* **2013**, *2* (4), 160–166. <https://doi.org/10.1089/wound.2012.0365>.
- (35) Noskovicova, N.; Schuster, R.; van Putten, S.; Ezzo, M.; Koehler, A.; Boo, S.; Coelho, N. M.; Griggs, D.; Ruminski, P.; McCulloch, C. A.; Hinz, B. Suppression of the Fibrotic Encapsulation of Silicone Implants by Inhibiting the Mechanical Activation of Pro-Fibrotic TGF- $\beta$ . *Nat Biomed Eng* **2021**, *5* (12), 1437–1456. <https://doi.org/10.1038/s41551-021-00722-z>.
- (36) Zamir, E.; Katz, M.; Posen, Y.; Erez, N.; Yamada, K. M.; Katz, B.-Z.; Lin, S.; Lin, D. C.; Bershadsky, A.; Kam, Z.; Geiger, B. *Dynamics and Segregation of Cell-Matrix Adhesions in Cultured Fibroblasts*; 2000; Vol. 2. [www.nature.com/ncb](http://www.nature.com/ncb).
- (37) Danen, E. H. J.; Sonneveld, P.; Brakebusch, C.; Fässler, R.; Sonnenberg, A. The Fibronectin-Binding Integrins A $\beta$ 1 and Av $\beta$ 3 Differentially Modulate RhoA-GTP Loading, Organization of Cell Matrix Adhesions, and Fibronectin Fibrillogenesis. *Journal of Cell Biology* **2002**, *159* (6), 1071–1086. <https://doi.org/10.1083/jcb.200205014>.
- (38) Noskovicova, N.; Hinz, B.; Pakshir, P. Implant Fibrosis and the Underappreciated Role of Myofibroblasts in the Foreign Body Reaction. *Cells*. MDPI July 1, 2021. <https://doi.org/10.3390/cells10071794>.

- (39) Witherel, C. E.; Abebayehu, D.; Barker, T. H.; Spiller, K. L. Macrophage and Fibroblast Interactions in Biomaterial-Mediated Fibrosis. *Advanced Healthcare Materials*. Wiley-VCH Verlag February 21, 2019. <https://doi.org/10.1002/adhm.201801451>.
- (40) Robotti, F.; Sterner, I.; Bottan, S.; Monné Rodríguez, J. M.; Pellegrini, G.; Schmidt, T.; Falk, V.; Poulikakos, D.; Ferrari, A.; Starck, C. Microengineered Biosynthesized Cellulose as Anti-Fibrotic in Vivo Protection for Cardiac Implantable Electronic Devices. *Biomaterials* **2020**, 229. <https://doi.org/10.1016/j.biomaterials.2019.119583>.

### 3 Comparison of human dermal and gingival fibroblast behaviour in response to varying elastic modulus. <sup>2</sup>

#### 3.1 Introduction

Cell morphology, migration, maturation, gene expression and adhesion formation have all been demonstrated to be affected by the elastic modulus of their culture substrata, irrespective of whether it represents a biomaterial or the extracellular matrix <sup>1-3</sup>. For example, alterations in elastic moduli are very well characterized in soft connective tissue wound healing, where resident fibroblast populations are forced to interpret and respond to constantly changing tissue stiffness in developing granulation tissue <sup>4</sup>.

In response to soft tissue injury, the wound healing process is initiated to repair the defect, beginning with clot formation, secretion of granulation tissue and in the case of skin, deposition of collagen dense scar tissue, all of which change tissue compliance from 10 – 1000 Pa, 18.5 kPa and ~80 kPa, respectively <sup>4-8</sup>. A wide range of elastic moduli is also present within the varying tissues of the body as well as in physiological conditions (healthy vs pathological) which potentially alter a cell's intrinsic response to such physical environments. For example, the alveolar bone, which supports and attaches to gingival connective tissue, possesses an elastic modulus of 12.7 GPa <sup>9</sup>, but in comparison, the tissues underlying the dermis possess an elastic modulus of only 100 – 400 kPa <sup>5,10,11</sup>. Analysis of cell physiology on surfaces of comparable elastic modulus has the potential to define mechanistic and physiological differences between human dermal and gingival cell populations. However, how the substratum mechanical property of elastic modulus differentially affects human dermal and gingival fibroblast physiology has never been directly compared.

Many aspects of cell behaviour, structure and human health are affected by the transmission of substratum linked mechanical load, imposed by elastic modulus, and

---

<sup>2</sup> A version of this chapter is being prepared for submission to American Journal of Physiology: Cell Physiology special issue "Decoding Fibrosis". Guest Editor: Dr Liliana Schaefer, Goethe University, Frankfurt, Germany.

detected in cells through their adhesion complexes <sup>12</sup>. In a process known as durotaxis, cells have a propensity to migrate toward stiffer substrata <sup>1</sup>. With increased elastic modulus, cell morphology becomes broader, and flatter and growth is most optimal when the substratum elasticity matched to the cells' intrinsic elasticity <sup>13</sup>. Additionally, through haptotaxis, cells migrate and attach to substrata with optimal adhesive properties which is influenced by the substratum surface elastic modulus <sup>14</sup>. Increasing our understanding of intrinsic cell properties and how cell origin impacts on healing can be utilized to alter physical and mechanical characteristics and optimize biomaterial design.

Previous research on dermal fibroblasts has shown that substratum elastic modulus regulates several aspects of cell physiology <sup>1,15</sup>. Gingival fibroblasts, however, are a cell population that remains uninvestigated. Gingiva exhibits a more regenerative wound healing capacity in comparison with skin which typically scars <sup>16</sup>. Direct comparison of human dermal and gingival fibroblasts therefore represents a logical method to investigate cellular mechanisms underlying scar formation versus tissue regeneration. The aim of this chapter was to investigate mechanistic differences in the induction of a wound healing/pro-fibrotic phenotype in fibroblasts of different origin and to quantify the role of elastic moduli in modulation of phenotype. An increase of substratum elastic modulus is hypothesized to increase cellular adhesion, proliferation, extracellular matrix production, and cell contractility. Specifically, comparative studies on adhesion assembly, integrin engagement, cytoskeleton structure, extracellular matrix secretion, proliferation, and signaling pathway activation of human dermal and gingival fibroblasts changes with varying elastic moduli were performed.

## 3.2 Materials and Methods

### 3.2.1 Dermal and gingival fibroblast isolation and culture

Isolation and experimental use of cells derived from human tissue were approved by the Western University Review Board for Health Sciences Research Involving Human Subjects and were in accordance with the 1964 Declaration of Helsinki. Human dermal fibroblasts (HDF) were isolated from skin removed under informed consent from patients

undergoing elective lower limb amputation at Victoria Hospital, London, Ontario. Human gingival fibroblasts (HGF) were isolated from patients undergoing elective periodontal procedures in the Oral Surgery Clinic at the Schulich School of Medicine and Dentistry, University of Western Ontario, London, Ontario. Human dermal and gingival fibroblast populations, each from 3 different patients, were used up to passage 6 and were maintained in Dulbecco's Modified Eagle Medium (DMEM; Thermo Fisher Scientific, Burlington, ON, Canada) supplemented with 10% fetal bovine serum (FBS) (Gibco Life Technologies, Burlington, ON, Canada) and 1% antibiotics and antimycotic (AA) solution (Gibco Life Technologies, Burlington, ON, Canada) in a humidified environment at 37°C, 5% CO<sub>2</sub>. Media is changed every 2 – 3 days. Prior to experimental use, the cells were incubated with serum free, high glucose DMEM supplemented with 1% antibiotics and antimycotic and maintained in a humidified environment at 37 °C, 5% CO<sub>2</sub> for 24 hr.

### 3.2.2 Varied elastic modulus substratum cell culture

Our study utilized prefabricated Cytosoft matrices, fabricated by silicone of elastic moduli 64 kPa, 8 kPa, and 0.2 kPa (Advanced Biomatrix Inc., San Diego, CA, United States) as well as control tissue culture plastic 6-well plates (VWR International, Mississauga, ON, Canada). Each surface was prepared for cell culture according to the Advanced Biomatrix Cytosoft 6 well plate preparation protocol. Each well was coated with 100 µg/mL PureCol Type I (Advanced Biomatrix Inc., San Diego, CA, United States) in Dulbecco's Phosphate Buffered Saline (dPBS). Wells were seeded with 5 000 cells/cm<sup>2</sup> and flooded with 2.5 mL high glucose DMEM containing 10% FBS and 1% AA. When indicated, transforming growth factor β1 (TGF-β1) (240-B/CF, R&D Systems, Minneapolis, MN, USA) treatment was added daily to the cell culture at a concentration of 5 ng/mL.

### 3.2.3 Adhesion and proliferation quantification

HDF and HGF attachment 1 h post seeding, and proliferation at 3- and 7-days post seeding was quantified using the CyQUANT assay (Thermo Fisher C7026).

### 3.2.4 Immunofluorescent labelling

Fibroblast structure was identified by F-actin (rhodamine phalloidin R415; Life Technologies),  $\alpha$ -smooth muscle actin (Sigma Aldrich A5228) and nuclei (Hoechst H3570 Invitrogen). Adhesion sites were identified by vinculin (focal adhesions; Millipore MAB3574), and tensin-1 (fibrillar adhesions; Novus biologicals NBP1-84129). Primary extracellular matrix protein was identified by fibronectin (Abcam Ab1954). Cells were then imaged upon a Zeiss Axio Imager M2.m fluorescence microscope under water immersion.

### 3.2.5 Western Blot

SDS-Page gel electrophoresis and Western blotting was performed as described by Abcam (Cambridge, United Kingdom) utilizing 4-20% gradient gels (Bio-Rad 4561093). Protein bands identified for  $\alpha$ -smooth muscle actin (Sigma Aldrich A5228) and vinculin (Millipore MAB3574) were normalized to GAPDH (Millipore MAB374).

### 3.2.6 Analysis of underlying mechanotransduction signalling pathways

A proteome profiler for human phospho-kinases (ARY003C, R&D Systems, Minneapolis, MN, USA) was used to quantify the activity of 43 different human kinases upon three independent HDF and HGF populations. Cells were seeded in collagen coated TCP, 64 kPa, 8 kPa and 0.2 kPa elastic moduli plates at a density of 16 000 cells/cm<sup>2</sup> and incubated under normal cell culture conditions for 24 hours. The assay was run according to the manufacturer's protocol with 50  $\mu$ g of total protein per assay.

### 3.2.7 Statistical analysis

In all experiments, 3 separate lines of HDFs and HGFs isolated from different individuals were used. The quantification of adhesion sites for quantity and size was made from a minimum of 10 cells per experiment from 3 different lines. Results were entered into a statistics software (Graphpad Software v.5, La Jolla, CA, USA) for one-way ANOVA, followed by a Bonferroni correction or Tukey post-test for multiple comparisons. For all statistical analyses,  $p \leq 0.05$  was considered significant.

## 3.3 Results

### 3.3.1 HDFs and HGFs exhibit differential adhesion and proliferation on surfaces of differing elastic modulus

Initial adhesion of HDF and HGF populations to surfaces of varying elastic moduli were quantified following a 1 h incubation (Figure 3-1). Dermal fibroblast adhesion on 64 kPa and 0.2 kPa elastic moduli surfaces significantly increased compared to tissue culture plastic surfaces ( $N = 3$ ,  $n = 5$ , two-way ANOVA, Tukey post-test for multiple comparisons,  $p < 0.05$ ). Human gingival fibroblasts demonstrated a greater adhesion to the 8 kPa elastic modulus surface following 1 h of incubation compared to tissue culture plastic ( $N = 3$ ,  $n = 5$ , two-way ANOVA, Tukey post-test for multiple comparisons,  $p < 0.05$ ). Following this, HDF and HGF proliferation was quantified through calculation of fold increase relative to cells seeded on day 0. The greatest increase in cell number was observed on 8 kPa elastic modulus surface following 7 days in cell culture for both HDF and HGF cultures ( $N = 3$ ,  $n = 2$ , ANOVA, Tukey post-test for multiple comparisons,  $p < 0.05$ ) (Figure 3-2).

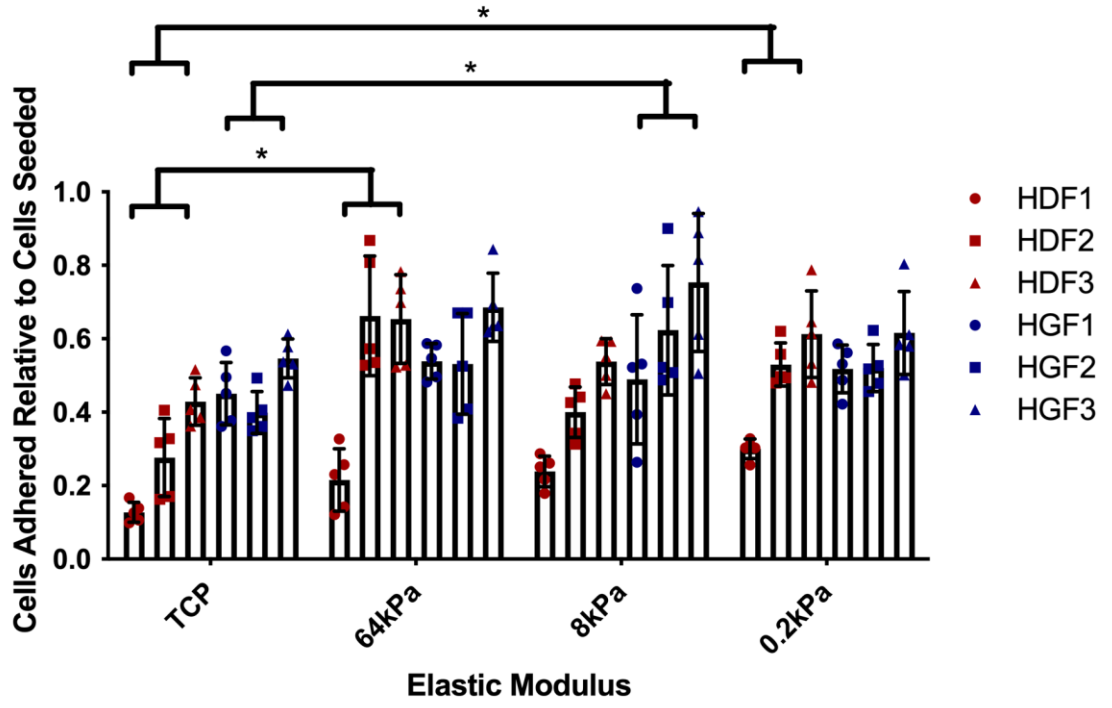




**Figure 3-1: HDF and HGF adhesion if effected by substratum elastic modulus**

Cells adhered relative to cells seeded vs elastic modulus for HDF and HGF at 64 kPa, 8 kPa and 0.2 kPa and on TCP following a 1 h incubation period. N = 3, n = 5, two-way ANOVA, Tukey post-test for multiple comparisons, \*  $p < 0.05$ .

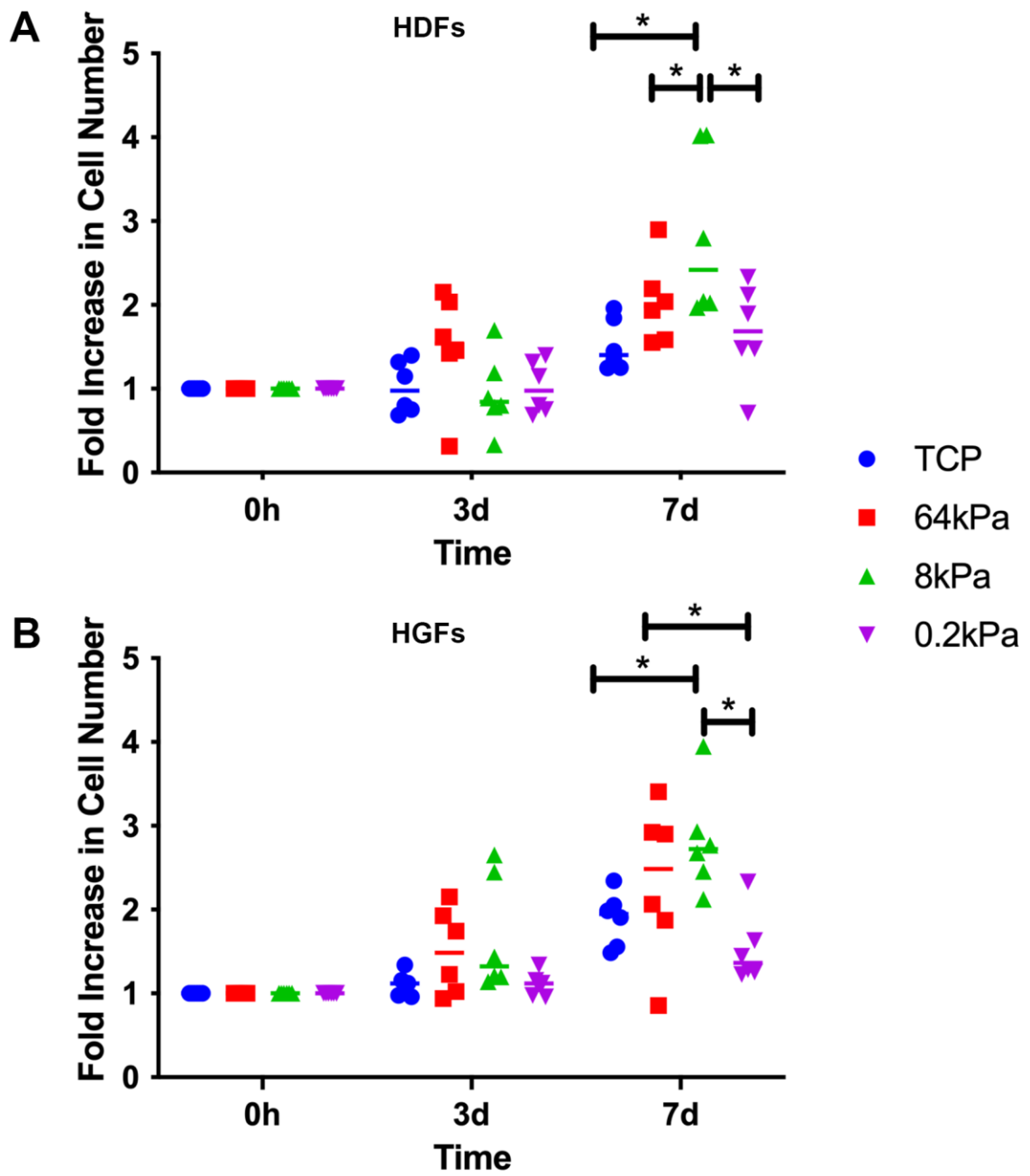


**Figure 3-2: HDF and HGF proliferation increases upon surfaces of low elastic moduli**

(A) HDF and (B) HGF cell proliferation (fold increase) upon cell culture surfaces of various elastic moduli at day 0, 3 and 7 post seeding. Cells were maintained under normal cell culture conditions with media changed every 3 days. All cell lines were normalized individually to day 0 of quantification. N = 3, n = 2, ANOVA, Tukey post-test for multiple comparisons \*  $p < 0.05$ .

### 3.3.2 HDF and HGF focal and fibrillar adhesion associated protein localization is altered by varying surface elastic modulus

Immunocytochemistry was performed for the focal adhesion associated protein, vinculin and the cytoskeletal component F-actin in both HDFs (Figure 3-3) and HGFs (Figure 3-4) on surfaces of 0.2, 8 and 64 kPa as well as on TCP. Both HDF and HGFs exhibited F-actin stress fibers on the TCP surface compared to cells cultured on lower elastic modulus surfaces. With an increase in surface elastic modulus, HDF and HGF demonstrated fewer vinculin associated focal adhesions (Figure 3-7A), however these adhesion sites had a greater area than those in cells on the 0.2 kPa elastic modulus surface (Figure 3-7B). The western blot quantification of vinculin protein expression was unchanged across all investigated surfaces by both HDFs and HGFs and did not increase irrespective of substratum compliance (Figure 3-5).

To evaluate fibrillar adhesion sites, immunocytochemistry with antibodies specific for tensin-1 in HDFs and HGFs on surfaces of 0.2, 8 and 64 kPa as well as TCP was performed (Figure 3-6). The highest number of tensin-1 associated fibrillar adhesions were evident in cells on culture substrata with an elastic modulus of 8 kPa (Figure 3-7C). The average fibrillar adhesion area was greatest upon the TCP control surface in both the HDF and HGF populations (Figure 3-7D).

As recruitment of vinculin and tensin-1 is associated with focal and fibrillar adhesion formation respectively, the next evaluation was the recruitment of integrin  $\alpha\beta3$  with vinculin and integrin  $\beta1$  with tensin-1, respectively (Figure 3-8). Integrin  $\alpha\beta3$  was observed to strongly co-localize with vinculin on TCP and 8 kPa surfaces in both HDF and HGFs. However, co-localization was attenuated on the 0.2 kPa elastic modulus surface with reduced integrin  $\alpha\beta3$  co-localization with vinculin observed in both HDFs and HGFs. In HDFs, integrin  $\beta1$  is abundant and ubiquitous, with strong tensin-1 co-localization in the center of the cell on all surfaces. Interestingly on 0.2 kPa, HDFs made prominent integrin  $\beta1$  associated filopodia which are not associated with tensin-1 (Figure 3-8). In HGFs on 0.2 kPa, while localized to adhesion sites, integrin  $\beta1$  does not associate with tensin-1 even in the central area of the cells. In general, integrin  $\beta1$ /tensin-1

associated adhesion sites are fewer in HGFs in comparison with HDFs, particularly on TCP (Figure 3-8).

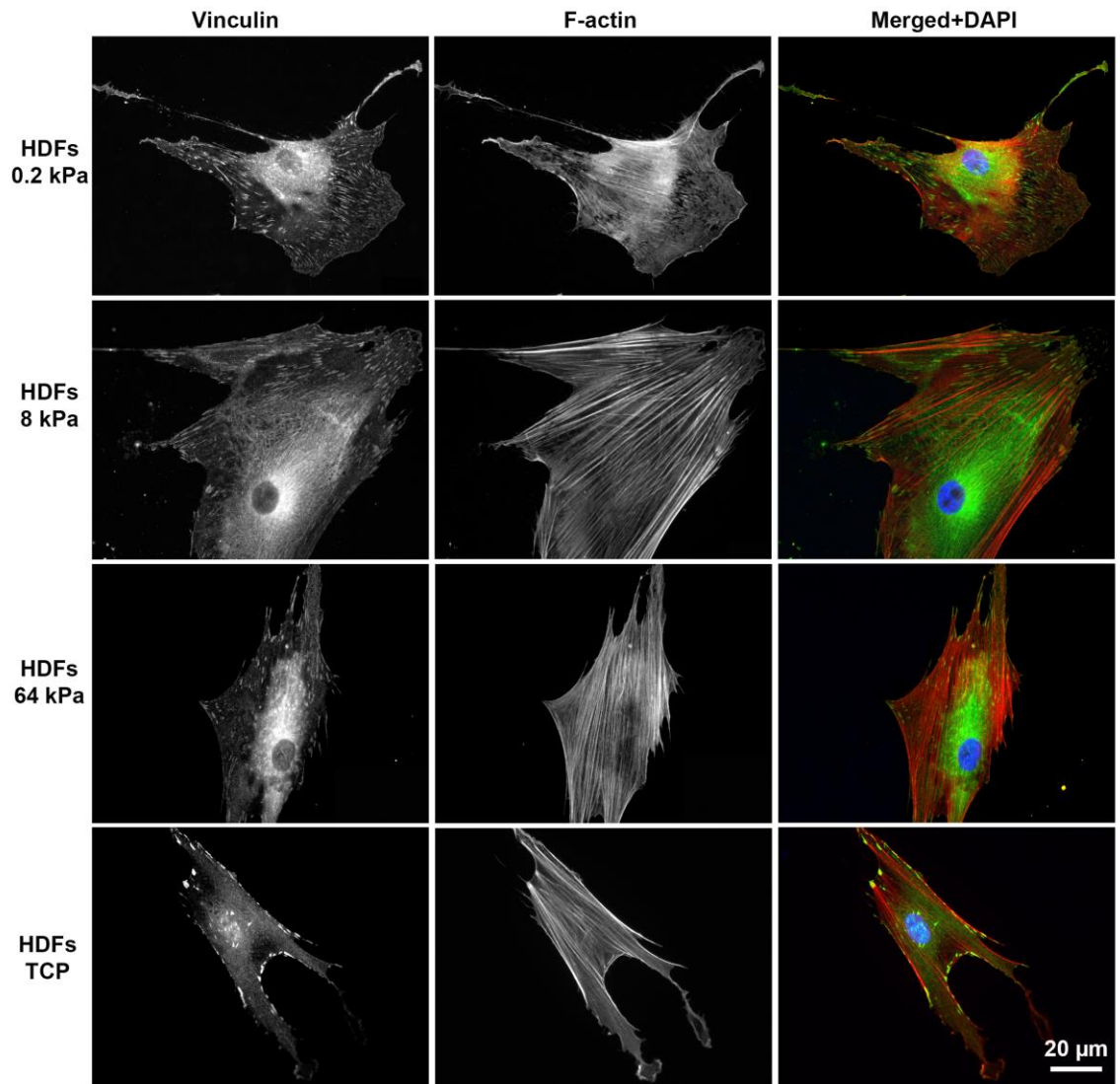


**Figure 3-3: A substratum of 0.2 kPa elastic modulus inhibits HDF F-actin stress fiber formation**

HDFs stained for adhesion protein, vinculin (green), and cytoskeleton component, f-actin (red), upon surfaces of various elastic moduli (64kPa, 8kPa and 0.2kPa) and traditional tissue culture plastic as a control. Micrographs were established under water immersion, 40X magnification. Fibroblasts were incubated for 24 h and labelled with Hoechst for nuclei identification (blue). Scale bar: 20 $\mu$ m.

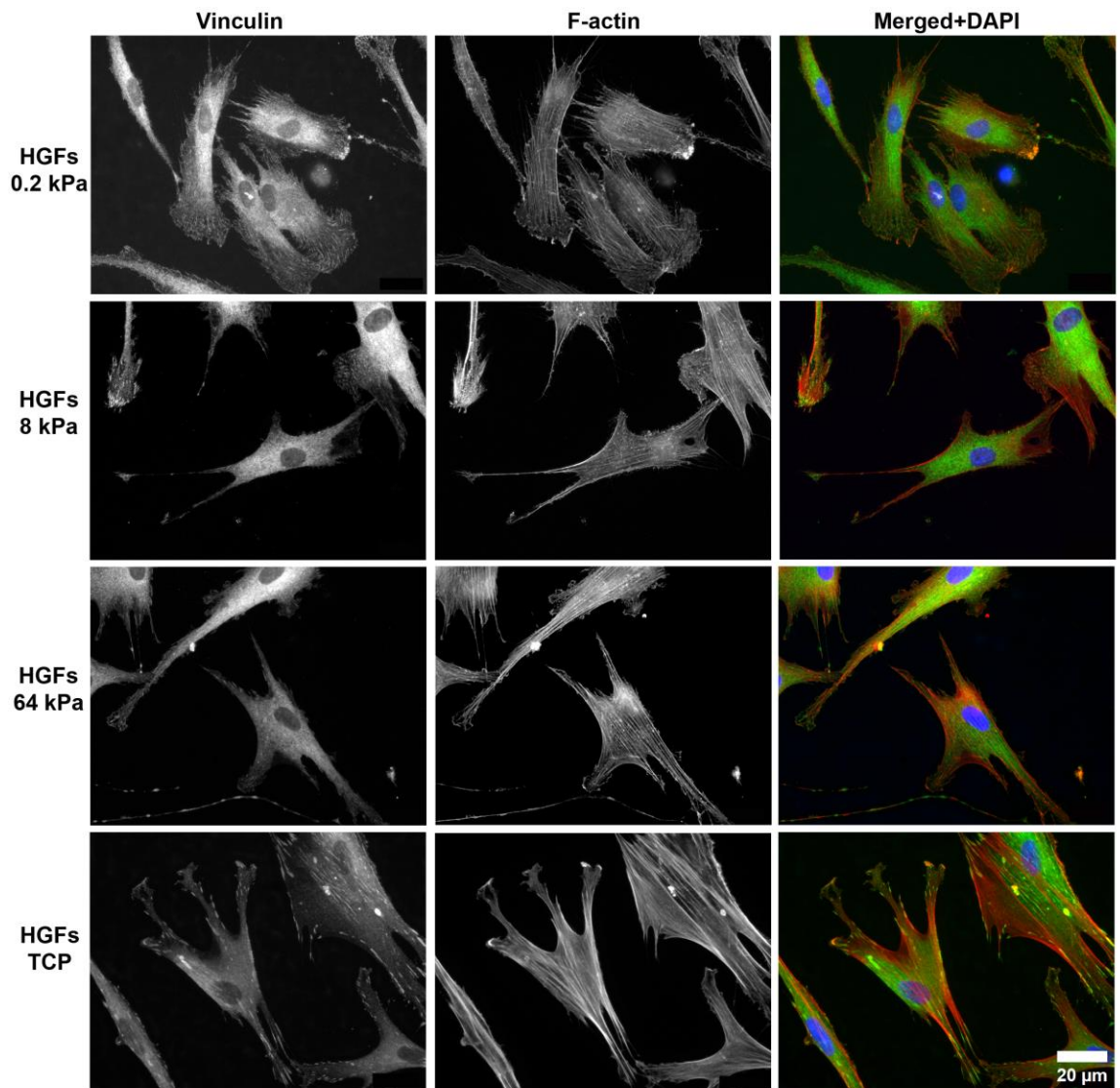




**Figure 3-4: Substrata of low elastic modulus inhibit HGF F-actin stress fiber formation.**

HGFs stained for adhesion protein, vinculin (green), and cytoskeleton component, f-actin (red), upon surfaces of various elastic moduli (64kPa, 8kPa and 0.2kPa) and traditional tissue culture plastic as a control. Micrographs were established under water immersion, 40X magnification. Fibroblasts were incubated for 24 hours and labelled with Hoechst for nuclei identification (blue). Scale bar: 20 $\mu$ m.

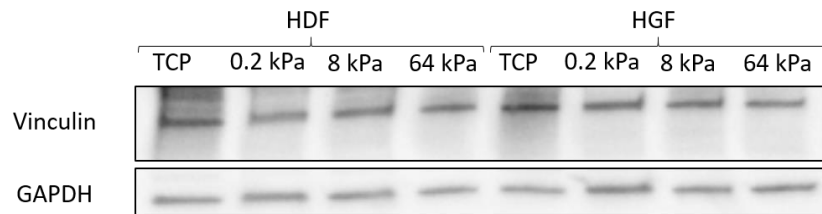
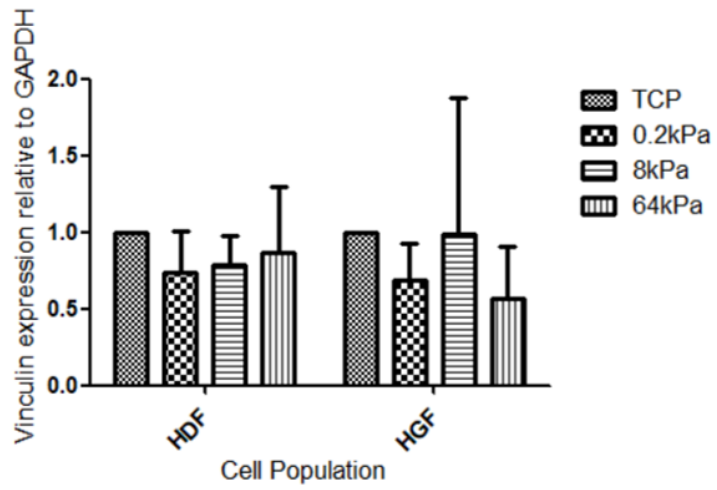


**Figure 3-5: HDF and HGF vinculin protein expression is unchanged by substratum elastic modulus**

HDF and HGF vinculin protein expression quantified through western blot analysis upon surfaces of varying elastic moduli (64 kPa, 8 kPa and 0.2 kPa) following a 24 h incubation period. N = 3. ANOVA, Tukey post-test for multiple comparisons, \*  $p < 0.05$ .

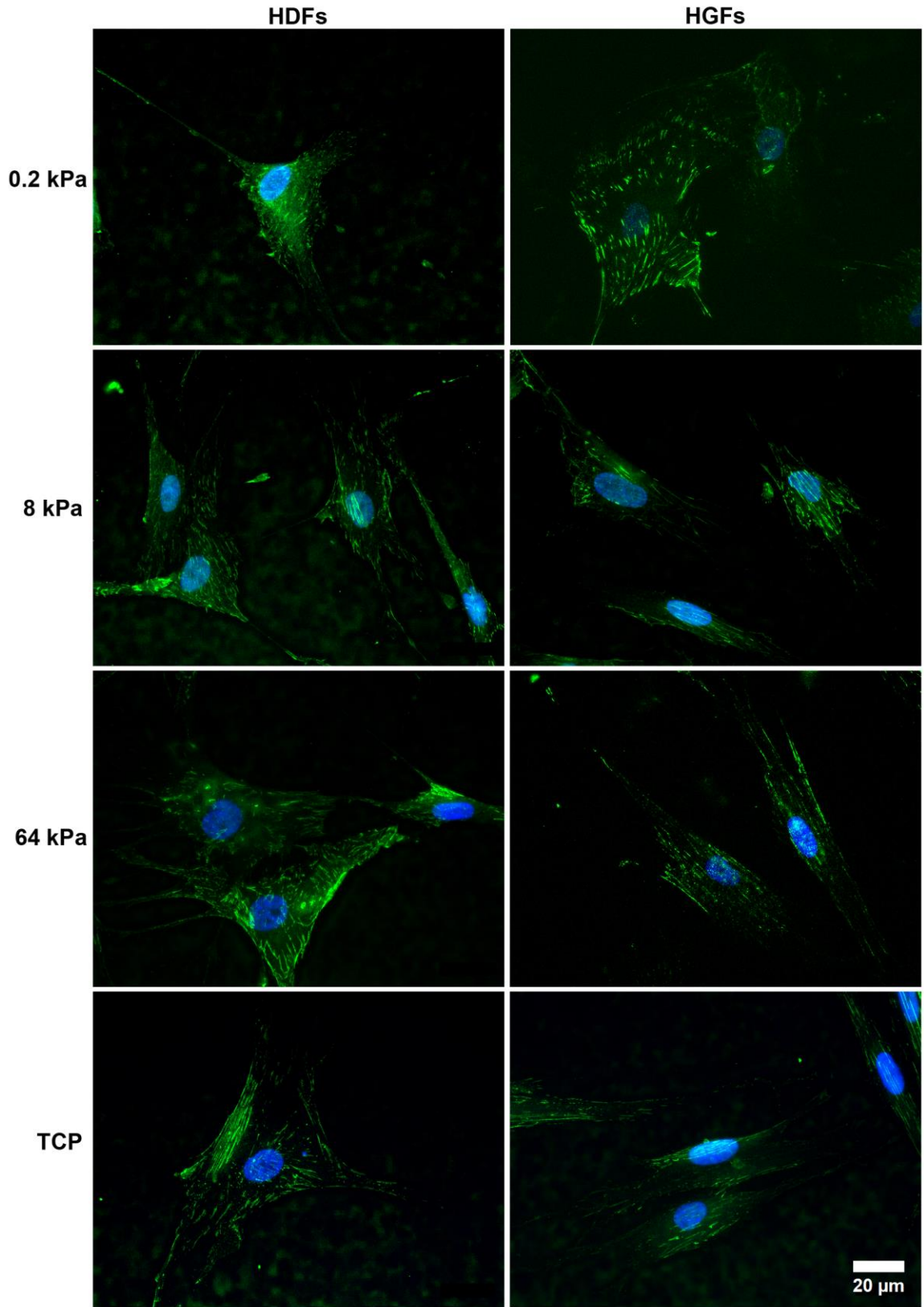


**Figure 3-6: HDF and HGF tensin-1 expression is centrally located upon TCP**

Immunocytochemistry of HDF and HGFs upon surfaces of varying elastic moduli for fibrillar adhesion marker tensin-1 (green) and nuclei (blue) following a 24 h incubation period. Scale: 20 $\mu$ m; Magnification 40X water immersion; N = 3, n = 10.

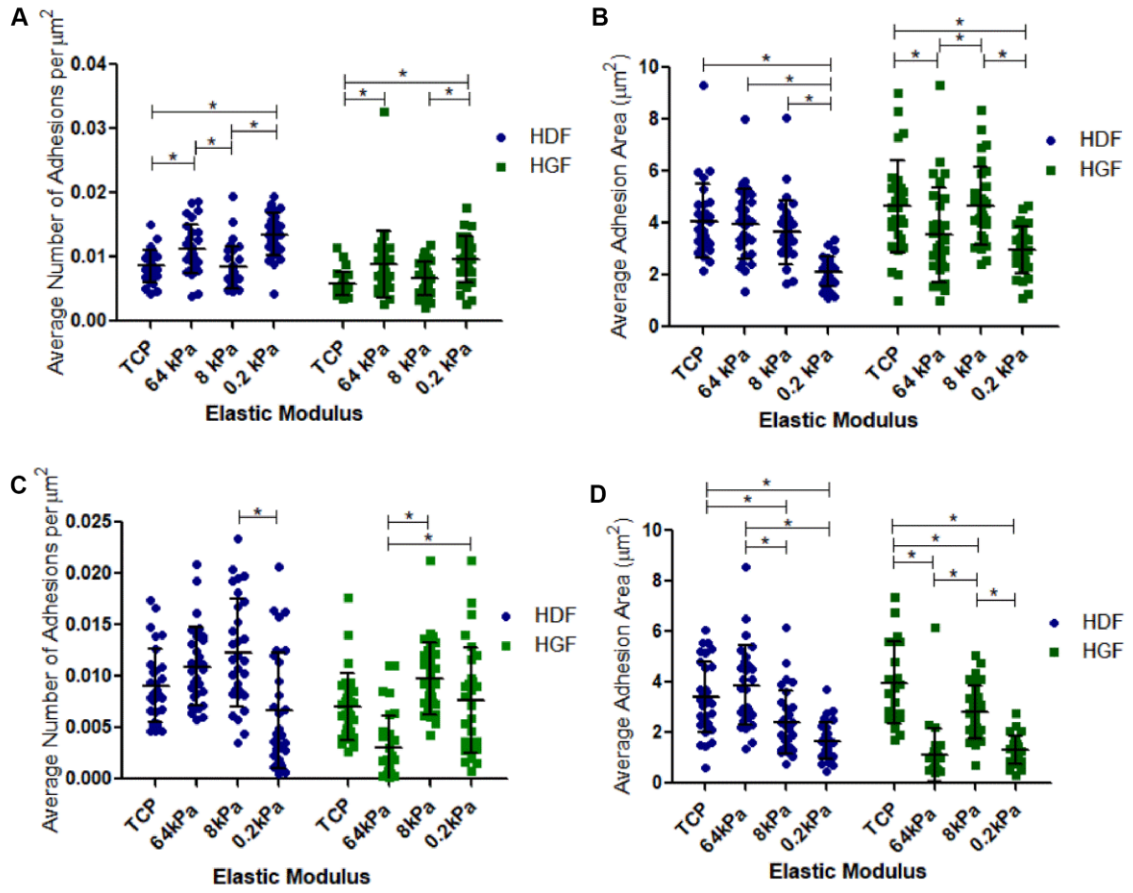


**Figure 3-7: HDF and HGF focal and fibrillar adhesion quantity and area is dependent upon substratum elastic modulus**

Average number of (A) focal adhesions and (C) fibrillar adhesions, normalized to planar cell area and the average adhesion area of (B) focal adhesions and (D) fibrillar adhesions were identified via vinculin and tensin-1 immunocytochemistry, respectively, upon surfaces of various elastic moduli. Micrographs of adhesion sites were obtained 24 h post seeding, under 20X magnification and quantified through image J software. HDF: blue. HGF: green. N = 3, n = 10, ANOVA, Bonferroni post-test, \*  $p < 0.05$ .

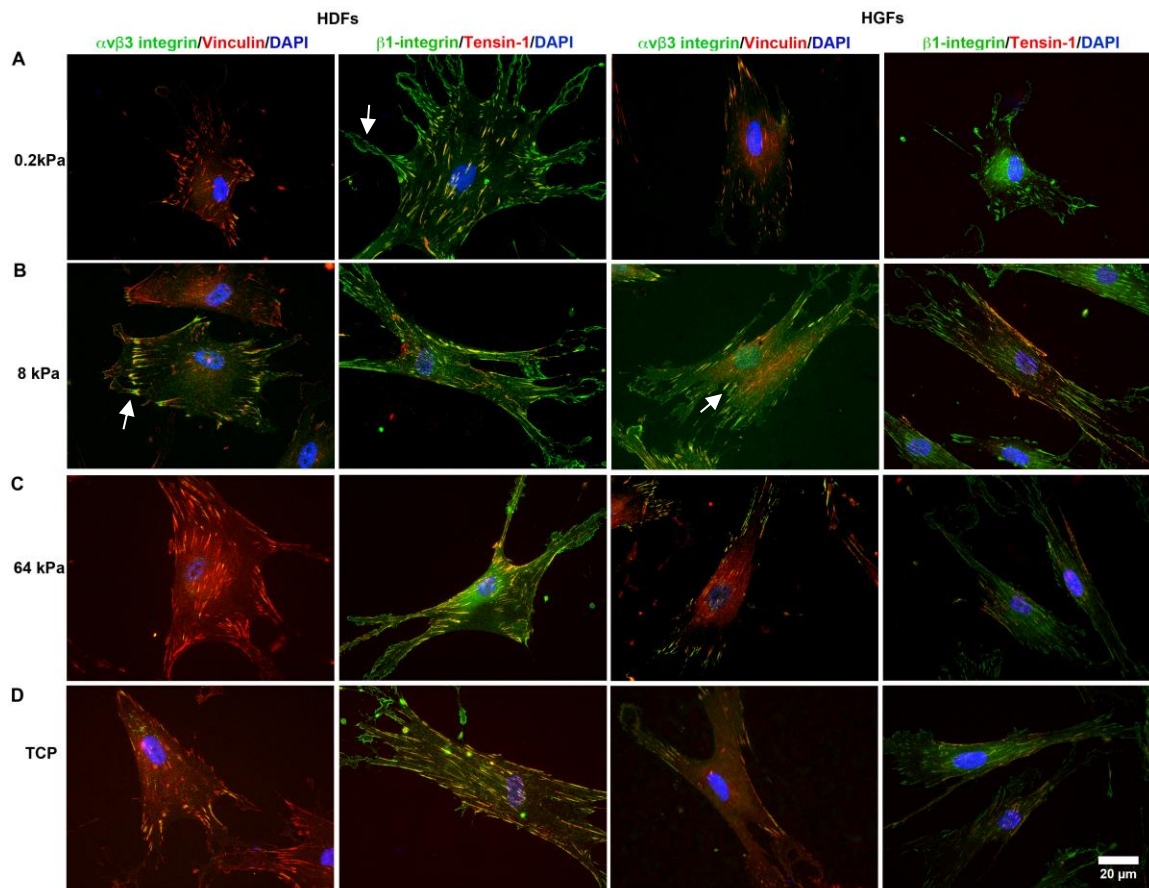




**Figure 3-8: HDF and HGF focal and fibrillar adhesions decrease in size upon substrata of low elastic modulus**

Immunocytochemistry of HDFs and HGFs upon surfaces of varying elastic moduli for focal adhesion markers vinculin (red) and integrin  $\alpha\beta3$  (green) and fibrillar adhesion markers tensin-1 (red) and integrin  $\beta1$  (green). White arrows indicate co-localization of vinculin and integrin  $\alpha\beta3$  upon the 8 kPa elastic modulus surface in both HDFs and HGFs. The localization of integrin  $\beta1$  in the periphery of the cell is also indicated by white arrows upon the 0.2 kPa elastic modulus surface within the HDF population. Nuclei (blue) are stained with Hoechst. Scale: 20  $\mu\text{m}$ ; Magnification 20X; N = 3, n = 10.

### 3.3.3 Extracellular matrix is differentially deposited upon surfaces of varying elastic modulus

To assess extracellular matrix production on surfaces of varying elastic moduli, immunocytochemistry for fibronectin was performed on HDF and HGF populations, with cytoskeletal component F-actin used to observe cell morphology. Fibronectin synthesis was assessed after 24 h (Figure 3-9) and 2 weeks (Figure 3-10). At 24 h post seeding both HDFs and HGFs deposit fibronectin on surfaces of 0.2 kPa and 8 kPa, but on 64 kPa and TCP, HDFs fibronectin immunoreactivity is restricted to the confines of the cell area. HGFs cultured on 64 kPa still secrete fibronectin, but this is attenuated on TCP similar to HDFs (Figure 3-9). After 2 weeks of culture, cells cultured on all experimental and control surfaces have established a fibrillar fibronectin matrix on the culture surfaces (Figure 3-10). Neither HDFs nor HGFs, form a confluent single cell layer on the 0.2 kPa elastic modulus surface, although all regions of cells are fibronectin dense. In general, HDFs secrete higher amounts of fibronectin than HGFs on 8 kPa, 64 kPa and TCP, with both cell populations establishing confluent cell layers.

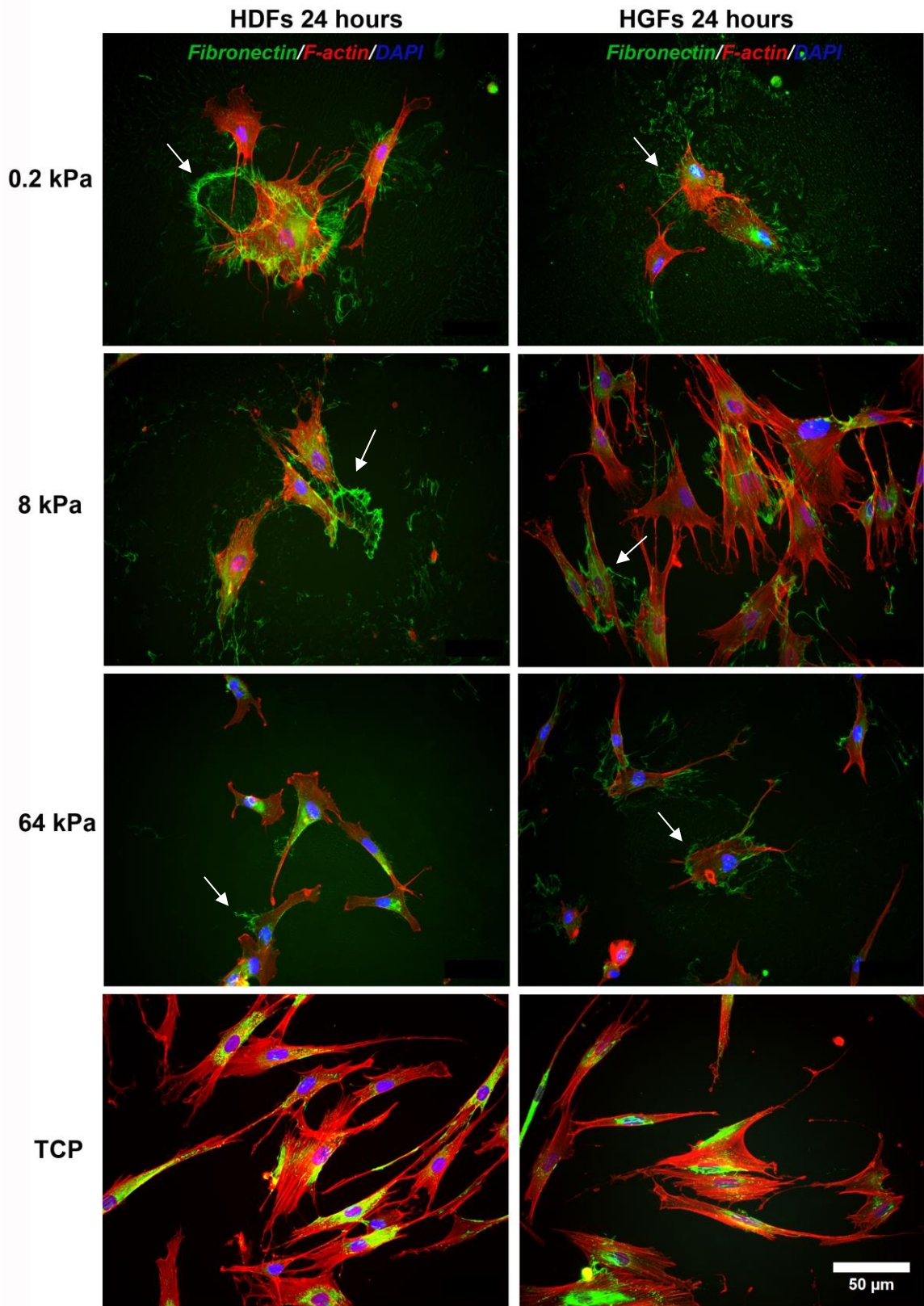


**Figure 3-9: HDF and HGF quickly establish fibronectin fibrils upon low elastic modulus surfaces**

HDFs (left) and HGFs (right) stained for extracellular matrix protein, fibronectin (green), and cytoskeleton component, F-actin (red), upon surfaces of various elastic moduli and TCP. White arrows indicate regions of extracellular fibronectin fibril formation. Micrographs established under water immersion, 20X magnification. Fibroblasts were incubated for 24 h. Cells were labelled with Hoechst for nuclei (blue) identification. Scale: 50  $\mu\text{m}$ ; N = 3.

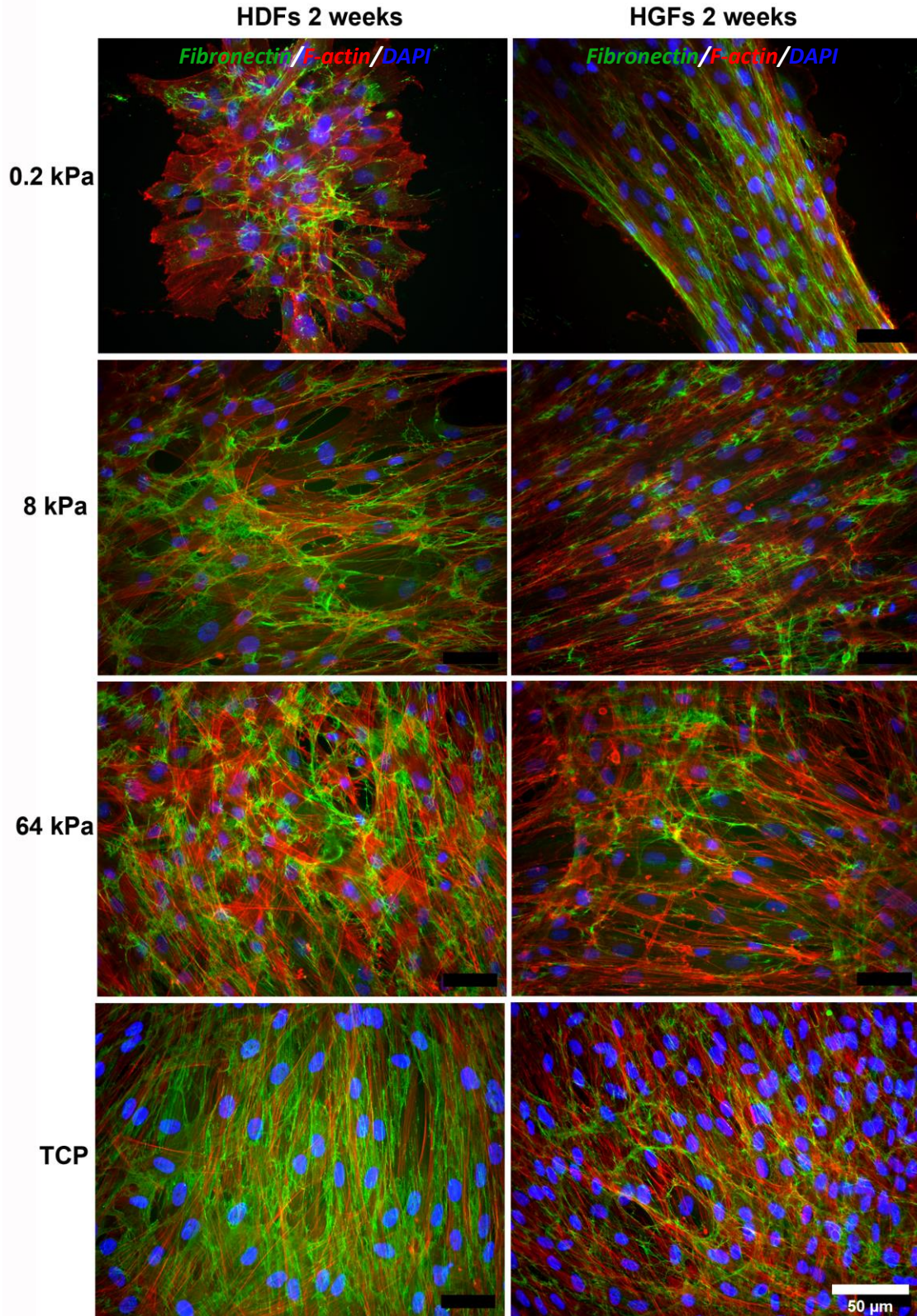


**Figure 3-10: A substrate elastic modulus of 0.2 kPa inhibits HDF and HGF extracellular matrix production following 2 weeks**

HDFs (left) and HGFs (right) labelled for extracellular matrix protein, fibronectin (green), and cytoskeleton component, F-actin (red), upon surfaces of various elastic modulus. Micrographs established under water immersion, 20X magnification. Fibroblasts were incubated for 14 days with media changes every 3 days. Cells were labelled with Hoechst for nuclei (blue) identification. Scale: 50  $\mu\text{m}$ ; N = 3.

### 3.3.4 HDF and HGF are capable of myofibroblast differentiation in a manner dependent on elastic modulus.

The hallmark characteristic of the myofibroblast is incorporation of  $\alpha$ -smooth muscle actin into F-actin stress fibre bundles<sup>17</sup>. In the next experiments, immunocytochemistry for  $\alpha$ -smooth muscle actin, and F-actin were performed on HDF (Figure 3-11) and HGF (Figure 3-12) on 0.2, 8, 64 kPa and TCP for 1, 3, and 5 days of culturing. As  $\alpha$ -smooth muscle actin expression is dependent on TGF- $\beta$ 1 as well as substratum stiffness, additional replicates were completed where HDF and HGF populations were incubated with 5 ng/mL TGF $\beta$ 1 treatment. Myofibroblast differentiation was quantified as the number of cells whose  $\alpha$ -SMA colocalized with F-actin, indicating stress fiber formation and positive myofibroblast differentiation. Western blot was performed to quantify  $\alpha$ -SMA protein expression (Figure 3-13).

In general, both HDF and HGF populations maintain the ability to differentiate into myofibroblasts irrespective of the substrata's elastic moduli (Figure 3-11 & Figure 3-12). Both HDFs and HGFs show 20% or less transition to the myofibroblast phenotype on any surface when untreated at all timepoints tested. With the addition of TGF- $\beta$ 1, there is an increase in the number of myofibroblast in HDF cultures, although this is only significant on 0.2 kPa surfaces at day 3. However, there is a significantly greater myofibroblast differentiation evident in HGFs on TCP controls compared to all other tested surfaces at all timepoints (N = 3; n = 100. RM-ANOVA; Bonferroni Post Hoc Test; \* p < 0.05) (Figure 3-12). HDF and HGF  $\alpha$ -SMA protein expression is unchanged by surface elastic modulus (Figure 3-13), except for HGF upon the 0.2 kPa elastic modulus surface, demonstrating it is the incorporation of  $\alpha$ SMA into stress fibers rather than overall expression that changes.

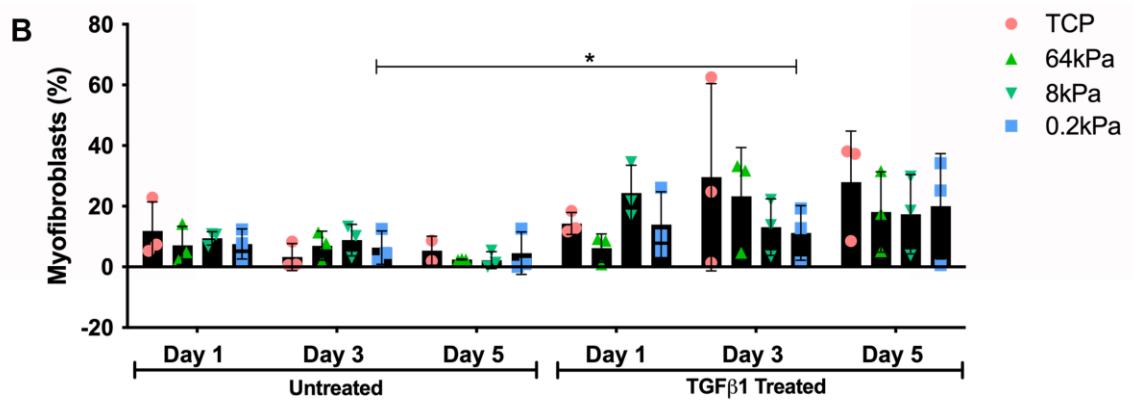
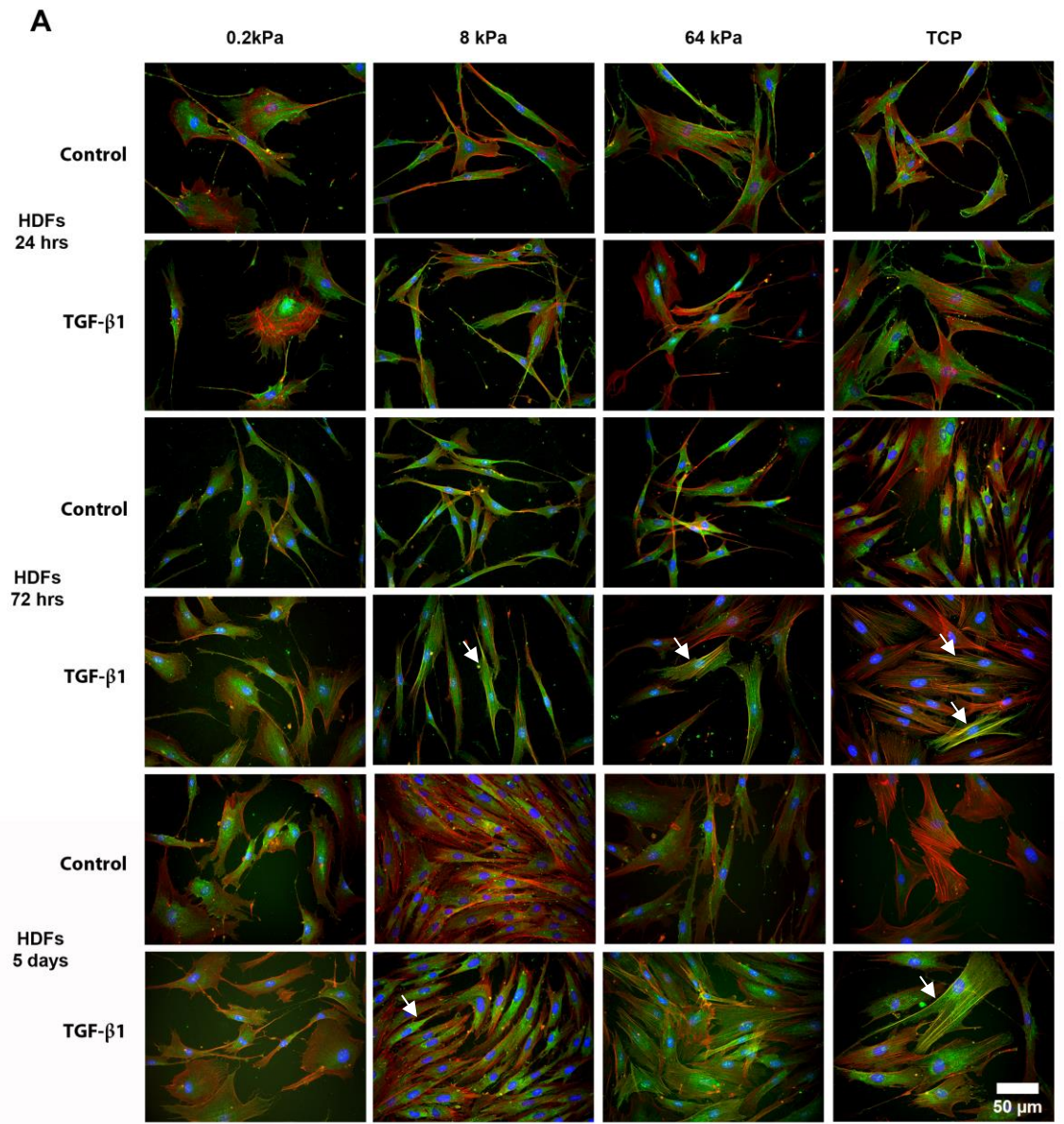




**Figure 3-11: HDF Myofibroblast differentiation is unaffected by substratum elastic modulus**

(A) HDFs stained for  $\alpha$ -SMA (green) and F-actin (red) to identify positive myofibroblast differentiation without (control) and with TGF- $\beta$ 1 treatment. Micrographs established under water immersion, 20X magnification. Fibroblasts were incubated for 1-, 3- and 5-days with or without 5 ng/mL TGF- $\beta$ 1 treatment. N = 3. Scale: 50  $\mu$ m. White arrows indicate example cells with  $\alpha$ -SMA incorporated F-actin stress fibers. (B) Quantification of human dermal fibroblast differentiation into myofibroblasts following a 1-, 3- and 5-day incubation with or without treatment of 5 ng/mL TGF $\beta$ 1. N = 3; n = 100. RM-ANOVA; Bonferroni Post Hoc Test; \* p < 0.05.

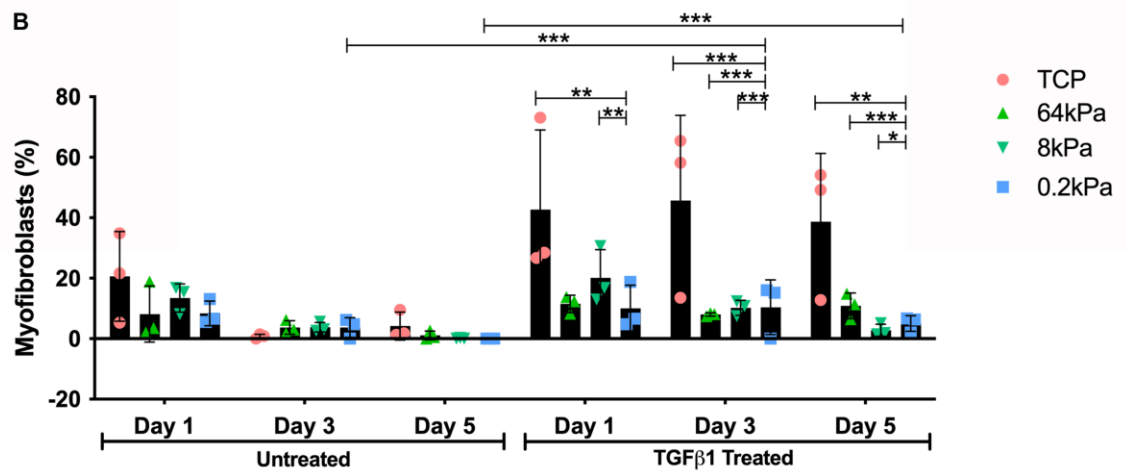
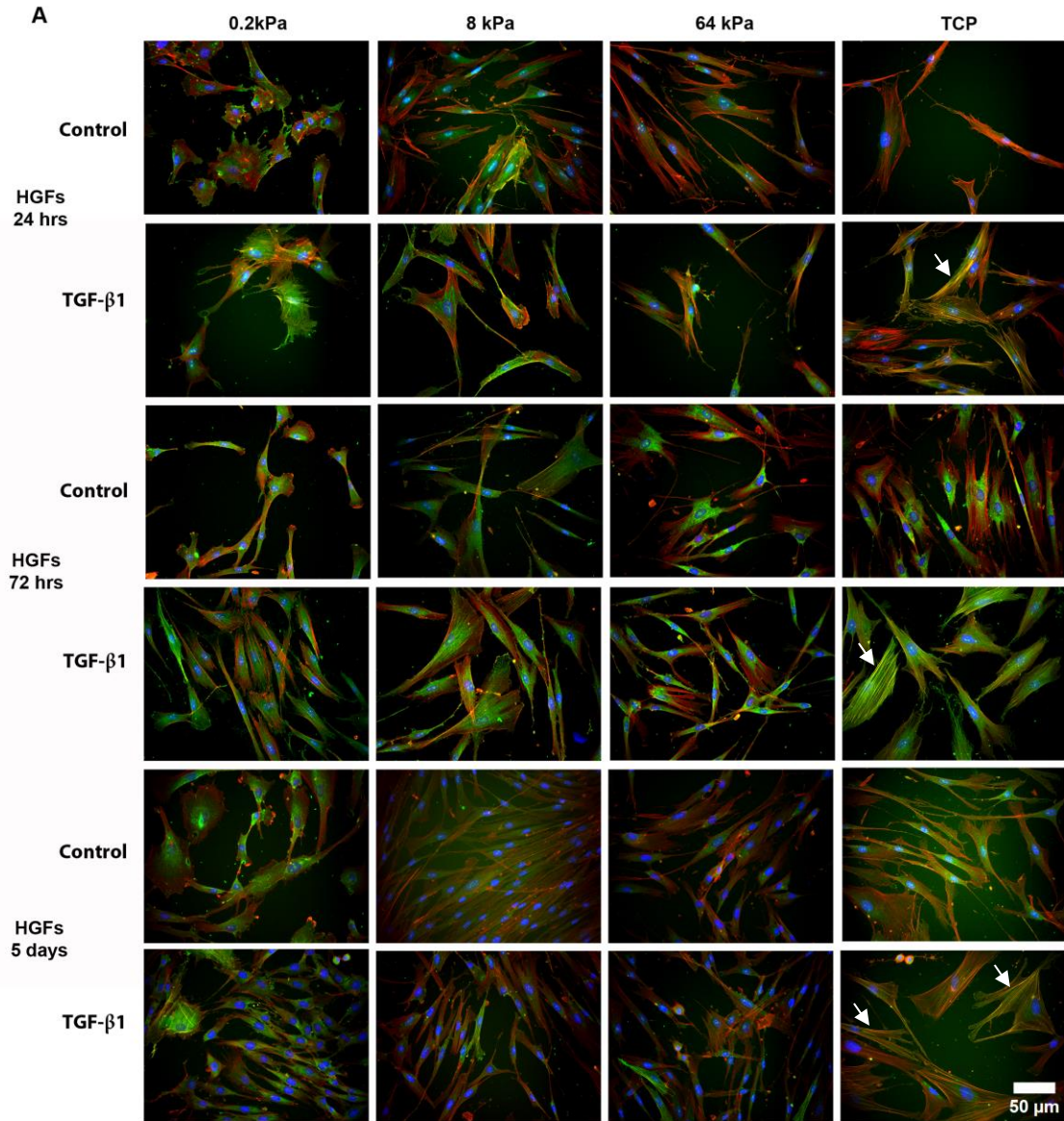


**Figure 3-12: TGF- $\beta$ 1 induces HGF myofibroblast differentiation upon TCP**

(A) HGFs stained for  $\alpha$ -SMA (green) and F-actin (red) to identify positive myofibroblast differentiation without (control) and with TGF- $\beta$ 1 treatment. Micrographs established under water immersion, 20X magnification. Fibroblasts were incubated for 1-, 3- and 5-days with or without 5 ng/mL TGF $\beta$ 1 treatment. White arrows indicate example cells with  $\alpha$ -SMA incorporated F-actin stress fibers. N = 3. Scale: 20  $\mu$ m. (B) Quantification of HGF differentiation into myofibroblasts following a 1-, 3- and 5-day incubation with or without treatment of 5 ng/mL TGF- $\beta$ 1. N = 3; n = 100. RM-ANOVA; Bonferroni Post Hoc Test; \* p < 0.05.

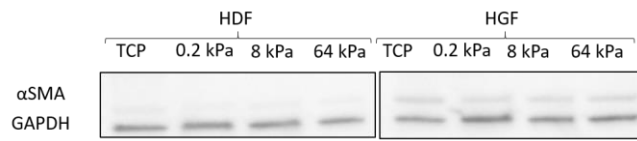
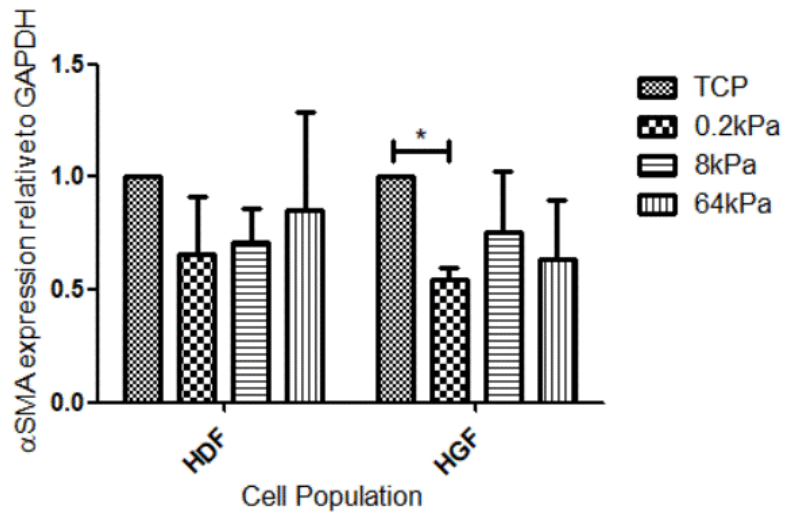


**Figure 3-13:  $\alpha$ -SMA expression by HDFs and HGFs shows minimal change by culturing on substrata of various elastic moduli**

HDF and HGF  $\alpha$ -SMA protein expression quantified through western blot analysis upon surfaces of varying elastic moduli following a 24 h incubation period. ANOVA, Tukey post-test for multiple comparisons, N = 3, \* p < 0.05.

### 3.3.5 Exogenous TGF- $\beta$ 1 treatment alters HGF adhesion composition

As HGFs showed an increased transition to myofibroblasts compared to HDFs, it was next assessed how myofibroblast differentiation of HGFs related to adhesion formation. Specifically, co-localization of tensin-1 with integrins  $\beta$ 1 and  $\alpha$ v $\beta$ 3 was performed to evaluate adhesion maturity and composition of HGFs on 0.2 kPa and TCP with no TGF- $\beta$ 1 treatment (Figure 3-14) and the exogenous addition of 5 ng/mL of TGF- $\beta$ 1 (Figure 3-15). In the absence of TGF- $\beta$ 1, on 0.2 kPa surfaces, HGFs exhibit  $\alpha$ v $\beta$ 3 in plaques at the periphery which do not localize with tensin-1 (Figure 3-14A). On TCP, HGFs exhibit larger  $\alpha$ v $\beta$ 3 plaques at the periphery, although tensin-1 localization is present. However, most tensin-1 plaques in HGFs on TCP are in the center of the cells and are more numerous than in HGFs on 0.2 kPa. These central plaques do not co-localize with  $\alpha$ v $\beta$ 3 (Figure 3-14A). With respect to  $\beta$ 1 integrins, HGFs contain many plaques throughout the cells on both 0.2 kPa and TCP (Figure 3-14B). However, on 0.2 kPa, only central  $\beta$ 1 integrin plaques co-localize with tensin-1, but in contrast, on TCP, most  $\beta$ 1 integrin adhesion sites co-localize with tensin-1 in all regions of the cells (Figure 3-14B).

With the addition of TGF-  $\beta$ 1, HGFs on the 0.2 kPa elastic modulus surface, show a loss of the  $\alpha$ v $\beta$ 3 plaques at the periphery, with tensin-1 localization largely unchanged relative to no TGF-  $\beta$ 1 treatment (Figure 3-15A). HGFs cultured on TCP appear similar to untreated cultures with respect to  $\alpha$ v $\beta$ 3 and tensin-1 localization. Similarly, the addition of TGF-  $\beta$ 1 does not significantly change  $\beta$ 1 integrin and tensin-1 localization compared to untreated controls in HGFs on TCP (Figure 3-15B). On 0.2 kPa surfaces, in the presence of TGF-  $\beta$ 1, there is qualitatively an increase in the number of  $\beta$ 1 integrin associated plaques, but very limited co-localization with tensin-1 (Figure 3-15B).

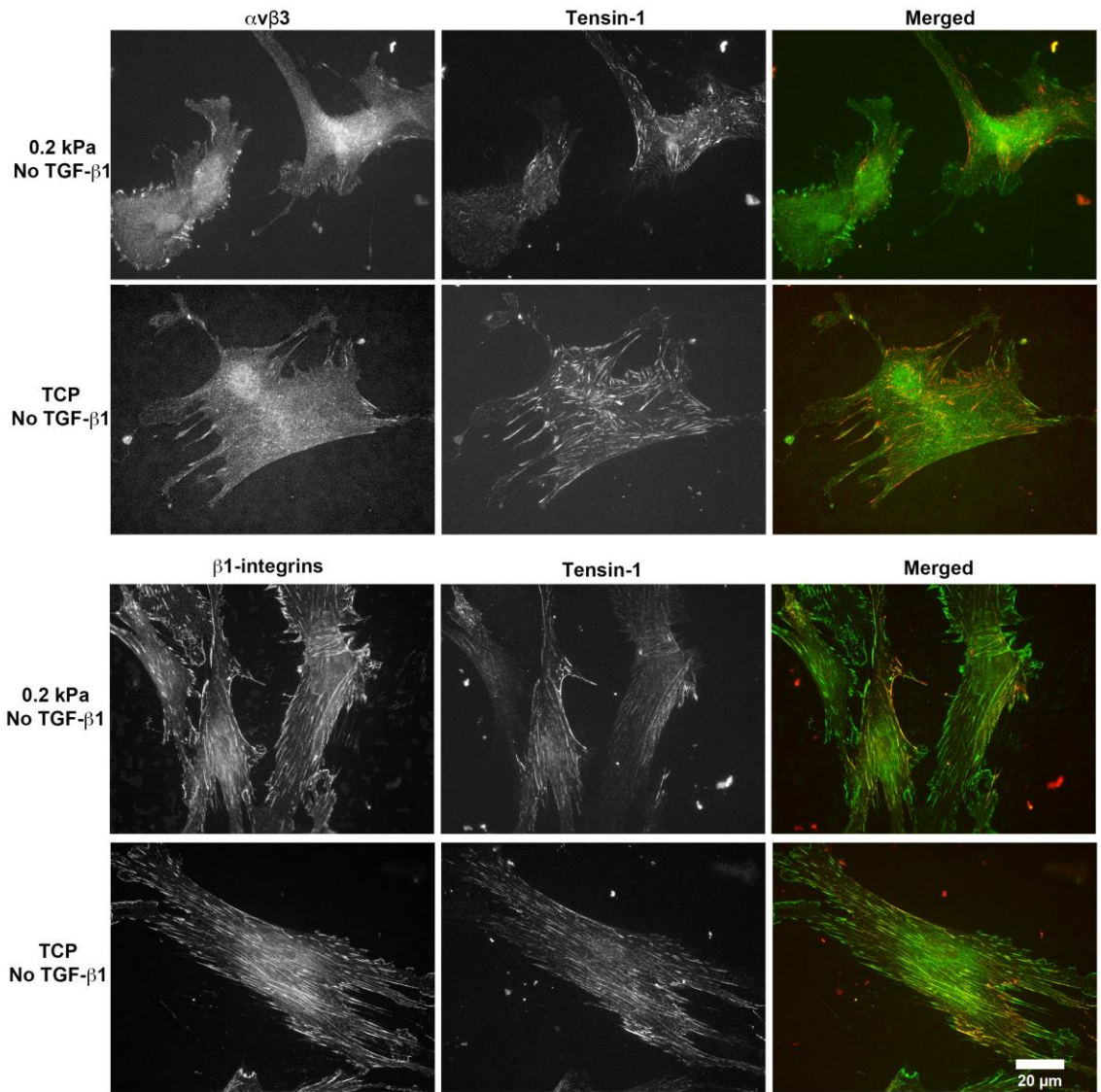


**Figure 3-14: Integrin  $\beta$ 1 and Tensin-1 exhibit greater co-localization upon TCP than 0.2 kPa elastic modulus surface among HGFs**

Immunocytochemistry of HGFs upon surfaces of varying elastic moduli evaluating the colocalization of tensin-1 (red), integrin  $\alpha$ v $\beta$ 3 (green) and integrin  $\beta$ 1 (green) after 24 h with no treatment. Scale: 20  $\mu$ m; Magnification 40X water immersion; N = 3.



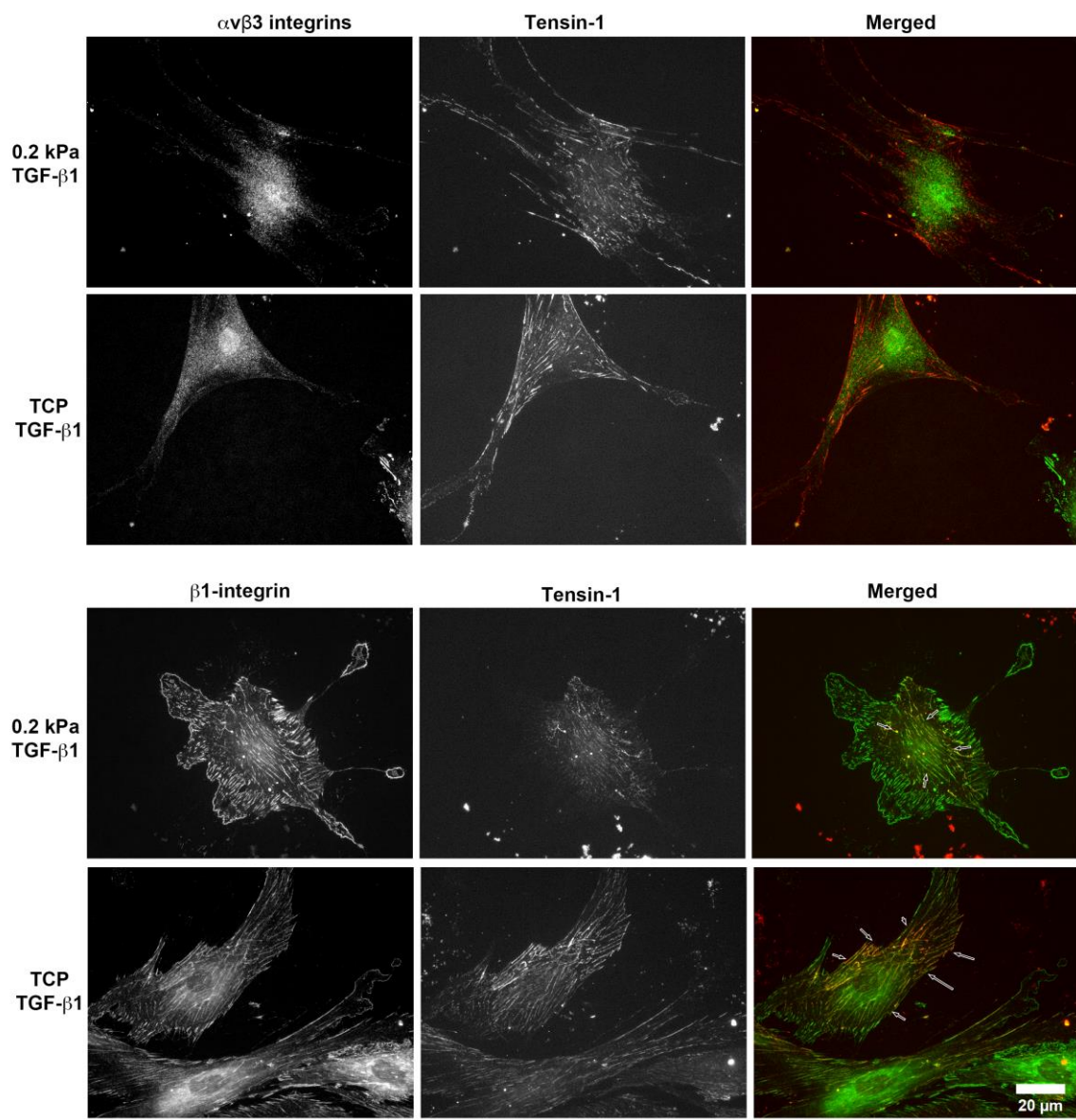


**Figure 3-15: TGF- $\beta$ 1 treatment switches integrin  $\alpha$  $\beta$ 3 adhesion engagement for integrin  $\beta$ 1 in HGFs**

Immunocytochemistry of HGFs upon surfaces of varying elastic moduli evaluating the colocalization of tensin-1 (red) with integrin  $\alpha$  $\beta$ 3 (green) and integrin  $\beta$ 1 (green) after 24 hours with 5 ng/mL TGF-  $\beta$ 1 treatment. White arrows indicate co-localization of the antibodies. Scale: 20  $\mu$ m; Magnification 40X water immersion; N = 3.

### 3.3.6 HDF and HGF intracellular signaling differs across substratum of varying elastic modulus

As adhesion sites represent a significant site for activation of intracellular signaling, we next cultured HDF and HGF on 0.2, 8, 64 kPa and TCP, and changes in phosphorylation of proteins were assessed using the human proteome profiler which assesses 37 different phospho-kinases (Appendix A). Of the proteins assessed at 24 hrs post seeding, in HDFs, two differences were noted, specifically ERK1/2 was seen to decrease on the 8 kPa elastic modulus surface compared to TCP. ERK1/2 phosphorylation upon the 64 kPa elastic modulus surface was similar to TCP, but greater than in cells cultured on the 8 and 0.2 kPa elastic modulus surfaces. GSK-3 $\alpha$  $\beta$  phosphorylation was significantly increased upon the 0.2 kPa elastic modulus surface as compared to the 8 kPa surface (Figure 3-16). Among HGFs, ERK1/2 was the only kinase to be differentially phosphorylated across the experimental surfaces; TCP had significantly reduced ERK1/2 phosphorylation compared to the 64 kPa elastic modulus surface (Figure 3-17).

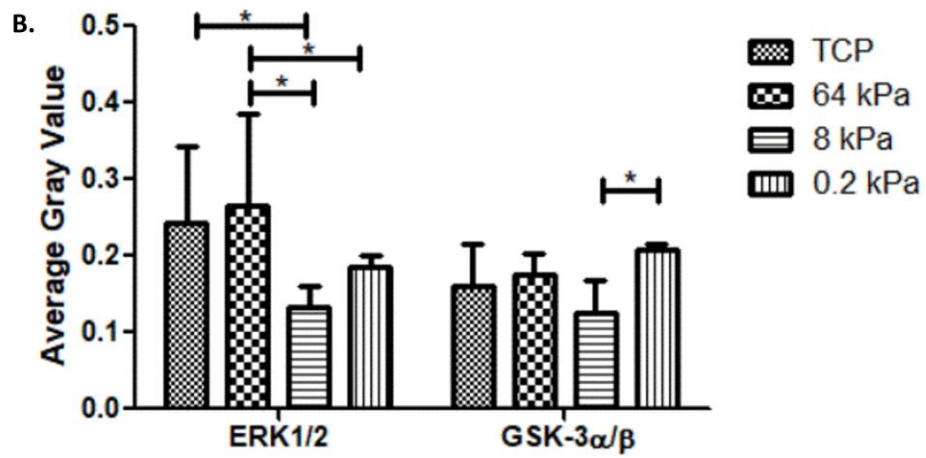
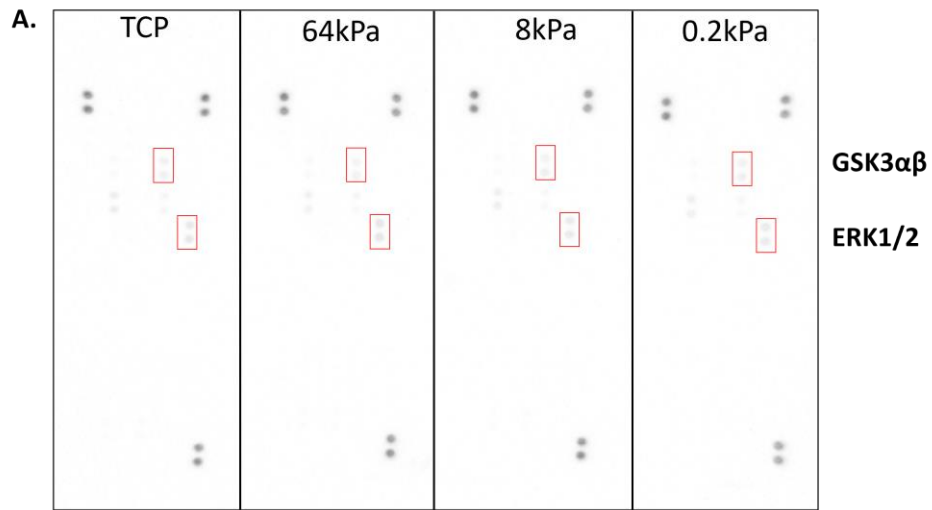


**Figure 3-16: HDF ERK1/2 and GSK3 $\alpha\beta$  phosphorylation is effected by culturing on surfaces of varying elastic moduli**

(A) Quantification of human HGF phospho-kinase activity as determined by the human proteome profile. (B) Average grey value of ERK1/2 and GSK3 $\alpha\beta$  phosphorylation upon TCP, 0.2, 8, and 64 kPa substrata. ERK1/2 and GSK3 $\alpha\beta$  demonstrated variable phosphorylation across the investigated surfaces. The average gray value was normalized to individual membrane reference points. Fibroblasts were incubated for 24 h. N = 3. ANOVA; Bonferroni Post Hoc Test; \* p < 0.05.

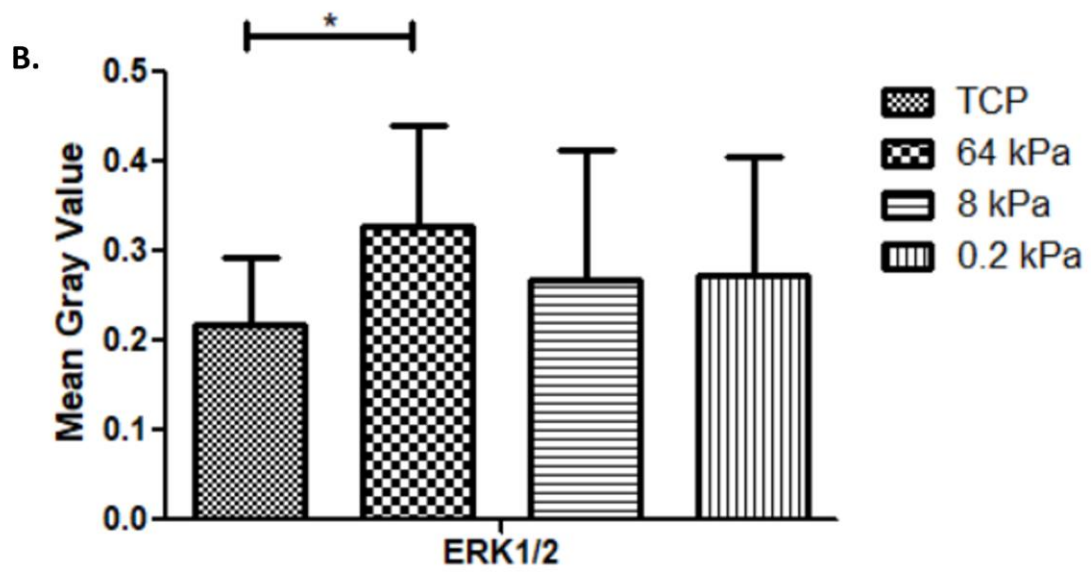
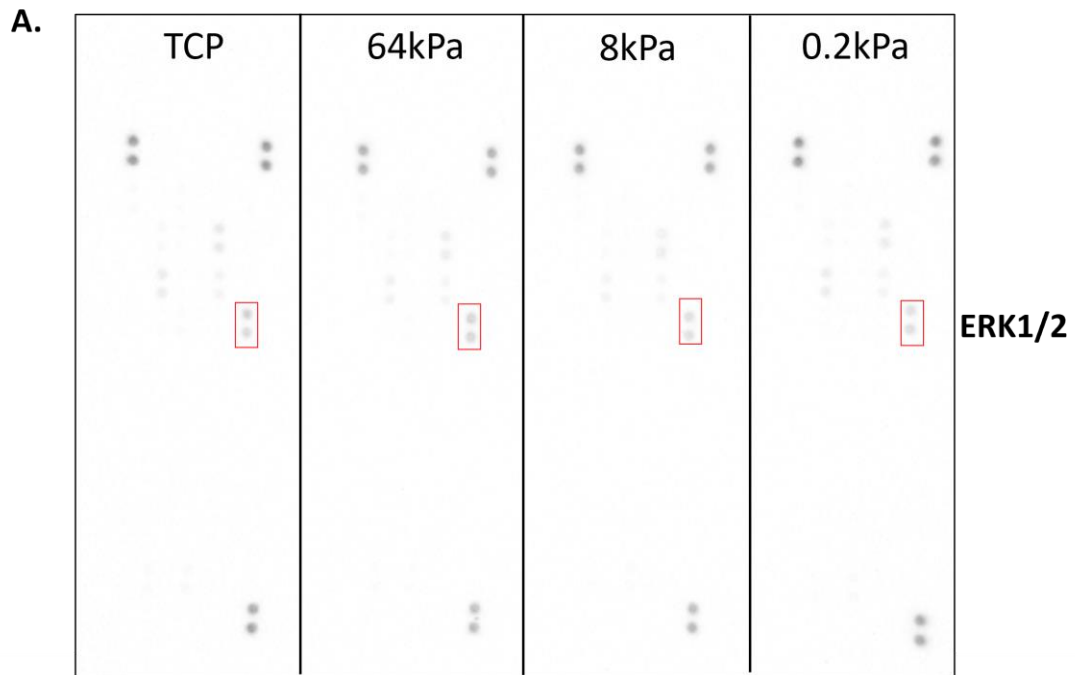


**Figure 3-17: HGF ERK1/2 phosphorylation is upregulated upon 64 kPa elastic modulus surface**

(A) Quantification of HGF phospho-kinase activity as determined by the human proteome profile. (B) Average grey value of ERK1/2 phosphorylation upon TCP, 0.2, 8, and 64 kPa substrata. ERK1/2 demonstrated variable phosphorylation across the investigated surfaces. The average gray value was normalized to individual membrane reference points. Fibroblasts were incubated for 24 hours. N = 3. ANOVA; Bonferroni Post Hoc Test; \*  $p < 0.05$ .

## 3.4 Discussion

As previously discussed in section 3.1, the elastic modulus of a culture substratum is known to influence cell behaviours including adhesion formation, morphology, migration, gene expression and matrix synthesis<sup>1-3</sup>. In this thesis, the influence of substratum elastic modulus on human dermal and gingival fibroblast physiology was determined, providing data on adhesion changes and intrinsic differences in cell behaviour based on tissue of origin which may underlie the propensity of these tissues to scar.

### 3.4.1 Tissue culture plastic reduces HDF and HGF initial cell adhesion and proliferation rate.

The level of cell adhesion and proliferation largely depend on the application of a biomaterial and the mechanical environment in which it is placed<sup>18</sup>. In the case of dental implants, the longevity of the implant is determined by adequate soft tissue integration, without the presence of fibrosis<sup>18</sup>. In contrast, biomaterials used for heart valve replacements and repairs are required to be biologically inert to prevent tissue adhesion<sup>18</sup>. TCP represents the normal in vitro culture substratum for cells, although it is considered far from an ideal substratum to maintain fibroblast phenotype as our group has previously shown<sup>19</sup>. Interestingly, direct tests of how TCP influences different cell types are sparse in the literature. Indeed, I demonstrate here for the first time that when HDFs and HGFs are seeded onto surfaces with different elastic moduli, they show higher adhesion at 1 h on lower elastic modulus surfaces. When cultured over 7 days, while all elastic moduli tested are capable of maintaining cell viability and supporting proliferation, the 8 kPa elastic modulus substratum provided the greatest cell number fold increase in both HDFs and HGFs. This illustrates clearly that TCP is unlikely to represent an optimal surface for cell culture and any data on which cells are cultivated on TCP must consider this a potential limitation.

It has previously been established that cells respond to specific elastic modulus with respect to spreading, adhesion, migration and proliferation<sup>1,13,14</sup>. From my work, TCP reduces initial adhesion and subsequent proliferation compared to lower elastic modulus substrata,



with a surface of 8 kPa elastic modulus having the larger influence on both HDF and HGF populations. Previous studies have also established key elastic modulus for fibroblast spreading at 10 kPa, while other studies show higher fibroblast proliferation on stiffness gradient gels nearer the 150 MPa elastic modulus range <sup>3,15</sup>. Although elastic modulus values may differ, it is important to recognize differences in cell populations. As TCP approximates an elastic modulus of 1 GPa <sup>8</sup>, it is evident that the fibroblast populations in this current study demonstrate greater proliferation and altered adhesion upon culture substrata of lesser elastic modulus.

This finding brings to question physiological changes induced by culturing cells upon traditional TCP. The concept of mechanical memory in fibroblasts was introduced in 2012 whereby it was determined that culturing lung fibroblasts on stiff substrata and transferring them to a soft substratum induced higher fibrotic activity than lung fibroblasts primarily cultured upon soft substrata <sup>20</sup>. As previously mentioned, during the process of wound healing, the elastic modulus of the extracellular environment progresses from 10 – 1000 Pa, 18.5 kPa and ~80 kPa during the inflammatory, proliferative, and remodelling phases respectively. <sup>4-8</sup>. In the case of fibrosis, the fibroblasts remain encased and contribute to a highly stiff environment <sup>4</sup>. If myofibroblast memory is preserved in these fibroblasts in scar tissue, epigenetic changes are likely to occur meaning a return to their non-contractile phenotypic state associated with resident fibroblasts in uninjured tissue is unlikely to occur. This process would further contribute to the sustained stiffness of fibrotic tissue and the lack of medical treatment for these types of conditions.

### **3.4.2 Influence of elastic modulus on HDF and HGF adhesion and cytoskeletal F-actin arrangement are population specific.**

Many aspects of cell behaviour (including proliferation) are affected by the sensing and transmission of substratum mechanical load, imposed by substratum elastic modulus, through cell adhesion complexes <sup>12,21</sup>. A pre-requisite for myofibroblast transition, formation of F-actin stress fiber bundles is a necessary configuration in fibroblasts. Important signaling pathways activated by adhesion mechanotransduction are the RhoA,

RacI and Cdc42 signaling cascades influencing actin stabilization, cell contraction, and adhesion formation and maturation<sup>22,23</sup>.

Human dermal and gingival fibroblast cytoskeletal F-actin immunofluorescence demonstrated less well-developed stress fiber bundles on surfaces of lower elastic modulus. HDFs showed minimal F-actin stress fibers upon the 0.2 kPa elastic modulus surface compared to TCP, while HGFs showed similar arrangement on both 0.2 kPa and 8 kPa elastic modulus surfaces. This result is supported by past studies indicating cell morphology, adhesions and cytoskeletal structure depend upon substratum elastic modulus<sup>3</sup>. I further establish that HDFs and HGFs require different substratum elastic moduli to initiate F-actin stress fibers, with 8 kPa sufficient for HDFs, but 64 kPa for HGFs. I postulate the elastic modulus of the cells' *in vivo* niche may contribute to this disparity. In healthy tissue, dermal fibroblasts are known to interact with a variety of elastic moduli *in vivo* ranging from 100 Pa to 10 kPa while HGFs lie in direct apposition to alveolar bone of ~13.7 GPa elastic modulus<sup>8,9</sup>. For this reason, HDFs must be able to function on a variety of elastic moduli, necessitating healthy F-actin fiber formation, unlike HGFs. Alternatively, HGFs may have developed a means of mitigating intracellular tension transferred from the extracellular matrix.

The process of mechanosensation, whereby the cell transmits the extracellular mechanical stimuli into discrete biological responses, is not yet completely understood. However, it is thought to be mediated through cell adhesion and the cytoskeleton<sup>22,24</sup>. Quantification indicates a decreased vinculin adhesion recruitment in focal adhesions across low elastic modulus surfaces. Generally, low elastic modulus substrata influence dermal and gingival fibroblasts to establish more focal adhesion sites with a decreased area. Neither population exhibit significant changes in vinculin protein levels, demonstrating that it is the recruitment and organization of vinculin in adhesion sites as opposed to changes in overall expression. Although focal adhesion formation appears similar between HDFs and HGFs, tensin-1 containing fibrillar adhesion sites show major differences. In HDFs, fibrillar adhesion sites decrease in frequency and increase in area with an increase in substratum elastic modulus with the exception of the 0.2 kPa surface where the dermal fibroblasts show smaller tensin-1 adhesion sites as demonstrated by quantity and area. HGFs tend to

adhere similarly upon TCP and the 8 kPa elastic modulus surface. In general, the lowest elastic modulus surface investigated, 0.2 kPa, attenuates formation of large adhesions and likely correlates with their ability to deposit extracellular matrix via their fibrillar adhesions, decreased intracellular tension and force necessary for surface contraction and ultimately myofibroblast differentiation. This work indicates HDF and HGF fibrillar adhesion composition is cell-type specific, especially on surfaces of variable elastic modulus. Aside from studies indicating that cells adhere preferentially to materials with optimal adhesive properties, and migrate toward stiffer substrata, to our knowledge the results of this current study are unique and provide a new avenue of investigation for tuning the adhesive properties of biomaterials (Brunette & Chehroudi, 1999; Pelham & Yu-Li, 1997).

### 3.4.3 HDFs and HGFs quickly alter low elastic modulus surfaces with extracellular matrix deposition

The organization and secretion of fibronectin by HDFs and HGFs upon tissue culture plates of varying elastic modulus follows a similar pattern across a 24-h incubation. Immunofluorescence showed higher fibronectin secretion after 24 h upon plates of lower elastic modulus than TCP. Allowing the same cell populations to incubate for 2 weeks indicated the decreased elastic modulus plates did not prevent fibronectin fibrillogenesis, but the density of it directly related to the plate stiffness. Recently, Nikoloudaki et al. have demonstrated fibroblasts obtained from the palate of mice express significantly greater fibronectin when cultured on 0.2 kPa elastic modulus surfaces<sup>25</sup>. This finding is confirmed in this thesis, suggesting that elastic moduli associated with early granulation tissue promotes fibronectin and likely other matrix molecules to be produced. Such a stiffness dependent effect would facilitate a timely formation of a supportive granulation tissue for cell infiltration.

Cell culture patterning was also observed following 2 weeks to establish holes within the confluent cell culture substratum, circular areas devoid of fibroblasts, unlike the denser fibrillogenesis evident in HGFs and HDFs on TCP. This observation may be due to a decreased adhesion ability of the fibroblasts upon lower elastic modulus substrata, as

discussed in section 3.4.2, or a method of cell adaptation to overcome the lack of tension provided by the substratum by adhering to neighboring cells which may provide an increased intracellular tension, a process similar to haptotaxis <sup>14</sup>.

#### 3.4.4 HGF myofibroblast differentiation is dependent upon the elastic modulus of the substratum, adhesion formation and TGF- $\beta$ 1.

A number of studies have outlined the potential for substratum elastic modulus to affect cell phenotypes and differentiation <sup>26-30</sup>. In the process of wound healing, the differentiation of fibroblasts into  $\alpha$ SMA expressing myofibroblasts, capable of contractility, is a vital process in wound closure and the formation of hypertrophic and keloid scar formation. In 1999, Arora et al. presented the combined influence of wound healing cytokines and mechanical forces upon myofibroblast differentiation and subsequent  $\alpha$ SMA expression <sup>30</sup>. Analysis of  $\alpha$ SMA expression following a 5-day incubation period indicated that the effect of elastic modulus upon myofibroblast differentiation was only evident when HGFs were treated with TGF- $\beta$ 1.

Myofibroblast differentiation was largely inhibited in HGFs with decreased substratum elastic modulus. This finding coincides with reduced F-actin stress fibre formation on the lower elastic modulus surfaces with respect to TCP, 64 kPa, 8 kPa and 0.2 kPa. However, HDFs showed a largely uniform response irrespective of the surface elastic modulus, with incorporation of  $\alpha$ SMA only evident with the addition of TGF-  $\beta$ 1. This result is supported by many studies demonstrating the influence of TGF- $\beta$ 1 upon fibroblast contractility, ultimately leading to myofibroblast differentiation and  $\alpha$ SMA expression <sup>31-33</sup>. HGFs have been shown to not utilize the TGF- $\beta$ 1 induced myofibroblast differentiation pathway <sup>34</sup>. My study suggests TGF- $\beta$ 1 induced myofibroblast differentiation among HGFs, but not HDFs, is dependent upon the elastic modulus of the substratum, specifically when cultured on surfaces of low elastic modulus.

My work highlights specifically the role of  $\alpha$ SMA incorporation in HDFs and whether the phenotype on TCP truly represents a fully differentiated myofibroblast. The hallmark of a

myofibroblast is the presence of  $\alpha$ SMA in the stress fibres. While HDFs exhibit stress fibre bundles on stiff culture substrata, it is not necessarily associated with  $\alpha$ SMA. In addition to  $\alpha$ SMA incorporated stress fibers, myofibroblast differentiation is also established by the formation of mature adhesions and a reduction in migration and proliferation<sup>17,35</sup>. It is possible that HDFs are themselves highly contractile cell populations through cytoskeletal actin-myosin contraction; a phenotype recently investigated in lung fibrosis<sup>36</sup>.

In lung fibroblasts, tensin-1, and subsequently  $\alpha$ SMA, is known to be upregulated as a result of TGF- $\beta$ 1 treatment (Bernau et al., 2017). Rather than examine the amount of tensin-1, I evaluated the formation of the adhesion sites with regards to integrin involvement upon TCP and the 0.2 kPa elastic modulus surface within the HGF population due to their increased  $\alpha$ SMA stress fiber incorporation, not observed within HDFs. The reduction in size of tensin-1 containing adhesion sites, previously established, does not appear to be mitigated by treatment with TGF- $\beta$ 1. However, with the addition of TGF- $\beta$ 1, HGFs drastically reduce the involvement of integrin  $\alpha$ v $\beta$ 3 in their adhesion sites which I have recently demonstrated are capable of integrin switching within the tensin-1 containing fibrillar adhesion sites<sup>38</sup>. It is evident that the treatment of HGF with TGF- $\beta$ 1 causes engagement of tensin-1 containing adhesion sites, driving them towards integrin  $\beta$ 1 containing fibrillar adhesions to increase stability and intracellular tension. However, the inhibitory effects of the low elastic modulus surfaces are too significant to be completely overcome by exogenous TGF- $\beta$ 1 treatment alone. These results suggest that HGFs and even HDFs are epigenetically programmed to not form stress fibres or become myofibroblasts on surfaces of 0.2 kPa elastic modulus irrespective of TGF- $\beta$ 1 treatment known to increase intracellular tension and HDF myofibroblast differentiation<sup>39</sup>.

### 3.4.5 Intracellular signaling in human dermal and gingival fibroblasts downstream of variation in elastic moduli.

Extracellular signal-regulated kinases-1/2 (ERK1/2) was identified as a differentially phosphorylated protein when HGF and HDF were cultured upon surfaces of varying elastic modulus. ERK1/2 is a member of the Ras-Raf-MEK-ERK signal cascade affiliated with

cell adhesion, growth, migration, differentiation, proliferation, and transcription<sup>40</sup>. Of greater relevance, ERK1/2 has previously been associated with epithelial and gingival cell proliferation and death<sup>41,42</sup>. The results of our current study are in agreement with these known interactions as it has been determined that HDF and HGF proliferate more on the 64 kPa elastic modulus surface, which coincides with an increase in ERK1/2 phosphorylation. However, the highest cell proliferation was identified upon the 8 kPa surface at 7 days, a contrast to the ERK1/2 phosphorylation at 1 day – this discrepancy is likely due to the time points at which the experiments were conducted. Due to the many roles of ERK1/2 further investigation is needed to ascertain its potential role in mechanotransduction.

Interestingly, HDFs, but not HGFs also exhibited increased glycogen synthase kinase 3 (GSK3 $\alpha/\beta$ ) phosphorylation on the 0.2 kPa elastic modulus surface compared to the 8 kPa elastic modulus surface. GSK3 $\beta$  is a known regulator of the Wnt/beta-catenin signalling pathway – a pathway known to regulate cell fate and migration<sup>43</sup>. GSK-3 $\beta$  has been associated with fibrosis in numerous organs including the heart, kidney, liver and lung<sup>44</sup>. Most relevant to our current study, the activation of GSK-3 $\beta$  is known to decrease fibroblast proliferation and increase apoptosis in keloid scars<sup>45</sup>. This finding corresponds to the decrease in proliferation observed between the 8 kPa and 0.2 kPa elastic modulus surface. 8 kPa elastic modulus may prove to be a pro-fibrotic elastic modulus for HDFs as compared to the 0.2 kPa elastic modulus. The lack of significance within the HGF population exhibiting the same proliferative trend suggests HDFs and HGFs activate different signal pathways as a result of the mechanical stimuli.

### 3.4.6 Conclusions

The elastic modulus plays an important role in cell adhesion and consequential behaviours. For the first time, I have defined how HDF and HGF adhesion patterns change with respect to substratum elastic modulus and demonstrated its relation to myofibroblast differentiation. The role of extracellular stimuli is undoubtedly complex and I show here that fibroblasts of different tissue origin contain intrinsic differences in

how they respond to the same external stimuli. This information will be of great importance in the continued development of materials both for cell culture and the field of regenerative medicine.

### 3.5 References

- (1) Pelham, R. J.; Yu-Li, W. Cell Locomotion and Focal Adhesions Are Regulated by Substrate Flexibility. *Proc Natl Acad Sci U S A* **1997**, *94*, 13661–13665. <https://doi.org/10.1073/pnas.94.25.13661>.
- (2) Tilghman, R. W.; Blais, E. M.; Cowan, C. R.; Sherman, N. E.; Grigera, P. R.; Jeffery, E. D.; Fox, J. W.; Blackman, B. R.; Tschumperlin, D. J.; Papin, J. A.; Parsons, J. T. Matrix Rigidity Regulates Cancer Cell Growth by Modulating Cellular Metabolism and Protein Synthesis. *PLoS One* **2012**, *7* (5). <https://doi.org/10.1371/journal.pone.0037231>.
- (3) Yeung, T.; Georges, P. C.; Flanagan, L. A.; Marg, B.; Ortiz, M.; Funaki, M.; Zahir, N.; Ming, W.; Weaver, V.; Janmey, P. A. Effects of Substrate Stiffness on Cell Morphology, Cytoskeletal Structure, and Adhesion. *Cell Motil Cytoskeleton* **2005**, *60* (1), 24–34. <https://doi.org/10.1002/cm.20041>.
- (4) Van De Water, L.; Varney, S.; Tomasek, J. J. Mechanoregulation of the Myofibroblast in Wound Contraction, Scarring, and Fibrosis: Opportunities for New Therapeutic Intervention. *Adv Wound Care (New Rochelle)* **2013**, *2* (4), 122–141. <https://doi.org/10.1089/wound.2012.0393>.
- (5) Clark, J. a.; Cheng, J. C. Y.; Leung, K. S. Mechanical Properties of Normal Skin and Hypertrophic Scars. *Burns* **1996**, *22* (6), 443–446. [https://doi.org/10.1016/0305-4179\(96\)00038-1](https://doi.org/10.1016/0305-4179(96)00038-1).
- (6) Corr, D. T.; Hart, D. A. Biomechanics of Scar Tissue and Uninjured Skin. *Adv Wound Care (New Rochelle)* **2013**, *2* (2), 37–43. <https://doi.org/10.1089/wound.2011.0321>.

- (7) Elliott, C. G.; Wang, J.; Guo, X.; Xu, S.; Eastwood, M.; Guan, J.; Leask, A.; Conway, S. J.; Hamilton, D. W. Periostin Modulates Myofibroblast Differentiation during Full-Thickness Cutaneous Wound Repair. *J Cell Sci* **2011**, *125* (Pt 1), 121–132.  
<https://doi.org/10.1242/jcs.087841>.
- (8) Garland, S. P.; McKee, C. T.; Chang, Y. R.; Raghunathan, V. K.; Russell, P.; Murphy, C. J. A Cell Culture Substrate with Biologically Relevant Size-Scale Topography and Compliance of the Basement Membrane. *Langmuir* **2014**, *30* (8), 2101–2108.  
<https://doi.org/10.1021/la403590v>.
- (9) Schwartz-Dabney, C. L.; Dechow, P. C. Variations in Cortical Material Properties throughout the Human Dentate Mandible. *Am J Phys Anthropol* **2003**, *120* (3), 252–277.  
<https://doi.org/10.1002/ajpa.10121>.
- (10) Levental, I.; Georges, P. C.; Janmey, P. A. Soft Biological Materials and Their Impact on Cell Function. *Soft Matter* **2007**, *3* (July 2006), 299–306.  
<https://doi.org/10.1039/b610522j>.
- (11) Solon, J.; Levental, I.; Sengupta, K.; Georges, P. C.; Janmey, P. A. Fibroblast Adaptation and Stiffness Matching to Soft Elastic Substrates. *Biophys J* **2007**, *93* (12), 4453–4461.  
<https://doi.org/10.1529/biophysj.106.101386>.
- (12) Bao, G.; Suresh, S. Cell and Molecular Mechanics of Biological Materials. *Nat Mater* **2003**, *2* (11), 715–725.
- (13) Discher, D. E.; Janmey, P.; Wang, Y.-L. Tissue Cells Feel and Respond to the Stiffness of Their Substrate. *Science* **2005**, *310* (5751), 1139–1143.  
<https://doi.org/10.1126/science.1116995>.
- (14) Brunette, D. M.; Chehroudi, B. The Effects of the Surface Topography of Micromachined Titanium Substrata on Cell Behavior in Vitro and in Vivo. *J Biomech Eng* **1999**, *121*, 49–57.
- (15) Hopp, I.; Michelmore, A.; Smith, L. E.; Robinson, D. E.; Bachhuka, A.; Mierczynska, A.; Vasilev, K. The Influence of Substrate Stiffness Gradients on Primary Human Dermal



- Fibroblasts. *Biomaterials* **2013**, *34* (21), 5070–5077.  
<https://doi.org/10.1016/j.biomaterials.2013.03.075>.
- (16) Fournier, B. P. J.; Larjava, H.; Häkkinen, L. Gingiva as a Source of Stem Cells with Therapeutic Potential. *Stem Cells Dev* **2013**, *22* (24), 3157–3177.  
<https://doi.org/10.1089/scd.2013.0015>.
- (17) Hinz, B.; Phan, S. H.; Thannickal, V. J.; Galli, A.; Bochaton-Piallat, M.-L.; Gabbiani, G. The Myofibroblast. *Am J Pathol* **2007**, *170* (6), 1807–1816.  
<https://doi.org/10.2353/ajpath.2007.070112>.
- (18) Khalili, A. A.; Ahmad, M. R. A Review of Cell Adhesion Studies for Biomedical and Biological Applications. *International Journal of Molecular Sciences*. 2015.  
<https://doi.org/10.3390/ijms160818149>.
- (19) Walker, J. T.; Flynn, L. E.; Hamilton, D. W. Lineage Tracing of Foxd1-Expressing Embryonic Progenitors to Assess the Role of Divergent Embryonic Lineages on Adult Dermal Fibroblast Function. *FASEB Bioadv* **2021**, *3* (7), 541–557.  
<https://doi.org/10.1002/FBA2.1219>.
- (20) Balestrini, J. L.; Chaudhry, S.; Sarrazy, V.; Koehler, A.; Hinz, B. The Mechanical Memory of Lung Myofibroblasts. *Integrative Biology* **2012**, *4* (4), 410–421.  
<https://doi.org/10.1039/c2ib00149g>.
- (21) Yang, S.; Plotnikov, S. V. Mechanosensitive Regulation of Fibrosis. *Cells*. MDPI May 1, 2021. <https://doi.org/10.3390/cells10050994>.
- (22) Vinarský, V.; Pagliari, S.; Forte, G.; Martino, F.; Perestrelo, A. R. Cellular Mechanotransduction: From Tension to Function. *Front Physiol* **2018**, *9* (July), 1–21.  
<https://doi.org/10.3389/fphys.2018.00824>.
- (23) Spiering, D.; Hodgson, L. Dynamics of the Rho-Family Small GTPases in Actin Regulation and Motility. *Cell Adhesion and Migration*. Taylor and Francis Inc. 2011, pp 170–180. <https://doi.org/10.4161/cam.5.2.14403>.

- (24) Geiger, B.; Yamada, K. M. Molecular Architecture and Function of Matrix Adhesions. *Cold Spring Harb Perspect Biol* **2011**, 1–22. <https://doi.org/10.1101/cshperspect.a005033>.
- (25) Nikoloudaki, G.; Snider, P.; Simmons, O.; Conway, S. J.; Hamilton, D. W. Periostin and Matrix Stiffness Combine to Regulate Myofibroblast Differentiation and Fibronectin Synthesis during Palatal Healing. *Matrix Biology* **2020**, *94*, 31–56. <https://doi.org/10.1016/j.matbio.2020.07.002>.
- (26) Bhana, B.; Iyer, R. K.; Chen, W. L. K.; Zhao, R.; Sider, K. L.; Likhitpanichkul, M.; Simmons, C. A.; Radisic, M. Influence of Substrate Stiffness on the Phenotype of Heart Cells. *Biotechnol Bioeng* **2010**, *105* (6), 1148–1160. <https://doi.org/10.1002/bit.22647>.
- (27) Tilghman, R. W.; Cowan, C. R.; Mih, J. D.; Koryakina, Y.; Gioeli, D.; Slack-Davis, J. K.; Blackman, B. R.; Tschumperlin, D. J.; Parsons, J. T. Matrix Rigidity Regulates Cancer Cell Growth and Cellular Phenotype. *PLoS One* **2010**, *5* (9), 1–13. <https://doi.org/10.1371/journal.pone.0012905>.
- (28) Wells, R. G. The Role of Matrix Stiffness in Hepatic Stellate Cell Activation and Liver Fibrosis. *J Clin Gastroenterol* **2005**, *39* (4 Suppl 2), S158-61. <https://doi.org/10.1097/01.mcg.0000155516.02468.0f>.
- (29) Yakut Ali, M.; Chuang, C.-Y.; Saif, M. T. A. HHS Public Access. *Soft Matter* **2014**, *10* (44), 8829–8837. <https://doi.org/10.1038/nbt.3121>.ChIP-nexus.
- (30) Arora, P. D.; Narani, N.; McCulloch, C. a. G. The Compliance of Collagen Gels Regulates Transforming Growth Factor- $\beta$  Induction of  $\alpha$ -Smooth Muscle Actin in Fibroblasts. *Am J Pathol* **1999**, *154* (3), 871–882. [https://doi.org/10.1016/S0002-9440\(10\)65334-5](https://doi.org/10.1016/S0002-9440(10)65334-5).
- (31) Montesano, R.; Orci, L. Transforming Growth Factor Beta Stimulates Collagen-Matrix Contraction by Fibroblasts: Implications for Wound Healing. *Proc Natl Acad Sci U S A* **1988**, *85* (13), 4894–4897. <https://doi.org/10.1073/pnas.85.13.4894>.

- (32) Hinz, B.; Celetta, G.; Tomasek, J. J.; Gabbiani, G.; Chaponnier, C. Alpha-Smooth Muscle Actin Expression Upregulates Fibroblast Contractile Activity. *Mol Biol Cell* **2001**, *12* (9), 2730–2741. <https://doi.org/10.1091/mbc.12.9.2730>.
- (33) Tomasek, J. J.; Gabbiani, G.; Hinz, B.; Chaponnier, C.; Brown, R. a. Myofibroblasts and Mechano-Regulation of Connective Tissue Remodelling. *Nat Rev Mol Cell Biol* **2002**, *3* (5), 349–363. <https://doi.org/10.1038/nrm809>.
- (34) Guo, F.; Carter, D. E.; Leask, A. MiR-218 Regulates Focal Adhesion Kinase-Dependent TGF $\beta$  Signaling in Fibroblasts. *Mol Biol Cell* **2014**, *25* (7), 1151–1158. <https://doi.org/10.1091/mbc.E13-08-0451>.
- (35) Hinz, B.; Gabbiani, G. Mechanisms of Force Generation and Transmission by Myofibroblasts. *Curr Opin Biotechnol* **2003**, *14* (5), 538–546. <https://doi.org/10.1016/j.copbio.2003.08.006>.
- (36) Southern, B. D.; Grove, L. M.; Rahaman, S. O.; Abraham, S.; Scheraga, R. G.; Niese, K. A.; Sun, H.; Herzog, E. L.; Liu, F.; Tschumperlin, D. J.; Egelhoff, T. T.; Rosenfeld, S. S.; Olman, M. A. Matrix-Driven Myosin II Mediates the pro-Fibrotic Fibroblast Phenotype. *Journal of Biological Chemistry* **2016**, *291* (12), 6083–6095. <https://doi.org/10.1074/jbc.M115.712380>.
- (37) Bernau, K.; Torr, E. E.; Evans, M. D.; Aoki, J. K.; Ngam, C. R.; Sandbo, N. Tensin 1 Is Essential for Myofibroblast Differentiation and Extracellular Matrix Formation. *Am J Respir Cell Mol Biol* **2017**, *56* (4), 465–476. <https://doi.org/10.1165/rcmb.2016-0104OC>.
- (38) Brooks, S.; Mittler, S.; Hamilton, D. W. Contact Guidance of Connective Tissue Fibroblasts on Submicrometer Anisotropic Topographical Cues Is Dependent on Tissue of Origin, B1 Integrins, and Tensin-1 Recruitment. *ACS Appl Mater Interfaces* **2023**, *15* (16), 19817–19832. <https://doi.org/10.1021/acsami.2c22381>.
- (39) Hinz, B. Formation and Function of the Myofibroblast during Tissue Repair. *Journal of Investigative Dermatology* **2007**, *127* (3), 526–537. <https://doi.org/10.1038/sj.jid.5700613>.

- (40) Roskoski, R. ERK1/2 MAP Kinases: Structure, Function, and Regulation. *Pharmacological Research*. August 2012, pp 105–143. <https://doi.org/10.1016/j.phrs.2012.04.005>.
- (41) Sharma, G. D.; He, J.; Bazan, H. E. P. P38 and ERK1/2 Coordinate Cellular Migration and Proliferation in Epithelial Wound Healing. Evidence of Cross-Talk Activation between Map Kinase Cascades. *Journal of Biological Chemistry* **2003**, 278 (24), 21989–21997. <https://doi.org/10.1074/jbc.M302650200>.
- (42) Kokubu, E.; Hamilton, D. W.; Inoue, T.; Brunette, D. M. Modulation of Human Gingival Fibroblast Adhesion, Morphology, Tyrosine Phosphorylation, and ERK 1/2 Localization on Polished, Grooved and SLA Substratum Topographies. *J Biomed Mater Res A* **2009**, 91 (3), 663–670. <https://doi.org/10.1002/jbm.a.32273>.
- (43) Kour Bali, S.; Bryce, D.; Prein, C.; Woodgett, J. R.; Beier, F.; Bali, S. K. Glycogen Synthase Kinase 3 Alpha/Beta Deletion Induces Precocious Growth Plate Remodeling in Mice. *J Mol Med* **2021**, 99, 831–844. <https://doi.org/10.1007/s00109-021-02049-3>/Published.
- (44) Zheng, H.; Yang, Z.; Xin, Z.; Yang, Y.; Yu, Y.; Cui, J.; Liu, H.; Chen, F. Glycogen Synthase Kinase-3 $\beta$ : A Promising Candidate in the Fight against Fibrosis. *Theranostics*. Ivyspring International Publisher 2020, pp 11737–11753. <https://doi.org/10.7150/thno.47717>.
- (45) Cai, Y.; Zhu, S.; Yang, W.; Pan, M.; Wang, C.; Wu, W. Downregulation of  $\beta$ -Catenin Blocks Fibrosis via Wnt2 Signaling in Human Keloid Fibroblasts. *Tumor Biology* **2017**, 39 (6). <https://doi.org/10.1177/1010428317707423>.

## 4 Fabrication of a novel, elastic moduli varied-topographic cell culture surface

### 4.1 Introduction

*In vivo*, many physical and chemical stimuli regulate different aspects of cell behaviour within the tissue microenvironment. Considering specifically the physical environment, one must consider both the material's elastic modulus and topography if the goal is to generate a realistic cell culture substratum to more closely mimic the *in situ* mechanical properties of native tissues. Although many culture models have been established to investigate the effects of substratum topography and elastic modulus, separately, upon various cell types, few studies have focused on combining a controlled elastic modulus and substratum topography into one cell culture device representing a large void yet to be explored in the depth required for the field of cellular biomechanics <sup>1-3</sup>.

The methods described by Garland et al. 2014 utilized PEG hydrogels to form a groove and ridge topography ranging in size from 800 - 2000 nm. The study performed by Al-Haque et al. in 2012 also established a topographical patterned hydrogel cell culture substratum, although the feature size was 50  $\mu\text{m}$  groove and ridge pattern, considerably beyond the average dimension of a cell. More recently, Comelles et al. have created 2  $\mu\text{m}$  grooves at a depth of 1  $\mu\text{m}$  in stiffness gradient polyacrylamide gels <sup>3</sup>. The novel topographic substrata used within the Hamilton Lab allow assessment of cell behaviour over large areas of patterning, including dots and line features, and at both a nanometric and micrometric level. By utilizing an elastic modulus tunable material, such as polyacrylamide, as used in previous studies investigating substratum elastic moduli <sup>3</sup>, in addition to the novel fabricated glass topographic surfaces already established within the Hamilton Lab, elastic moduli varied-topographic cell culture surface will be fabricated.

Successful fabrication of devices with varying elastic moduli and topographic features for cell culture surfaces is an important step to facilitate a more complete analysis of the physiological effects of a varying elastic modulus and topographical extracellular environment. The investigation by Al-Haque et al. 2012 demonstrated the influence of combined substratum topography and stiffness upon cardiac fibroblast morphology and

migration. The dependence upon combined topography and elastic modulus within mechanosensation was established <sup>1</sup>. However, a further need to investigate the combined effect of topography and elastic modulus and mechanisms involved is identified <sup>1</sup>. Comelles et al. demonstrated actomyosin contractility on soft grooves and tubulin polymerization on stiff grooves are important for stiffness regulated contact guidance <sup>3</sup>. It is the goal of this research to quantify preliminary observations regarding the combined effect of elastic modulus and sub-micron topography upon the morphology and contact guidance of HDF and HGF in the realm of wound healing and fibrosis development.

## 4.2 Materials and Methods

### 4.2.1 Elastic Moduli Varied-Topographical Substratum Fabrication

A total of 4 surfaces are to be constructed; topographical nanogrooves of 900 nm periodicity will be combined with a material of tunable elastic modulus. Flat control surfaces of the same elastic modulus will also be fabricated.

Negatives of glass nanotopographical surfaces are established in polyvinylsiloxane VP mix (PVS) (Henry Schein, Niagara-on-the-Lake, ON, Canada). Glass topographic surfaces are placed topography upright within 50 mm cell culture dishes. The topographies are coated in PVS and compressed until dried, approximately 5 min. The molds are gently removed from the cell culture dishes, labelled and stored in a cool, dry location.

#### 4.2.1.1 Polyacrylamide Surfaces

Utilizing an established protocol and mimicking the work of Al-Haque et al. <sup>1</sup>, polyacrylamide surfaces were fabricated of various elastic moduli by increasing the percentage of acrylamide (A3553, Millipore Sigma Canada Ltd., Oakville, ON, Canada) and bis-acrylamide (146072, Millipore Sigma Canada Ltd., Oakville, ON, Canada) to increase the elastic modulus and vice-versa <sup>4</sup>. The PVS topographic negatives are filled with either 3% / 0.1% or 15% / 0.3% acrylamide to bis-acrylamide, and polymerized with the addition of ammonium persulfate (APS) (AMP001, Bioshop Canada Inc., Burlington,

ON, Canada) and N, N, N', N' tetramethyl - ethylenediamine (TEMED) (T9281, Millipore Sigma Canada Ltd., Oakville, ON, Canada). Samples were placed in a vacuum for 5 min to degas and left covered with a glass coverslip for 1 hour to polymerize.

#### 4.2.1.2 Photocol Collagen Surfaces

Utilizing the protocol provided by Advanced Biomatrix for PhotoCol (Methacrylated Collagen 5198, Advanced Biomatrix, Carlsbad, CA, USA), a surface approximating 1 kPa, is prepared within a tissue culture plastic 6-well plate (10062-892, VWR International, Mississauga, ON, Canada). A topographic negative is overlaid upon the Photocol substratum prior to gel formation. The collagen substratum is left to incubate at 37°C for 1h. The topographic negative is floated off of the collagen gel with PBS.

#### 4.2.1.3 Silicone Topographic Elastomers

Silicone elastomers (Medical Grade Elastomer A-103, Factor II Inc., Lakeside, AZ, USA) are prepared via an adapted protocol <sup>5</sup>. Silicone elastomers are polymerized in PVS topographic surface negative molds, 2 cm x 2 cm x 2 mm, at different ratios of elastomer to curing agent (Table 4-1). Silicone elastomers are released from their molds with forceps and PBS. The silicone elastomers are processed into uniform, circular culture constructs by an 8 mm biopsy punch. The samples are stored dry, protected from light, at room temperature, for future use. Prior to use, the surfaces are prepared for cell culture using an argon plasma cleaner. This process is summarized in Figure 4-1.

**Table 4-1: Silicone elastomer polymerization specifications**

<b>Base/Curing agent ratio by weight</b>	<b>Curing temperature</b>	<b>Curing time</b>
10 : 1	60 °C	24 h
5 : 1	60 °C	24 h



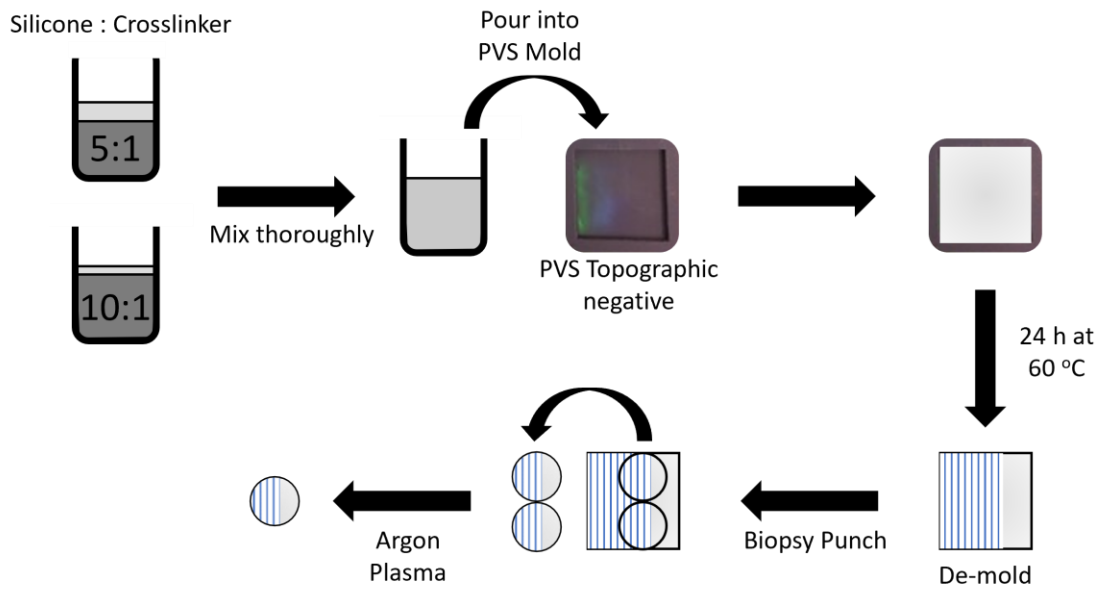


**Figure 4-1: Schematic detailing the fabrication process of the topographic silicone elastomers**

Silicone monomer is mixed with the crosslinker at 10:1 and 5:1 ratios and gently poured into the PVS topographic negative for a 900 nm periodicity nanogroove. After 24 h at 60 °C, the silicone elastomers are gently removed from their PVS mold. An 8 mm biopsy punch is used to create uniform cell culture constructs containing an area of topography and a flat control. The final step prior to cell culture is to charge the surface with argon plasma.

## 4.2.2 Material Characterization

### 4.2.2.1 Surface Topography Analysis

Atomic force microscopy was performed by Dr. Heng-Yong Nie at Surface Science Western using a Park Systems XE-100. The surface morphology was imaged with the dynamic force mode using a silicon cantilever having a nominal spring constant of 40 N/m and resonant frequency of 325 kHz. The radius of the apex of the AFM tip at the free end of the cantilever was nominally 8 nm. The AFM images were obtained in air at 256 x 256 pixels.

### 4.2.2.2 Elastic Modulus Analysis

Elastic modulus is determined using the Cell Scale UniVert system in compression with a 10 N load cell at a 20 % strain at a rate of 0.005 s<sup>-1</sup>. Surfaces, 8 mm diameter and 2 mm thick, will undergo testing after 1- and 5-days following polymerization to determine short term shelf life. In addition, surfaces are tested following incubation under normal cell culture conditions (high glucose DMEM containing 10% FBS and 1% AA, 37°C, 5% CO<sub>2</sub>) for 1 and 5 days. Force displacement data were processed in Microsoft Excel into stress-strain curves from which the elastic modulus was calculated by the slope of the linear portion.

### 4.2.2.3 Contact Angle Analysis

Sessile drop goniometry was performed by Dr. Heng-Yong Nie at Surface Science Western using a DSA30E Drop Shape Analyzer (KRÜSS). 2 µL ultra-pure water was used to measure the contact angle upon all surfaces.

### 4.2.3 Dermal and Gingival Fibroblast Isolation and Culture

In accordance with the guidelines of the University's Research Ethics Board for Health Sciences Research, *in vitro* studies are performed utilizing human dermal fibroblasts (HDF) populations isolated from skin tissue under informed consent from patients undergoing elective limb amputation. Human gingival fibroblasts (HGF) are isolated from tissue retrieved under informed patient consent during elective periodontal procedures in the Oral Surgery Clinic at the Schulich School of Medicine and Dentistry, University of Western Ontario. Human dermal and gingival fibroblasts populations, each from 3 different patients, are maintained under passage 6 in high glucose (4.5 g/L) Dulbecco's Modified Eagle Medium (DMEM; Thermo Fisher Scientific, Burlington, ON, Canada) supplemented with 10% fetal bovine serum (FBS) (Gibco Life Technologies, Burlington, ON, Canada) and 1% antibiotics and antimycotic (AA) solution (Gibco Life Technologies, Burlington, ON, Canada) at 37 °C, 5% CO<sub>2</sub>. Media is changed every 2 - 3 days.

### 4.2.4 Elastic Moduli Varied-Topographic Substratum Cell Culture

Silicone gel processing for cell culture is adapted from previous protocols established for polyacrylamide gel cell culture substrata<sup>4,6-8</sup>. The surfaces are sterilized using an argon plasma cleaner and rinsed in sterile PBS 3 times. The gels are primed for cell culture with media for 24 h at 37 °C, 5% CO<sub>2</sub>. The media is aspirated, cells are seeded at a density of 5000 cells/cm<sup>2</sup>, allowed to adhere for 1 h at 37°C, 5% CO<sub>2</sub>, and flooded with cell culture media. Cells are incubated under normal conditions at 37 °C, 5% CO<sub>2</sub>.

### 4.2.5 Immunofluorescence

Cells were fixed with 4% paraformaldehyde for 5 min, rinsed in 1X phosphate buffered saline, incubated within 0.1% Triton X-100 solution for 5 min, rinsed, and blocked by a 1% bovine serum albumin solution (Millipore Sigma) for 30 min. F-actin was labelled with Rhodamine conjugated phalloidin (R415; Life Technologies, Grand Island, New York), and nuclei counterstained with Hoechst (H3560; Invitrogen, Burlington, ON). Images were

taken on a Carl Zeiss Axio Imager M2m microscope (Zeiss Microscopes, North York, ON) under 20X magnification and processed using Zen Pro software.

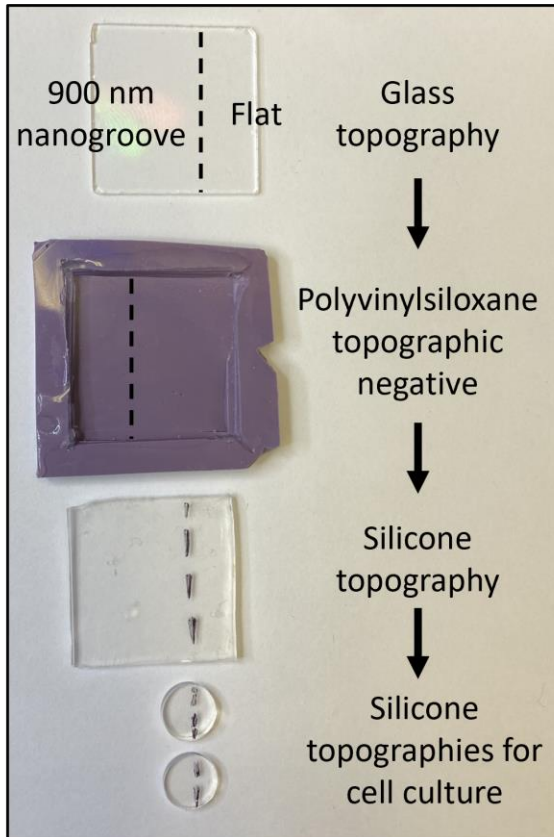
## 4.3 Results

### 4.3.1 Silicone provides an optically translucent, structural polymer with negligible swelling to fabricate topographic surfaces of various elastic modulus

Initial attempts to fabricate a device with topographic patterning in materials of defined elastic modulus with were performed using polyacrylamide and collagen (Photocol) as the base materials. Both polyacrylamide and collagen gels were successfully formed in the PVS topographic negatives. Optically translucent materials were fabricated, plasma cleaned and transferred to cell culture plates. When placed under normal cell culture conditions, submerged in cell culture media, significant swelling was observed in both polyacrylamide and collagen gels. No further examination was conducted upon either material as swelling eliminated the controlled topographical feature dimensions.

Silicone elastomers with varying silicone to crosslinker ratios were next used to fabricate culture devices with 900 nm nanogroove PVS topographic negatives the selected feature size (Figure 4-2). The presence of interference colours upon the surface of the silicone elastomers demonstrated the presence of a topography prior to and post incubation within normal cell culture conditions. The presence of topography was confirmed via atomic force microscopy (Figure 4-3). Digital palpation of the silicone elastomers suggested a variation in elastic modulus was present. Again, these preliminary results were confirmed through mechanical testing following incubation under normal cell culture conditions (Figure 4-5).

A.



B.

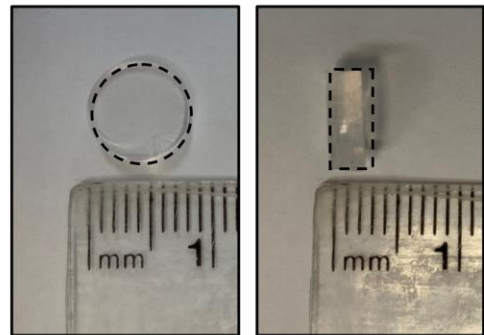


**Figure 4-2: Fabrication process of topographic, silicone elastomers**

(A) The progression of glass topographical surfaces fabricated by HeCd laser nanolithography to elastic modulus varied, topographic silicone surfaces through PVS topographic negative molds is depicted. The division of the flat surface from the topography is indicated by the dashed line. (B) Top and side view of the finalized elastic modulus varied, silicone topographic surface of 8 mm diameter to be utilized for *in vitro* experimentation.

### 4.3.2 Silicone reliably fabricates submicron topographic cell culture substrata

Atomic force microscopy (AFM) was performed upon both the template glass topographic surfaces and the newly fabricated varied elastic modulus, silicone topographic surfaces (Figure 4-3). The AFM images confirmed the accuracy of the fabrication process through the reproducibility of the topographic structure within the silicone elastomers (Figure 4-4).



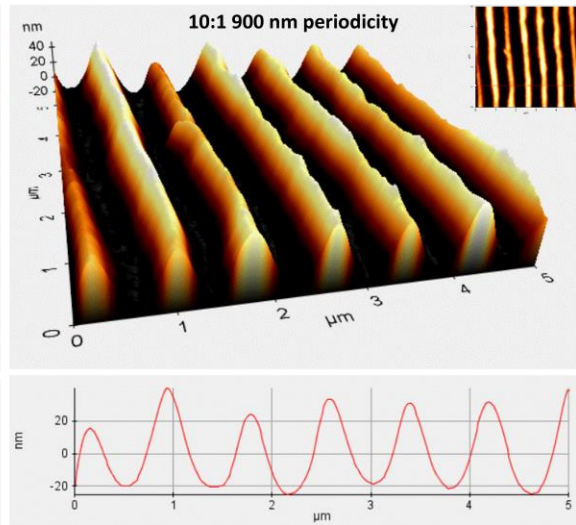
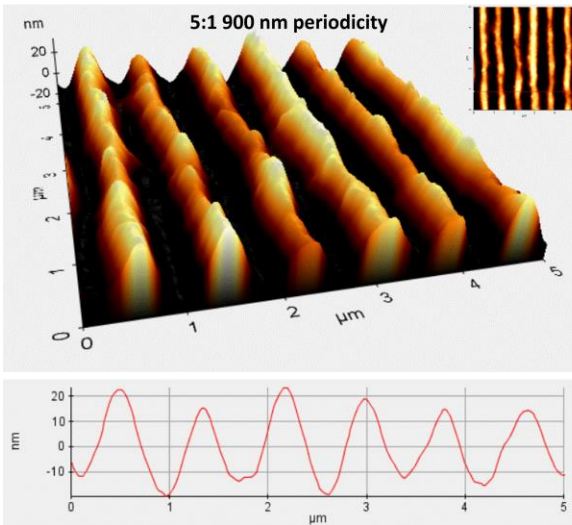
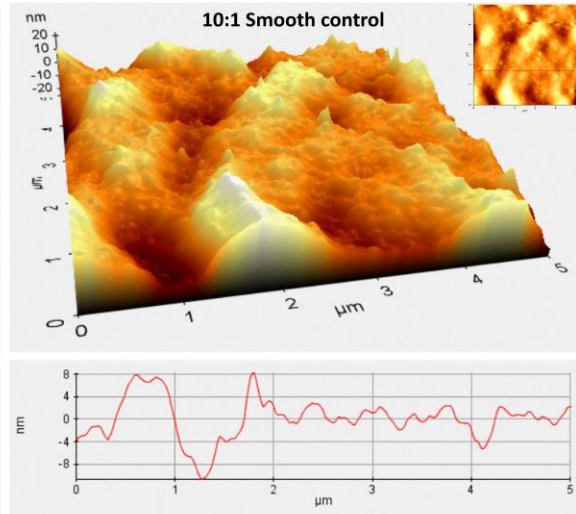
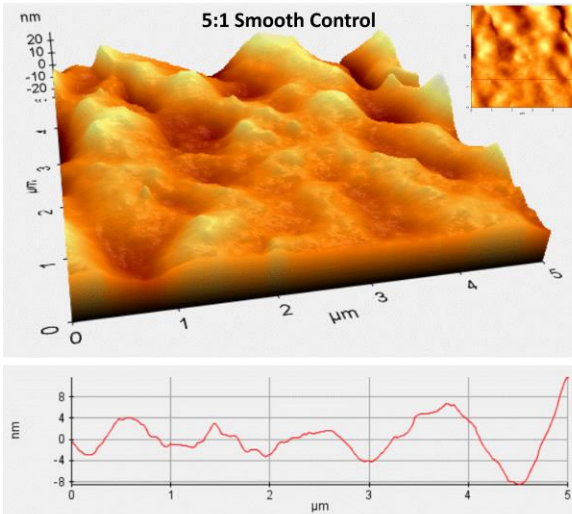


**Figure 4-3 Atomic force microscopy images of the elastic modulus varied topographic silicone elastomers.**

Atomic force microscopy (dynamic mode) 3D rendering and ridge and peak profiles of flat controls and 900 nm periodicity, repeating groove topographical structures within silicone elastomers. Silicone elastomers were fabricated at silicone to crosslinker ratios of 5:1 and 10:1.

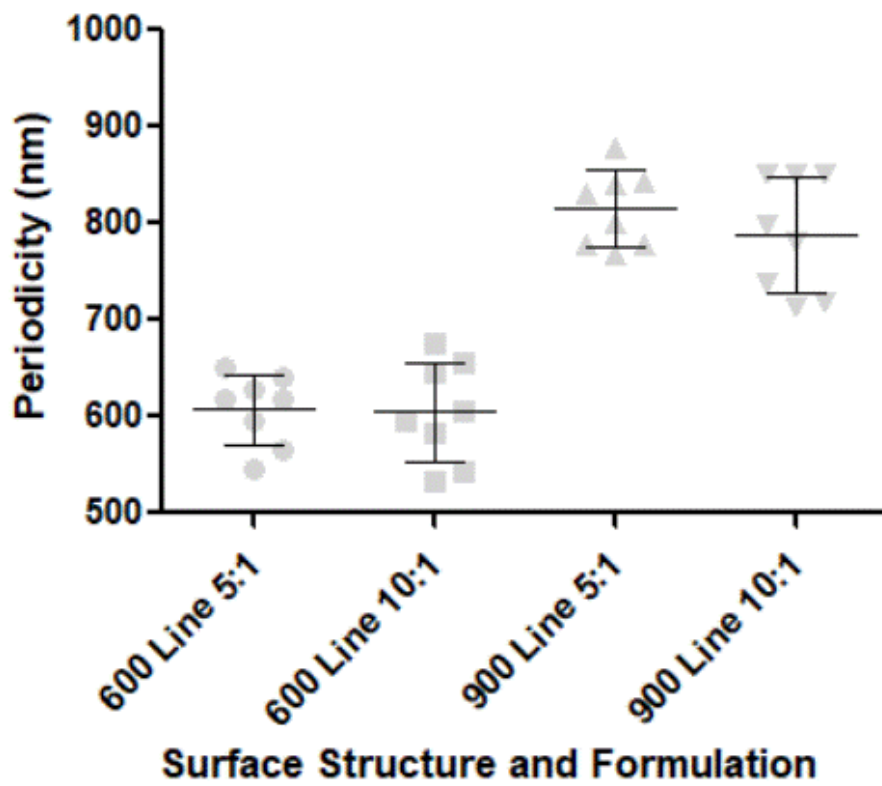


**Figure 4-4: Periodicity of peak-to-peak topographic structures within silicone elastomers with varied elastic modulus.**

The consistency of topographic structures and reproducibility through the experimental silicone elastomer fabrication process is determined through the measurement of peak-to-peak structures upon the AFM images. Linear nanogroove structures of 600 nm and 900 nm were quantified at silicone to crosslinker ratios of 5:1 and 10:1.  $n = 8$ .

### 4.3.3 Silicone allows reliable fabrication of submicron topographic cell culture substrata of varying elastic modulus

The elastic moduli of the topography containing silicone elastomers, as determined through compression testing, were variable. All measurements were obtained across the entire 8 mm circular silicone elastomer containing the nanogroove topography and flat control. By varying the ratio of silicone to crosslinker, the resultant silicone elastomers containing submicron topographies exhibited a consistent variability in their elastic modulus. At a 5:1 ratio of silicone to crosslinker, the elastomer exhibits an average elastic modulus of  $738.9 \pm 308.2$  kPa at 1-day post-fabrication and  $844.8 \pm 174.4$  kPa at 5-days post-fabrication (Figure 4-5A). When the silicone and crosslinker is mixed at a ratio of 10:1, the elastomer exhibits an average elastic modulus of  $1047 \pm 81.57$  kPa following 1-day and  $1145 \pm 171.9$  kPa following 5-days (Figure 4-5B).

Under normal cell culture conditions, the elastic modulus is reduced over time. Regarding the 5:1 silicone elastomer, the average elastic modulus 1-day post-fabrication is  $878.2 \pm 171.2$  kPa, this is reduced to  $688.2 \pm 36.2$  kPa at 5-days post-fabrication in normal cell culture conditions (Figure 4-5C). Similarly, the average elastic modulus of the 10:1 silicone elastomer at 1-day post-fabrication is  $1262 \pm 52$  kPa, and 5-days post-fabrication in normal cell culture conditions is  $849.3 \pm 156.7$  kPa (Figure 4-5D).

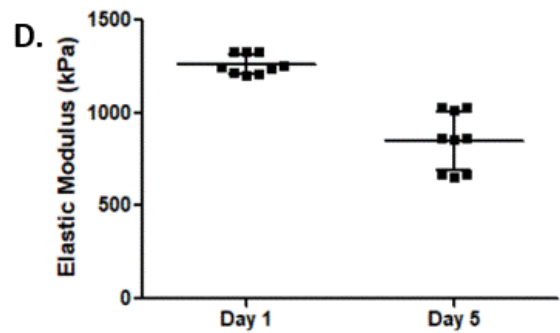
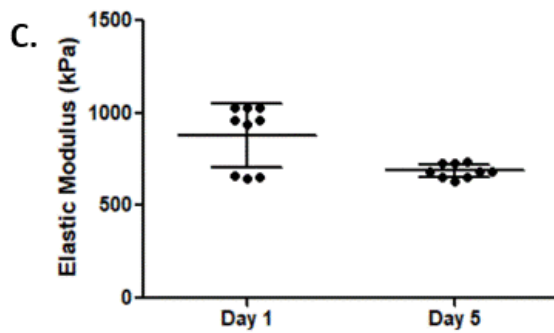
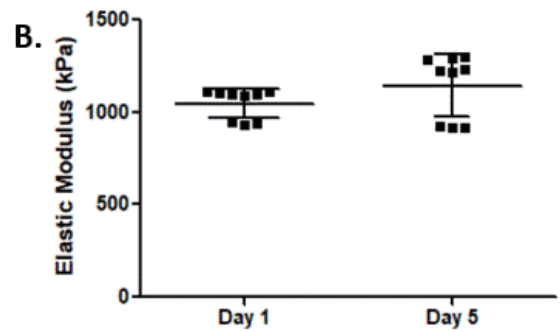
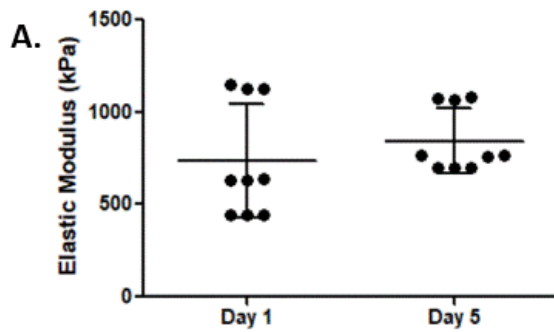


**Figure 4-5: Elastic modulus of the fabricated silicone elastomers patterned with topographic features.**

Compression testing was utilized to determine the elastic modulus of the silicone elastomers. The elastic modulus of silicone elastomers polymerized at a 5:1 ratio of silicone to crosslinker at 1-day and 5-days post fabrication stored under (A) dry conditions and (C) normal cell culture conditions. The elastic modulus of silicone elastomers polymerized at a 10:1 ratio of silicone to crosslinker is quantified under (B) dry conditions and (D) normal cell culture conditions; N = 3, n = 3.

#### 4.3.4 Plasma treated silicone with submicron topographic features are hydrophilic

Through sessile drop goniometry, the contact angle of the 5:1 and 10:1 silicone formulations with 900 nm periodicity nanogrooves was determined (Figure 4-6). The results are summarized in Table 4-2; N = 4. All surfaces exhibited an average contact angle  $< 45^\circ$ , indicating a hydrophilic surface.



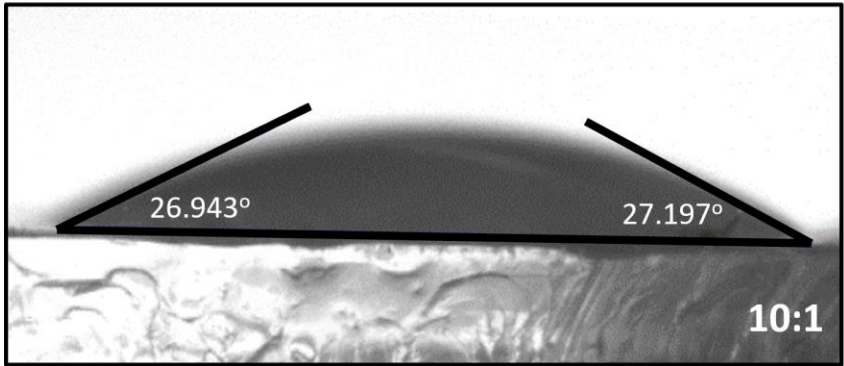
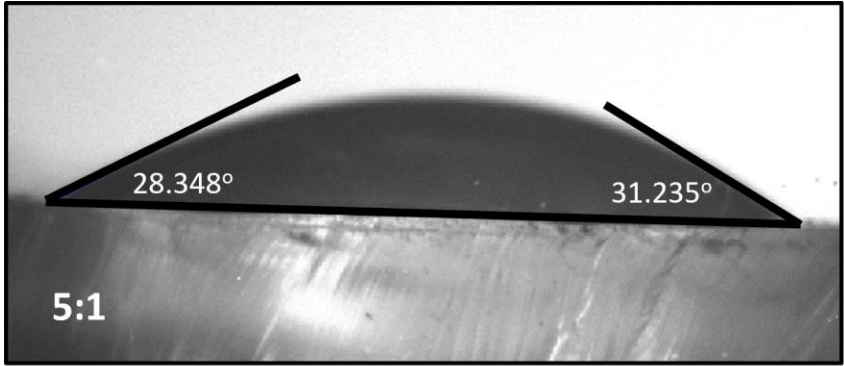


**Figure 4-6: Contact angle measurement upon plasma cleaned 5:1 and 10:1 topographic silicone elastomers**

Surface wettability of silicone elastomers was determined through sessile drop goniometry with 2  $\mu\text{L}$  ultra-pure water was used to measure the contact angle upon all surfaces immediately following argon plasma processing. N = 4.

**Table 4-2 Surface contact angle determined through sessile drop goniometry**

<b>Surface</b>	<b>Average Contact Angle (°)</b>	<b>Standard Deviation (°)</b>
5:1 silicone with 900 nm periodicity nanogroove	29.823	4.013
10:1 silicone with 900 nm periodicity nanogroove	32.569	3.827

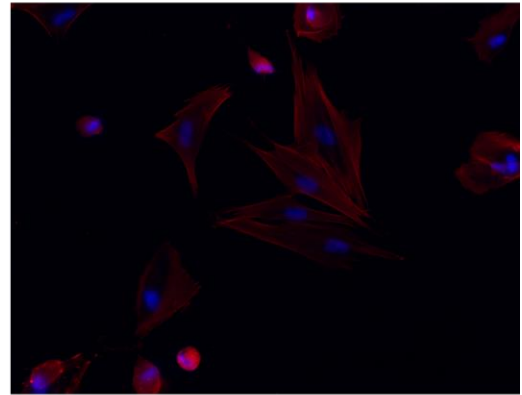
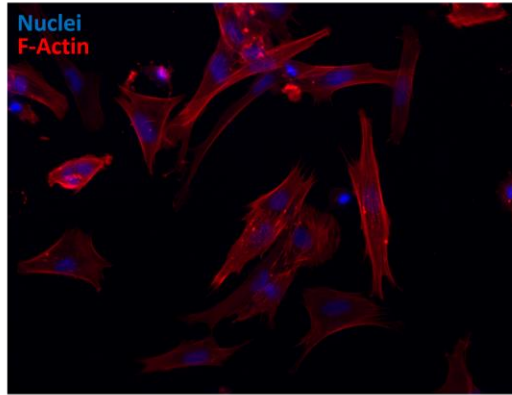
#### 4.3.5 Silicone surfaces with submicron topographic details provides a viable means of cell culture

Following a 24 h incubation period under normal cell culture conditions, HDF and HGF were fixed and stained to visualize their cellular F-actin and nuclei. HDF and HGF adhere, spread and are viable following a 24 h incubation period upon both 5:1 and 10:1 topographic silicone elastomers (Figure 4-7).

HDF

HGF

5:1



10:1

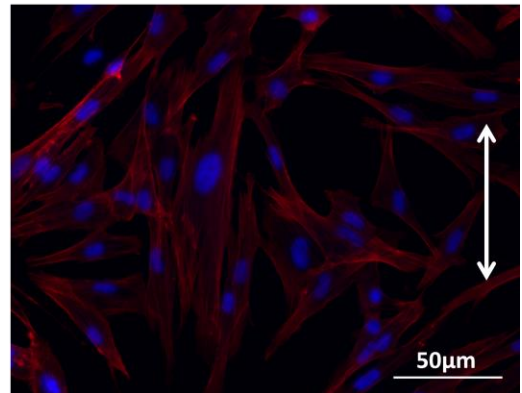
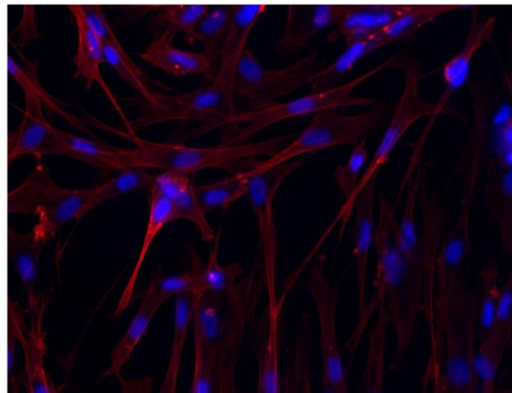


**Figure 4-7: HDF and HDF upon silicone surfaces with a sub-micron topography**

Immunofluorescent imaging of HDF and HGF upon the 5:1 and 10:1 silicone surfaces containing a microgroove topography, 900 nm in periodicity (direction indicated by the white arrow), for cellular F-Actin (red) and nuclei (blue) following a 24 h incubation period. Images obtained at 20X magnification. N = 2. Scale bar = 50  $\mu\text{m}$ .

## 4.4 Discussion

Surface topography and elastic modulus are key extracellular material characteristics which influence cell adhesion, migration, differentiation, protein expression and intracellular signaling cascades <sup>9</sup>. Combining both stimuli in one cell culture device is an important step to better recapitulate the native tissue environment for in vitro studies. However, fabrication of combined topography and modulated elastic modulus cell culture constructs has proved to be difficult <sup>2</sup>. As a result, very few studies have been conducted with human cells upon constructs possessing defined topographic details and an elastic modulus less than tissue culture plastic <sup>1,10</sup>.

Recently, Comelles et al. have established a means of fabricating a hydrogel with < 10um topographic details <sup>10</sup>. Previous work demonstrated that hydrogels patterned with topographic details in the humid cell culture environment lost the intended geometries of the features due to the swelling properties of the hydrogels <sup>2</sup>. I negated the potential effects of swelling and were able to maintain submicron topographic grooves in an elastic modulus tunable material by utilizing silicone elastomers.

### 4.4.1 Silicone provides an optically translucent, structural polymer with negligible swelling to fabricate topographic surfaces of various elastic modulus

In order to reliably reproduce the topographies fabricated in silica described and utilized within the second chapter, a negative impression of the topography had to be accurately produced. The use of PVS as a casting material for topographic negatives was successful as indicated by the presence of interference colours upon the PVS and may be replicated for experimental consistency. The PVS mold volumetric capacity is adequate for the required amount of fabrication material, 2 g silicone elastomer, and are an appropriate size for cell culture and various experimental procedures.

Initial efforts to fabricate elastic modulus varied topographic substratum from the PVS molds were made using polyacrylamide and collagen gels. Polyacrylamide is a well-

established material for the fabrication of tunable elastic modulus tissue culture constructs and has demonstrated its use in numerous studies <sup>2,6,10-12</sup>.

Though the polymerization of polyacrylamide gels within the topographic negatives was successful, the use of polyacrylamide gel, inlaid with a topography, within the cell culture environment had characteristic flaws. Both acrylamide and bis-acrylamide possess high water solubility. Within the tissue culture environment, the processing required of the polyacrylamide gels maintains the polymers in a highly aqueous environment with solutes necessary for cell growth, proliferation and maintenance of life. Polyacrylamide gels swell as result of many conditions including pH, temperature, solutes and water presence (Boyde, 1976). Cell culture requires incubation at 37°C within glucose containing media. Unfortunately, polyacrylamide polymers have been demonstrated to display increased swelling properties to both high temperatures and glucose exposure <sup>13</sup>. A 0.5 M glucose presence leads to a polyacrylamide weight increase of 31% because of swelling while water increases the polyacrylamide gel weight by 18 % (Boyde, 1976). These unavoidable components of the cell culture environment lead to a great level of polyacrylamide gel swelling, thus eliminating any topographical features imprinted within the gel prior to processing. Garland et al. demonstrated the adhesion of the polyacrylamide to an underlying stable constraint can restrict swelling to the depth of the material and topography, however this would establish undesirable groove depths of greater than 100 nm.

Like polyacrylamide, the material provided by Advanced Biomatrix, Photocol, proved successful in fabricating a tunable compliance substratum. However, Photocol is a collagen hydrogel and the use of this material to produce topographic substratum again failed due to the significant amount of swelling that occurred, preventing the maintenance of the topography within the material. The swelling behaviour of hydrogels is well documented and can be controlled by an effective crosslinker, which reduces the pore size and diffusion rate of nutrients and other chemical components thus impacting osmolarity <sup>14</sup>. Photocol utilizes UV irradiation as the primary crosslinking method, inducing chemical and physical changes in the collagen-1 structure <sup>15</sup>. Using this method of crosslinking, one may increase the time under UV to increase the level of crosslinking. Unfortunately, collagen is



susceptible to degradation with increased UV exposure <sup>15</sup>. For this reason, it is not a feasible method to establish minimal swelling within the collagen hydrogels to maintain the defined topographic features.

Ultimately, the use of silicone elastomer in the production of topographic elastomer surfaces has proved most successful. Even though silicone has a greater elastic modulus than polyacrylamide gels, its elastic modulus is much less than that of tissue culture plastic <sup>16</sup>. The methods described in the adapted protocol allow for surfaces to be produced with a variety of elastic moduli and silicone has previously been used to fabricate microgroove topographies <sup>17</sup>.

Through AFM and compression testing, I have established the presence of 900 nm periodicity nanogroove structures, with a depth approximating 100 nm, within varied elastic modulus silicone polymers (Figure 3-5). The nanogrooves are reliably reproducible using the PVS molds and are uniform amongst the silicone elastomers at both 5:1 and 10:1 silicone to crosslinker ratios. The elastic modulus between 5:1 and 10:1 silicone to crosslinker ratios increases from  $738.9 \pm 308.2$  kPa to  $1047 \pm 81.57$  kPa respectively. The established elastic modulus is much greater than the documented elastic modulus of the prefabricated elastic modulus varied tissue culture plates utilized in objective 2. However, it is important to note the conditions under which mechanical testing of the silicone elastomer used in the Cytosoft plates used within objective 2 is not documented. To compare and contrast results obtained from the Cytosoft tissue culture plates, mechanical testing should be completed under the same conditions, including humidity and strain rate, as our topographic silicone elastomers. In this study I focus on the effects of a varied elastic modulus rather than the value of the material elastic modulus. However, future investigations into the effects of specific elastic modulus should be conducted to optimize biomaterial application.

In regard to shelf life, the topographic silicone elastomers appeared to be relatively stable over a period of 5 days, however under normal cell culture conditions the elastic modulus decreases after the same period of time. The elastic modulus of silicone is known to be affected by temperature <sup>18</sup>. The results from objective 2 indicate HDF and HGF alter their

underlying substratum when on lower elastic moduli surfaces, compared to TCP, through extracellular matrix production. With this in mind, the effect of the cell culture substratum over time will decrease as cells become confluent and make fewer adhesions with the underlying tissue culture construct. Therefore, the change in elastic modulus over 5 days in cell culture conditions is of little concern. Overall, the investigated shelf-life is suitable for *in vitro* studies.

#### 4.4.2 The fabricated topographic silicone elastomers establish development of a novel cell culture device.

Following argon plasma cleaning, the topographic silicone elastomers are very hydrophilic as demonstrated by their contact angle measurement. It is also a well-established method for sterilizing biomaterials for use both *in vitro* and *in vivo*<sup>19</sup>. Together, the topographic silicone elastomers are favourably prepared for cell culture.

Preliminary *in vitro* investigation into HDF and HGF adhesion and viability upon the topographic silicone elastomers demonstrated promising results. The culturing of both HDF and HGF upon the investigative surfaces was successful. Both HDF and HGF adhere and exhibit varying degrees of cell spreading, similar to behaviour observed in objective 2. Despite the higher elastic modulus than previously investigated in objective 2, the difference in elastic modulus is still capable of eliciting a differential response by HDFs and HGFs. I can now proceed with comparative studies between HDFs and HGFs to determine how the combined effects of topography and substratum elastic modulus impact their cellular physiology while referencing what I have learned from the investigations into each mechanical stimulus independently. This step is crucial to understanding how the mechanical stimuli direct cell behavior *in vivo*.

In conclusion, I have laid a foundation for future *in vitro* studies on cell culture substrata containing topographical features and a varied elastic modulus. These surfaces enable *in vitro* investigations with greater physiological relevance. This system better mimics the native tissue, allowing for a more accurate translation of observed cellular mechanisms from the *in vitro* to *in vivo* environment in a means not previously available.

## 4.5 References

- (1) Al-Haque, S.; Miklas, J. W.; Feric, N.; Chiu, L. L. Y.; Chen, W. L. K.; Simmons, C. A.; Radisic, M. Hydrogel Substrate Stiffness and Topography Interact to Induce Contact Guidance in Cardiac Fibroblasts. *Macromol Biosci* **2012**, *12* (10), 1342–1353. <https://doi.org/10.1002/mabi.201200042>.
- (2) Garland, S. P.; McKee, C. T.; Chang, Y. R.; Raghunathan, V. K.; Russell, P.; Murphy, C. J. A Cell Culture Substrate with Biologically Relevant Size-Scale Topography and Compliance of the Basement Membrane. *Langmuir* **2014**, *30* (8), 2101–2108. <https://doi.org/10.1021/la403590v>.
- (3) Comelles, J.; Fernández-Majada, V.; Acevedo, V.; Rebollo-Calderon, B.; Martínez, E. Soft Topographical Patterns Trigger a Stiffness-Dependent Cellular Response to Contact Guidance. *Mater Today Bio* **2023**, *19*. <https://doi.org/10.1016/j.mtbio.2023.100593>.
- (4) Bhana, B.; Iyer, R. K.; Chen, W. L. K.; Zhao, R.; Sider, K. L.; Likhitpanichkul, M.; Simmons, C. A.; Radisic, M. Influence of Substrate Stiffness on the Phenotype of Heart Cells. *Biotechnol Bioeng* **2010**, *105* (6), 1148–1160. <https://doi.org/10.1002/bit.22647>.
- (5) Wang, J.; Zheng, M.; Wang, W.; Li, Z. *Optimal Protocol for Moulding PDMS with a PDMS Master*; 2010.
- (6) Pelham, R. J.; Yu-Li, W. Cell Locomotion and Focal Adhesions Are Regulated by Substrate Flexibility. *Proc Natl Acad Sci U S A* **1997**, *94*, 13661–13665. <https://doi.org/10.1073/pnas.94.25.13661>.
- (7) Elliott, C. G.; Wang, J.; Guo, X.; Xu, S.; Eastwood, M.; Guan, J.; Leask, A.; Conway, S. J.; Hamilton, D. W. Periostin Modulates Myofibroblast Differentiation during Full-Thickness Cutaneous Wound Repair. *J Cell Sci* **2011**, *125* (Pt 1), 121–132. <https://doi.org/10.1242/jcs.087841>.
- (8) Tilghman, R. W.; Cowan, C. R.; Mih, J. D.; Koryakina, Y.; Gioeli, D.; Slack-Davis, J. K.; Blackman, B. R.; Tschumperlin, D. J.; Parsons, J. T. Matrix Rigidity Regulates

- Cancer Cell Growth and Cellular Phenotype. *PLoS One* **2010**, 5 (9), 1–13.  
<https://doi.org/10.1371/journal.pone.0012905>.
- (9) Khalili, A. A.; Ahmad, M. R. A Review of Cell Adhesion Studies for Biomedical and Biological Applications. *International Journal of Molecular Sciences*. 2015.  
<https://doi.org/10.3390/ijms160818149>.
- (10) Comelles, J.; Fernández-Majada, V.; Berlanga-Navarro, N.; Acevedo, V.; Paszkowska, K.; Martínez, E. Microfabrication of Poly(Acrylamide) Hydrogels with Independently Controlled Topography and Stiffness. *Biofabrication* **2020**, 12 (2).  
<https://doi.org/10.1088/1758-5090/ab7552>.
- (11) Denisin, A. K.; Pruitt, B. L. Tuning the Range of Polyacrylamide Gel Stiffness for Mechanobiology Applications. *ACS Appl Mater Interfaces* **2016**, 8 (34), 21893–21902.  
<https://doi.org/10.1021/acsami.5b09344>.
- (12) Mih, J. D.; Sharif, A. S.; Liu, F.; Marinkovic, A.; Symer, M. M.; Tschumperlin, D. J. A Multiwell Platform for Studying Stiffness-Dependent Cell Biology. *PLoS One* **2011**, 6 (5), 1–10. <https://doi.org/10.1371/journal.pone.0019929>.
- (13) Boyde, T. R. C. Swelling and Contraction of Polyacrylamide Gel Slabs in Aqueous Solutions. *J Chromatogr A* **1976**, 124 (2), 219–230. [https://doi.org/10.1016/S0021-9673\(00\)89737-X](https://doi.org/10.1016/S0021-9673(00)89737-X).
- (14) Dubey, N. K.; Deng, W.-P. Polymeric Gels for Cartilage Tissue Engineering. In *Polymeric Gels*; Elsevier, 2018; pp 505–525. <https://doi.org/10.1016/b978-0-08-102179-8.00020-x>.
- (15) Jiang, Y.-H.; Lou, Y.-Y.; Li, T.-H.; Liu, B.-Z.; Chen, K.; Zhang, D.; Li, T. *Cross-Linking Methods of Type I Collagen-Based Scaffolds for Cartilage Tissue Engineering*; 2022; Vol. 14. [www.ajtr.org](http://www.ajtr.org).
- (16) Feng, L.; Li, S.; Feng, S. Preparation and Characterization of Silicone Rubber with High Modulus via Tension Spring-Type Crosslinking. *RSC Adv* **2017**, 7 (22), 13130–13137.  
<https://doi.org/10.1039/c7ra00293a>.

- (17) Schmidt, J. A.; Van Recum, A. F. Texturing of Polymer Surfaces at the Cellular Level. *Biomaterials* **1991**, *12*, 385–389.
- (18) Rey, T.; Chagnon, G.; Le Cam, J. B.; Favier, D. Influence of the Temperature on the Mechanical Behaviour of Filled and Unfilled Silicone Rubbers. *Polym Test* **2013**, *32* (3), 492–501. <https://doi.org/10.1016/j.polymertesting.2013.01.008>.
- (19) Mozaffari, A.; Gashti, M. P.; Mirjalili, M.; Parsania, M. Argon and Argon-Oxygen Plasma Surface Modification of Gelatin Nanofibers for Tissue Engineering Applications. *Membranes (Basel)* **2021**, *11* (1), 1–13. <https://doi.org/10.3390/membranes11010031>.

## 5 Discussion

### 5.1 General Discussion

In this thesis, I investigated how fibroblast, attachment, adhesion, spreading, morphology, proliferation, and phenotypic modulation was influenced by geometrical and physical stimuli present in the tissue microenvironment, specifically substratum topography and variations in elastic modulus. Additionally, by comparing fibroblasts from different tissues of origin, dermis associated with scarring, and gingiva associated with regeneration, the cellular mechanisms associated with these disparate functional outcomes can begin to be parsed out. In this thesis I established significant differences in adhesion formation and composition in human dermal and gingival fibroblasts which was manifest in matrix secretion and contractile ability, processes which are known to contribute to tissue repair and fibrosis. In short, the tissue of origin of fibroblasts as well as the individual from which they are isolated are both major determinants of their response to topographical cues and elastic moduli. To take these kinds of studies forward, in the third aim of my thesis, I also developed a novel cell culture device which combines both elastic modulus and sub-micron level topography. This is a significant step for future investigations into how combining these physical cues can be manipulated to control cell phenotype and tissue repair.

#### 5.1.1 Quantification and comparison of human dermal and gingival fibroblast adhesion composition and behaviours on materials patterned with anisotropic sub-micron topographies

When considering biomaterial design, surface modification of materials has been investigated to optimize tissue formation and cellular response upon implantation, with pH, scaffold porosity, elemental charge, temperature, and ionic strength all shown to be important parameters to control <sup>1</sup>. Surface modification through topographic patterning has been widely investigated, particularly for the incorporation of bone interfacing materials such as replacement hip/knee joints and dental implants, with the aim of speeding osseointegration <sup>1</sup>. Research into topographic manipulation of soft tissue interfacing materials has only recently become a focus due to advances in methods of fabrication <sup>2</sup>.

The process of contact guidance, mechanosensation and response to underlying substratum topography, is known to influence cell morphology, adhesion formation and migration<sup>3</sup>. This process is crucial for tissue development, wound repair and is also evident in several pathological processes<sup>4-6</sup>. Research has shown human dermal fibroblasts increase fibronectin secretion, guided migration, decreased planar cell surface area, and decreased MMP protein expression on topographic substratum compared to surfaces lacking a distinct topography<sup>7,8</sup>. However, gingival fibroblasts have been less of a focus in comparison<sup>9</sup>.

In this thesis, I have investigated the role of topography on contact guidance of human dermal and gingival fibroblasts, tissues associated with scar and regeneration after healing, respectively. I hypothesized that the addition of anisotropic submicron level topographies would decrease cellular adhesion, proliferation, extracellular matrix production and cell contractility. I provide unique insight into the effects of topographic contact guidance between a scarring and non-scarring cell population, observing a differential adhesion formation upstream of mechanosensation, information that can be used to guide biomaterial fabrication.

Specifically, I established both HGFs and HDFs exhibit morphological and adhesion alignment with respect to the long axis of sub-micron groove topographies. When a repeated groove structure, with periodicities of 600 nm and 900 nm, is patterned on the culture substratum, both HGFs and HDFs align their cell long axis, as well as vinculin containing focal adhesion sites and tensin-1 containing fibrillar adhesion sites and newly deposited fibronectin matrix with the direction of the groove structure. Most studies point to the physiological relevance of topography with structure periodicities ranging from 2 – 50  $\mu\text{m}$  due to similar scale features as collagen fibrils in the extracellular matrix<sup>10</sup>. However, it has been determined that rat fibroblasts require ligand spacing of ~60 – 140 nm for regular focal adhesion and stress fiber formation<sup>11</sup>. Micrometric topographic details may elicit the desired response from many cell types, but in reality, the cellular mechanosensory capacity is on a much smaller scale. I demonstrate HDF and HGF contact guidance on nanometric depth topographies and have provided mechanistic differences through adhesion site composition and response to submicron topography. *In vivo*, the cells behaviour may in fact be a response to stimuli much smaller than the ECM fibrils, including

the various extracellular proteins such as periostin, known to influence HGF adhesion to the extracellular matrix <sup>12</sup>.

When investigating the mechanisms underlying the observed contact guidance, I confirmed integrins  $\alpha\beta3$  and  $\beta1$  play a critical role in cell spreading and elongation, however the inhibition of integrin  $\alpha\beta3$  still enables HDF and HGF cell adhesion and spreading, though impaired. I also identified integrin  $\beta1$  as a critical mechanosensory component for alignment and contact guidance in HDFs, but not in HGFs. In HDFs, but not HGFs, inhibition of  $\beta1$  integrins induces tensin-1 recruitment to focal adhesion sites located near the periphery of the cell. It has previously been established that topographic details can disrupt extracellular matrix deposition <sup>9</sup>. The disruption of tensin-1 and integrin  $\beta1$  adhesion sites also inhibit extracellular matrix deposition <sup>13</sup>. As such, my research suggests topographic modulation of integrin  $\beta1$  and tensin-1 may open new avenues for inhibiting fibrosis around dermis implanted materials.

### 5.1.2 Quantification and comparison of human dermal and gingival fibroblast adhesion composition and behaviours on materials of varying elastic moduli.

Substratum elastic modulus is a robust mechanical stimulus that alters cell physiology and is itself a result of cell behaviour and signaling activity <sup>14</sup>. The elastic modulus of a cell's underlying substratum is known to influence cell behaviours including adhesion formation, morphology, migration, gene expression and matrix synthesis <sup>15-17</sup>. *In vivo*, the elastic modulus of the cellular microenvironment varies dramatically from 13.7 GPa in alveolar bone to as little as 100 Pa in neural tissue <sup>18,19</sup>. Currently, it is accepted that cellular adhesion sites and associated cytoskeletal components are prerequisites for cell sensing any variations in substratum elastic modulus; however more research is needed to completely understand the role of adhesions and their associated components in this observation <sup>20</sup>.

This thesis investigated the influence of substratum elastic modulus on human dermal and gingival fibroblast physiology, focusing on adhesion changes related to contraction and



extracellular matrix formation. An increase in substratum elastic modulus was hypothesized to increase cell adhesion, proliferation, extracellular matrix production, and cell contractility in a manner dependent on tissue of origin. I demonstrated HDFs and HGFs show different responses to substratum elastic modulus in terms of adhesion size and composition, F-actin arrangement, myofibroblast differentiation and extracellular matrix deposition.

It was determined HDFs and HGFs exhibit higher adherence to surfaces with lower elastic modulus, and the 8 kPa elastic modulus substratum promoted the highest increase in cell number at day 5 post-seeding. As prior research, both in the literature as well as in this thesis, demonstrates a higher elastic modulus establishes more stable, larger adhesion sites in cells, the finding that lower elastic modulus surfaces of 0.2 kPa and 8 kPa promote increased adherence and proliferation compared to TCP was somewhat unexpected. With respect to wound healing, this finding may highlight cellular processes needed or associated with, the transition from clot to granulation tissue to scarring. As granulation tissue matures, the environment in which dermal fibroblasts are present increases in elastic modulus<sup>21,22</sup>. Fibroblasts are required to adhere within the granulation tissue, of low elastic modulus, to migrate into and within the wound site, reconstruct the extracellular matrix and differentiate into myofibroblasts<sup>21,22</sup>. The proliferation of fibroblasts during this same phase progression is expected to decrease as cells assume a myofibroblast contractile phenotype<sup>23</sup>.

Additionally, the increased early adhesion as well as temporal proliferation on lower elastic modulus surfaces speaks to the conditions of which many *in vitro* studies take place – on tissue culture plastic. Previous studies have stated that tissue culture plastic is not an optimal experimental construct to recapitulate *in vivo* conditions<sup>24</sup>. It has also been postulated that cells have an intrinsic elastic modulus and their physiology is optimized upon surfaces which match this mechanical property<sup>3,15,25</sup>. This thesis provides useful data regarding the preferential elastic moduli of HDF and HGF adhesion and proliferation and can direct future studies which aim to investigate these characteristics.

This thesis further determines that elastic modulus can modulate HGF differentiation. HDF differentiation into myofibroblasts however, is strongly regulated by TGF- $\beta$ 1 signaling irrespective of the substratum elastic modulus. The contrast in HGF and HDF response to exogenous TGF- $\beta$ 1 upon various substratum elastic modulus pointed to a mechanistic difference. Myofibroblast differentiation has traditionally been associated with an increase in intracellular tension including the incorporation of  $\alpha$ SMA into stress fibers and large fibrillar adhesion sites<sup>26</sup>. Through the evaluation of tensin-1 involved fibrillar adhesions formed by HGFs upon 0.2 kPa and TCP with exogenous TGF- $\beta$ 1 I found a disruption of integrin engagement in the adhesion sites. Integrin  $\beta$ 1 became expressed in the periphery of the cell, traditionally known to possess focal adhesions, and tensin-1 colocalization was disrupted upon the 0.2 kPa elastic modulus surface. This finding points to a unique means of disrupting integrin  $\beta$ 1 engagement, an integrin implicated in fibrosis<sup>27,28</sup>, and tensin-1 recruitment. Overall, this study provides important insights into the interplay between substratum elastic modulus, fibroblast behavior, and potential implications for tissue engineering and wound healing.

### 5.1.3 The fabrication of a novel, combined, elastic modulus varied, topographic cell culture device to quantitate human dermal and gingival fibroblast behavior.

The structure of the ECM provides cells with both topographic and mechanical cues to which they respond based on the properties of the matrix<sup>29</sup>. To the best of our knowledge, this is the first time a submicron topography has been successfully incorporated into a tunable elastic modulus material for cell culture applications. I have demonstrated submicron topographies are capable of augmenting HDF and HGF adhesion formation and as a result impact underlying behaviours such as matrix production and myofibroblast differentiation. In combination with the research presented in this thesis and recent literature demonstrating cellular control through elastic modulus modulated substratum containing micrometric topographic details<sup>30</sup>, the submicron topographic silicone elastomers provides a means to determine how cells integrate these mechanical stimuli and give insight into their effects *in vivo*.

## 5.2 Contributions to the Literature

### 5.2.1 Tissue of Origin as a Variant in Fibroblast response to topography and variations in elastic moduli

In its simplest form, a fibroblast is considered a work horse cell type, which produces and turns over the extracellular matrix maintaining tissue homeostasis and architecture <sup>31</sup>. In the context of wound healing, a fibroblast is also responsible for contraction of the wound site and contributing to the immune response by upregulation of adhesion markers and pro-inflammatory cytokines <sup>32,33</sup>. Even though both HDF and HGFs are classified as fibroblasts, literature has identified quintessential differences between the two populations. Beginning with their embryonic origin, human gingival and dermal fibroblasts arise from the neural crest and mesoderm, respectively; HGFs also have distinct gene expression, response to inflammatory mediators and reduced FAK expression <sup>34-36</sup>. Most notably, gingival cells have been said to have fetal like characteristics, a capacity of tissue regeneration rather than scarring as observed within HDFs <sup>34</sup>. The physiological divide between HDFs and HGFs in wound healing is unexpected and remains an area of active investigation. By understanding the processes in gingiva that result in regeneration without scarring, potential targets could be identified to reduce fibrosis in organs and skin.

Through this work I have identified differences in HDF and HGF behavior, quantifying mechanistic differences which help to understand their role of differential healing outcomes in their respective tissues of origin. Previous research has demonstrated a species dependent mechanism of oral wound healing between rat and pig <sup>12,37</sup>. In rat gingival healing, myofibroblasts are sparse <sup>12</sup>. However, the elevated level of myofibroblasts in oral wound healing of red Duroc pigs is postulated as a key element to their reduced scar formation <sup>37</sup>. These observations bring to question the relatability of animal research in mimicking human cellular response, and it is clear only certain models of pigs are similar to humans, while rats don't recapitulate human healing at all with regards to myofibroblasts. One also cannot rule out variability that would be observed between individual animals. It is well known that animals are not perfect models of human disease

– they present anatomical and physiological differences, with no one model encompassing the complexity of wound healing in humans<sup>38</sup>. With this work, I demonstrate the variation and complexity of adhesion formation may be even greater than thought and this directly impacts on healing outcomes.

### 5.2.2 Hierarchical Adhesion Theory: Are $\beta 1$ integrins the real determinant of contraction, but not necessarily of adhesion maturity?

The prominent theory in cellular adhesion formation was published by Zaidel-Bar et al. in 2004 where it was proposed that a hierarchical assembly of adhesions from focal complexes to focal adhesions to fibrillar adhesions exists, with each type of adhesion representing increasing maturity of attachment<sup>39</sup>. Additionally, it is the cross talk between FAK, phosphorylated paxillin and force transduction that leads to the transition between focal adhesions and tensin-1 engaged fibrillar adhesions (Zaidel-Bar et al., 2007). In this thesis, I investigated focal and fibrillar adhesion formation. Classically defined, focal adhesions are matured intermediate adhesion complexes characterized by a recruitment of zyxin, integrin  $\alpha v\beta 3$ , talin, vinculin, and increased adhesion area (3 - 10  $\mu\text{m}$ ) at the terminus of actin stress fibers<sup>41-44</sup>. Fibrillar adhesions have been defined as  $\alpha 5\beta 1$  integrin and tensin-1 association elongated along the fibronectin matrix<sup>45-47</sup>.

We are challenging these theories and definitions as our data has demonstrated adhesion composition is cell population and culture condition dependent. I have demonstrated fibroblasts are capable of forming adhesion sites with tensin-1 and integrin  $\alpha v\beta 3$  when integrin  $\beta 1$  is inaccessible. I have also found integrin  $\beta 1$  to be present in the periphery of the cell, not associated with tensin-1, but in regions normally associated with focal adhesions. This change is notable in HGFs when treated with TGF- $\beta 1$ ; a treatment seen to induce myofibroblast differentiation in both HDFs and HGFs on TCP. In combination with the previous finding that HGF adhesion to periostin requires integrin  $\beta 1$  (Kim et al., 2019), I confirm in this thesis that integrin  $\beta 1$  is required for adhesion outside of the traditional fibrillar adhesion formation. Our work demonstrates the theories proposed by Zaidel-Bar

et al. are accurate solely under the conditions in which they were investigated<sup>39</sup>. I propose integrin  $\beta 1$  recruitment is not maturity dependent but rather a cellular resource to form stable adhesions, especially under conditions of poor adhesive properties and when integrin  $\alpha v\beta 3$  is inaccessible, to enable intracellular tension and the transition into myofibroblasts.

### 5.2.3 How to engage an Integrin.

As shown in this thesis, both fibroblast populations contain all the proteins required to form focal and fibrillar adhesion sites. The differential engagement of integrins into these adhesion sites by HDF and HGF points to a potential disparity in mechanisms underlying integrin recruitment. Research suggests integrin recruitment is regulated by several processes including conformational changes to alter their ligand affinity, integrin clustering by increasing bonds with the substratum, vesicular tracking to the plasma membrane and force transduction via the ECM or actomyosin-mediated intracellular tension<sup>48</sup>. The rigidity of a substratum is thought to impact the rate of turnover in integrin engagement dependent upon the amount of force being transduced over them<sup>49</sup>.

In this research, I demonstrate both topography and substratum elastic modulus effect integrin engagement in a cell population dependent manner. I found HDFs require integrin  $\beta 1$  engagement for contact guidance while HGFs do not. I also found integrin  $\beta 1$  engages in adhesion complexes with both vinculin and tensin-1. Finally, I propose integrin  $\beta 1$  is a robust protein, and serves a vital role in establishing cell attachment and intracellular tension. As integrin  $\beta 1$  has been implicated in fibrosis<sup>27</sup>, our research can aid in biomaterial design to mitigate integrin  $\beta 1$  involvement and reduce the potential of fibrotic encapsulation of implanted biomaterials by incapacitating traditional fibrillar adhesion sites resulting in the disruption of extracellular matrix deposition.

#### 5.2.4 Topography VS Elastic Modulus: Is one more important than the other?

As indicated throughout this thesis, there is considerable research on both substratum elastic modulus and topography and their effects on cellular physiology. Though current work is focused on combining the two stimuli to create more accurate *in vitro* investigations <sup>2</sup>, as I establish in this work, questions remain on the importance of both stimuli to biomaterial design. In mice, reduction of implant stiffness by coating with a soft silicone layer can reduce collagen deposition and myofibroblast activation <sup>50</sup>. Work in the Hamilton Lab has demonstrated randomly organized pitting on titanium can disrupt HGF fibrillar adhesion formation, decrease adhesion stability, and inhibit myofibroblast differentiation and fibronectin deposition <sup>9</sup>. Evidently, even upon a material with a high elastic modulus such as titanium, topographic effects still prevail with reduction of profibrotic behaviours.

In conjunction with the literature <sup>9,50</sup>, the contents of this thesis indicate by harnessing the antifibrotic properties of topography and elastic modulus, significant progress can be made in reducing fibrotic events relating to implanted biomaterials. I postulate a combination of a low elastic modulus with an anisotropic sub-micron topography will inhibit stable fibroblast adhesion formation and subsequent myofibroblast differentiation and extracellular matrix production.

### 5.3 Experimental Limitations

All cell experiments conducted in this thesis were completed using primary fibroblast lines obtained from multiple individual donors. Based on human ethics protocols related to tissue harvest, I have limited access to information about each individual donor. As a result of this, these cell lines are likely quite variable as a result of age, sex, ethnicity, genetics and potential morbidities. Age is a well-known determinant of wound healing; elderly humans experience a slower rate of wound healing within each temporal phase with a lesser degree of remodeling and poorer collagen organization <sup>51</sup>. Additionally, it has been suggested testosterone increases the rate of oral wound healing, while females experience a greater

rate of dermal wound healing <sup>52</sup>. Many comorbidities such as diabetes, autoimmune conditions and radiation exposure are also known to impact wound healing capacity <sup>31</sup>.

In our laboratory, fibroblast are isolated from dermal and gingival tissue explants using digestion and media to optimize fibroblast separation. It is important to recognize the results presented in this thesis are a combination of fibroblast subpopulations retrieved from the dermis including papillary, reticular, and follicular fibroblasts <sup>53</sup>. As I identify differences between dermal and gingival fibroblasts, these subpopulations also possess distinct characteristics including extracellular matrix production and organization, and production of growth factors and cytokines <sup>53</sup>. There are also inherent limitations when working with primary human cell lines.

In chapter 3, I use pre-fabricated tissue culture plates coated with silicone elastomers of various elastic moduli from Advanced Biomatrix. In the process of fabricating the topographic silicone elastomers of chapter 4, the elastic modulus is determined under specific conditions including temperature, pH, strain rate and material dimensions. To accurately compare and contrast results obtained from the Cytosoft tissue culture plates, mechanical testing should be completed under the same conditions as our topographic silicone elastomers. This process would allow us to manipulate the fabrication process of the topographic silicone elastomers to achieve a comparable elastic modulus to that of the Cytosoft tissue culture plates and enable accurate conclusions to be drawn upon the effect of combined elastic modulus and topographic stimuli.

## 5.4 Future Directions

With a working cell culture device to investigate the combined effects of topography and elastic modulus, future experiments will establish how the two stimuli integrate to effect HDF and HGF cell adhesion patterns and their resultant behaviour. The topographic silicone elastomers should also be compared directly to the Cytosoft tissue culture plates from Advanced Biomatrix by conducting mechanical testing under the same conditions. This comparison will further define the topographic silicone elastomers with regards to a

commercially available product and allow other research groups to compare their own data collected upon the Cytosoft surfaces to our work upon the topographic silicone elastomers. Additional topographic silicone elastomers should also be fabricated to match the elastic modulus of native skin,  $\sim 100 - 400$  kPa<sup>29</sup>, to determine if topography can alter HDF behaviour under *in vivo* mechanical stimuli.

The extracellular matrix niche is a complex microenvironment. A variety of mechanical, chemical, and electrical stimuli are present at any given time with which a cell must sense, integrate, and respond<sup>54</sup>. The complexity of the extracellular environment makes it difficult to understand the processes underlying each stimulus and how they affect cell behaviour. It is for this reason the reductionist approach improves the understanding of mechanisms and is the basis for the experimental design in my thesis. In this thesis I analyze the effects of topography and elastic modulus, to understand the individual effects followed by the complex combined effect upon HDF and HGF physiology. In general, a variety of mechanical, chemical, and electrical cues have been investigated in isolation however, combinations of these stimuli have yet to be modelled in an accurate and controllable manner<sup>55,56</sup>. I now have established an accurate and controllable cell culture device to investigate the combined effects of multiple mechanical stimuli and will work to combine chemical and electrical cues present in the *in vivo* environment as well.

Future studies will assess how our topographic silicone elastomers influence capsule formation and fibrosis using *in vivo* models. Using a porcine model, due to their largely similar skin structure to humans<sup>57</sup>, the topographic silicone elastomers could be implanted and evaluated for fibrotic capsule formation. Recently, micrometric hexagonal topographic features have been found to reduce fibrotic capsule formation upon pacemakers<sup>58</sup>.

With any human study, I can continue to strengthen the findings by investigating more patients and how different patient demographics impact the investigated cell behaviours, both in HDF and HGF. Sex hormones are known to modulate many disease states including diabetes, diabetes, and osteoporosis<sup>59</sup>. Estrogens also inhibit the development of tissue fibrosis<sup>59</sup>. Additionally, an individuals' advanced age is well established predisposition for pulmonary and cardiac fibrosis<sup>60</sup>.



## 5.5 Conclusions

First, I demonstrated human dermal and gingival fibroblasts exhibit differential responses to the same topographies and found  $\beta 1$  integrins are crucial for HDF cell alignment to submicron grooves. HDF and HGFs do not incorporate the same proteins for use as mechanosensory machinery. I further indicated HDF and HGF exhibit different sensitivity to changes in substratum elastic modulus. HDFs are more likely to exhibit a contractile phenotype despite the substratum's low elastic modulus. I have fabricated a submicron groove topography in a tunable elastic modulus material to enable investigations into cell physiology upon a topographic material not available previously. Finally, I conclude, fibroblasts from different tissue origins exhibit distinct responses to these stimuli, emphasizing the need for tissue-specific considerations in biomaterial design.

## 5.6 References

- (1) Devgan, S.; Sidhu, S. S. Evolution of Surface Modification Trends in Bone Related Biomaterials: A Review. *Mater Chem Phys* **2019**, *233*, 68–78.  
<https://doi.org/10.1016/j.matchemphys.2019.05.039>.
- (2) Comelles, J.; Fernández-Majada, V.; Berlanga-Navarro, N.; Acevedo, V.; Paszkowska, K.; Martínez, E. Microfabrication of Poly(Acrylamide) Hydrogels with Independently Controlled Topography and Stiffness. *Biofabrication* **2020**, *12* (2).  
<https://doi.org/10.1088/1758-5090/ab7552>.
- (3) Brunette, D. M.; Chehroudi, B. The Effects of the Surface Topography of Micromachined Titanium Substrata on Cell Behavior in Vitro and in Vivo. *J Biomech Eng* **1999**, *121*, 49–57.
- (4) Britland, S.; Morgan, H.; Wojciak-Stodart, B.; Riehle, M.; Curtis, a; Wilkinson, C. Synergistic and Hierarchical Adhesive and Topographic Guidance of BHK Cells. *Exp Cell Res* **1996**, *228* (228), 313–325. <https://doi.org/10.1006/excr.1996.0331>.
- (5) Curtis, A. S. G.; Clark, P. The Effects of Topographic and Mechanical Properties of Materials on Cell Behaviour. *Critical Reviews in Biocompatibility* **1990**, *5*, 343–362.
- (6) Brunette, D. M. The Effects of Surface Topography on the Behaviour of Cells on Implants. *International Journal of Oral and Maxillofacial Implantology* **1988**, *3*, 231–246.
- (7) Mudera, V. C.; Pleass, R.; Eastwood, M.; Tarnuzzer, R.; Schultz, G.; Khaw, P. Molecular Responses of Human Dermal Fibroblasts to Dual Cues : Contact Guidance and Mechanical Load. *Cell Motil Cytoskeleton* **2000**, *45* (September 1999), 1–9.
- (8) Chou, L.; Firth, J. D.; Uitto, V.; Brunette, D. M. Substratum Surface Topography Alters Cell Shape and Regulates Fibronectin mRNA Level , mRNA Stability , Secretion and Assembly in Human Fibroblasts. *J Cell Sci* **1995**, *108*, 1563–1573.

- (9) Kim, S. S.; Wen, W.; Prowse, P.; Hamilton, D. W. Regulation of Matrix Remodelling Phenotype in Gingival Fibroblasts by Substratum Topography. *J Cell Mol Med* **2015**, *19* (6), 1183–1196. <https://doi.org/10.1111/jcmm.12451>.
- (10) Leclech, C.; Villard, C. Cellular and Subcellular Contact Guidance on Microfabricated Substrates. *Frontiers in Bioengineering and Biotechnology*. Frontiers Media S.A. October 22, 2020. <https://doi.org/10.3389/fbioe.2020.551505>.
- (11) Cavalcanti-adam, E. A.; Volberg, T.; Micoulet, A.; Kessler, H.; Geiger, B.; Spatz, J. P. Cell Spreading and Focal Adhesion Dynamics Are Regulated by Spacing of Integrin Ligands. **2007**, *92* (April), 2964–2974. <https://doi.org/10.1529/biophysj.106.089730>.
- (12) Kim, S. S.; Nikoloudaki, G. E.; Michelsons, S.; Creber, K.; Hamilton, D. W. Fibronectin Synthesis, but Not  $\alpha$ -Smooth Muscle Expression, Is Regulated by Periostin in Gingival Healing through FAK/JNK Signaling. *Sci Rep* **2019**, *9* (1). <https://doi.org/10.1038/s41598-018-35805-6>.
- (13) Danen, E. H. J.; Sonneveld, P.; Brakebusch, C.; Fässler, R.; Sonnenberg, A. The Fibronectin-Binding Integrins A5 $\beta$ 1 and Av $\beta$ 3 Differentially Modulate RhoA-GTP Loading, Organization of Cell Matrix Adhesions, and Fibronectin Fibrillogenesis. *Journal of Cell Biology* **2002**, *159* (6), 1071–1086. <https://doi.org/10.1083/jcb.200205014>.
- (14) Yang, S.; Plotnikov, S. V. Mechanosensitive Regulation of Fibrosis. *Cells*. MDPI May 1, 2021. <https://doi.org/10.3390/cells10050994>.
- (15) Pelham, R. J.; Yu-Li, W. Cell Locomotion and Focal Adhesions Are Regulated by Substrate Flexibility. *Proc Natl Acad Sci U S A* **1997**, *94*, 13661–13665. <https://doi.org/10.1073/pnas.94.25.13661>.
- (16) Tilghman, R. W.; Blais, E. M.; Cowan, C. R.; Sherman, N. E.; Grigera, P. R.; Jeffery, E. D.; Fox, J. W.; Blackman, B. R.; Tschumperlin, D. J.; Papin, J. A.; Parsons, J. T. Matrix Rigidity Regulates Cancer Cell Growth by Modulating Cellular Metabolism and Protein Synthesis. *PLoS One* **2012**, *7* (5). <https://doi.org/10.1371/journal.pone.0037231>.

- (17) Yeung, T.; Georges, P. C.; Flanagan, L. A.; Marg, B.; Ortiz, M.; Funaki, M.; Zahir, N.; Ming, W.; Weaver, V.; Janmey, P. A. Effects of Substrate Stiffness on Cell Morphology, Cytoskeletal Structure, and Adhesion. *Cell Motil Cytoskeleton* **2005**, *60* (1), 24–34. <https://doi.org/10.1002/cm.20041>.
- (18) Corr, D. T.; Hart, D. A. Biomechanics of Scar Tissue and Uninjured Skin. *Adv Wound Care (New Rochelle)* **2013**, *2* (2), 37–43. <https://doi.org/10.1089/wound.2011.0321>.
- (19) Schwartz-Dabney, C. L.; Dechow, P. C. Variations in Cortical Material Properties throughout the Human Dentate Mandible. *Am J Phys Anthropol* **2003**, *120* (3), 252–277. <https://doi.org/10.1002/ajpa.10121>.
- (20) Li, L.; Eyckmans, J.; Chen, C. S. Designer Biomaterials for Mechanobiology. *Nature Materials*. 2017. <https://doi.org/10.1038/nmat5049>.
- (21) Li, B.; Wang, J. H. C. Fibroblasts and Myofibroblasts in Wound Healing: Force Generation and Measurement. *J Tissue Viability* **2011**, *20* (4), 108–120. <https://doi.org/10.1016/j.jtv.2009.11.004>.
- (22) Rodrigues, M.; Kosaric, N.; Bonham, C. A.; Gurtner, G. C. Wound Healing: A Cellular Perspective. *Physiol Rev* **2019**, *99* (1), 665–706. <https://doi.org/10.1152/physrev.00067.2017>.
- (23) Hinz, B. The Role of Myofibroblasts in Wound Healing. *Curr Res Transl Med* **2016**, *64* (4). <https://doi.org/10.1016/j.retram.2016.09.003>.
- (24) Walker, J. T.; Flynn, L. E.; Hamilton, D. W. Lineage Tracing of Foxd1-Expressing Embryonic Progenitors to Assess the Role of Divergent Embryonic Lineages on Adult Dermal Fibroblast Function. *FASEB Bioadv* **2021**, *3* (7), 541–557. <https://doi.org/10.1002/FBA2.1219>.
- (25) Discher, D. E.; Janmey, P.; Wang, Y.-L. Tissue Cells Feel and Respond to the Stiffness of Their Substrate. *Science* **2005**, *310* (5751), 1139–1143. <https://doi.org/10.1126/science.1116995>.

- (26) Hinz, B.; Phan, S. H.; Thannickal, V. J.; Galli, A.; Bochaton-Piallat, M.-L.; Gabbiani, G. The Myofibroblast. *Am J Pathol* **2007**, *170* (6), 1807–1816. <https://doi.org/10.2353/ajpath.2007.070112>.
- (27) Leask, A. Integrin B1: A Mechanosignaling Sensor Essential for Connective Tissue Deposition by Fibroblasts. *Adv Wound Care (New Rochelle)* **2013**, *2* (4), 160–166. <https://doi.org/10.1089/wound.2012.0365>.
- (28) Leask, A. The Hard Problem: Mechanotransduction Perpetuates the Myofibroblast Phenotype in Scleroderma Fibrosis. *Wound Repair Regen* **2021**, *29* (4), 582–587. <https://doi.org/10.1111/wrr.12889>.
- (29) Garland, S. P.; McKee, C. T.; Chang, Y. R.; Raghunathan, V. K.; Russell, P.; Murphy, C. J. A Cell Culture Substrate with Biologically Relevant Size-Scale Topography and Compliance of the Basement Membrane. *Langmuir* **2014**, *30* (8), 2101–2108. <https://doi.org/10.1021/la403590v>.
- (30) Comelles, J.; Fernández-Majada, V.; Acevedo, V.; Rebollo-Calderon, B.; Martínez, E. Soft Topographical Patterns Trigger a Stiffness-Dependent Cellular Response to Contact Guidance. *Mater Today Bio* **2023**, *19*. <https://doi.org/10.1016/j.mtbio.2023.100593>.
- (31) Gurtner, G. C.; Werner, S.; Barrando, Y.; Longaker, M. T. Wound Repair and Regeneration. *Nature* **2008**, *453*, 314–321. <https://doi.org/10.1159/000339613>.
- (32) Zhao, T.; Zhao, W.; Chen, Y.; Li, V. S.; Meng, W.; Sun, Y. Platelet-Derived Growth Factor-D Promotes Fibrogenesis of Cardiac Fibroblasts. *Am J Physiol Heart Circ Physiol* **2013**, *304* (12), H1719-26. <https://doi.org/10.1152/ajpheart.00130.2013>.
- (33) Cialdai, F.; Risaliti, C.; Monici, M. Role of Fibroblasts in Wound Healing and Tissue Remodeling on Earth and in Space. *Front Bioeng Biotechnol* **2022**, *10*, 958381. <https://doi.org/10.3389/fbioe.2022.958381>.
- (34) Fournier, B. P. J.; Larjava, H.; Häkkinen, L. Gingiva as a Source of Stem Cells with Therapeutic Potential. *Stem Cells Dev* **2013**, *22* (24), 3157–3177. <https://doi.org/10.1089/scd.2013.0015>.

- (35) Sriram, G.; Bigliardi, P. L.; Bigliardi-Qi, M. Fibroblast Heterogeneity and Its Implications for Engineering Organotypic Skin Models in Vitro. *Eur J Cell Biol* **2015**, *94* (11), 483–512. <https://doi.org/10.1016/j.ejcb.2015.08.001>.
- (36) Guo, F.; Carter, D. E.; Mukhopadhyay, A.; Leask, A. Gingival Fibroblasts Display Reduced Adhesion and Spreading on Extracellular Matrix: A Possible Basis for Scarless Tissue Repair? *PLoS One* **2011**, *6* (11), 1–9. <https://doi.org/10.1371/journal.pone.0027097>.
- (37) Mak, K.; Manji, A.; Gallant-Behm, C.; Wiebe, C.; Hart, D. A.; Larjava, H.; Häkkinen, L. Scarless Healing of Oral Mucosa Is Characterized by Faster Resolution of Inflammation and Control of Myofibroblast Action Compared to Skin Wounds in the Red Duroc Pig Model. *J Dermatol Sci* **2009**, *56* (3), 168–180. <https://doi.org/10.1016/j.jdermsci.2009.09.005>.
- (38) Grada, A.; Mervis, J.; Falanga, V. Research Techniques Made Simple: Animal Models of Wound Healing. *Journal of Investigative Dermatology*. Elsevier B.V. October 1, 2018, pp 2095-2105.e1. <https://doi.org/10.1016/j.jid.2018.08.005>.
- (39) Zaidel-Bar, R.; Cohen, M.; Addadi, L.; Geiger, B. Hierarchical Assembly of Cell-Matrix Adhesion Complexes. *Biochem Soc Trans* **2004**, *32* (Pt3), 416–420. <https://doi.org/10.1042/BST0320416>.
- (40) Zaidel-Bar, R.; Milo, R.; Kam, Z.; Geiger, B. A Paxillin Tyrosine Phosphorylation Switch Regulates the Assembly and Form of Cell-Matrix Adhesions. *J Cell Sci* **2007**, *120* (1), 137–148. <https://doi.org/10.1242/jcs.03314>.
- (41) Geiger, B.; Spatz, J. P.; Bershadsky, A. D. Environmental Sensing through Focal Adhesions. *Nat Rev Mol Cell Biol* **2009**, *10* (1), 21–33. <https://doi.org/10.1038/nrm2593>.
- (42) Balaban, N. Q.; Schwarz, U. S.; Riveline, D.; Goichberg, P.; Tzur, G.; Sabanay, I.; Mahalu, D.; Safran, S.; Bershadsky, A.; Addadi, L.; Geiger, B. Force and Focal Adhesion Assembly: A Close Relationship Studied Using Elastic Micropatterned Substrates. *Nat Cell Biol* **2001**, *3* (5), 466–472. <https://doi.org/10.1038/35074532> [pii].

- (43) Prager-Khoutorsky, M.; Lichtenstein, A.; Krishnan, R.; Rajendran, K.; Mayo, A.; Kam, Z.; Geiger, B.; Bershadsky, A. D. Fibroblast Polarization Is a Matrix-Rigidity-Dependent Process Controlled by Focal Adhesion Mechanosensing. *Nat Cell Biol* **2011**, *13* (12), 1457–1465. <https://doi.org/10.1038/ncb2370>.
- (44) Marquis, M.-E.; Lord, E.; Bergeron, E.; Drevelle, O.; Park, H.; Cabana, F.; Senta, H.; Faucheux, N. Bone Cells-Biomaterials Interactions. *Frontiers in Bioscience* **2009**, *14*, 1023–1067. <https://doi.org/10.2741/3293>.
- (45) Chen, W. T.; Hasegawa, T.; Hasegawa, C.; Weinstock, C.; Yamada, K. M. Development of Cell Surface Linkage Complexes in Cultivated Fibroblasts. *Journal of Cell Biology* **1985**, *100*, 1103–1114.
- (46) Zamir, E.; Katz, M.; Posen, Y.; Erez, N.; Yamada, K. M.; Katz, B.-Z.; Lin, S.; Lin, D. C.; Bershadsky, A.; Kam, Z.; Geiger, B. Dynamics and Segregation of Cell– Matrix Adhesions in Cultured Fibroblasts. *Nat Cell Biol* **2000**, *2* (4), 191–196. <https://doi.org/10.1038/35008607>.
- (47) Zhong, C.; Chrzanowska-Wodnicka, M.; Brown, J.; Shaub, A.; Belkin, A. M.; Burridge, K. Rho-Mediated Contractility Exposes a Cryptic Site in Fibronectin and Induces Fibronectin Matrix Assembly. *Journal of Cell Biology* **1998**, *141* (2), 539–551. <https://doi.org/10.1083/jcb.141.2.539>.
- (48) Iwamoto, D. V.; Calderwood, D. A. Regulation of Integrin-Mediated Adhesions. *Current Opinion in Cell Biology*. 2015. <https://doi.org/10.1016/j.ceb.2015.06.009>.
- (49) Elosegui-Artola, A.; Bazellières, E.; Allen, M. D.; Andreu, I.; Oria, R.; Sunyer, R.; Gomm, J. J.; Marshall, J. F.; Jones, J. L.; Trepats, X.; Roca-Cusachs, P. Rigidity Sensing and Adaptation through Regulation of Integrin Types. *Nat Mater* **2014**, *13* (6). <https://doi.org/10.1038/nmat3960>.
- (50) Noskovicova, N.; Schuster, R.; van Putten, S.; Ezzo, M.; Koehler, A.; Boo, S.; Coelho, N. M.; Griggs, D.; Ruminski, P.; McCulloch, C. A.; Hinz, B. Suppression of the Fibrotic Encapsulation of Silicone Implants by Inhibiting the Mechanical Activation of Pro-

- Fibrotic TGF- $\beta$ . *Nat Biomed Eng* **2021**, 5 (12), 1437–1456.  
<https://doi.org/10.1038/s41551-021-00722-z>.
- (51) Gerstein, A. D.; Phillips, T. J.; Rogers, G. S.; Gilchrest, B. A. Wound Healing and Aging. *Dermatol Clin* **1993**, 11 (4), 749–757.
- (52) Engeland, C. G.; Sabzehei, B.; Marucha, P. T. Sex Hormones and Mucosal Wound Healing. *Brain Behav Immun* **2009**, 23 (5), 629–635.  
<https://doi.org/10.1016/j.bbi.2008.12.001>.
- (53) Dellambra, E.; Dimri, G. P. Cellular Senescence and Skin Aging. *Skin Aging Handbook: An Integrated Approach to Biochemistry and Product Development* **2009**, 129–148.  
<https://doi.org/10.1016/B978-0-8155-1584-5.50011-9>.
- (54) Khalili, A. A.; Ahmad, M. R. A Review of Cell Adhesion Studies for Biomedical and Biological Applications. *International Journal of Molecular Sciences*. 2015.  
<https://doi.org/10.3390/ijms160818149>.
- (55) Bose, S.; Robertson, S. F.; Bandyopadhyay, A. Surface Modification of Biomaterials and Biomedical Devices Using Additive Manufacturing. *Acta Biomater* **2018**, 66, 6–22.  
<https://doi.org/10.1016/j.actbio.2017.11.003>.
- (56) Pacelli, S.; Manoharan, V.; Desalvo, A.; Lomis, N.; Johda, K. S.; Prakash, S.; Paul, A. Tailoring Biomaterial Surface Properties to Modulate Host- Implant Interactions: Implication in Cardiovascular and Bone Therapy. *J Mater Chem B* **2016**, 4 (9), 1586–1599. <https://doi.org/10.4172/2157-7633.1000305>.Improved.
- (57) Summerfield, A.; Meurens, F.; Ricklin, M. E. The Immunology of the Porcine Skin and Its Value as a Model for Human Skin. *Molecular Immunology*. Elsevier Ltd July 1, 2015, pp 14–21. <https://doi.org/10.1016/j.molimm.2014.10.023>.
- (58) Robotti, F.; Sterner, I.; Bottan, S.; Monné Rodríguez, J. M.; Pellegrini, G.; Schmidt, T.; Falk, V.; Poulikakos, D.; Ferrari, A.; Starck, C. Microengineered Biosynthesized Cellulose as Anti-Fibrotic in Vivo Protection for Cardiac Implantable Electronic Devices. *Biomaterials* **2020**, 229. <https://doi.org/10.1016/j.biomaterials.2019.119583>.



- (59) Garate-Carrillo, A.; Gonzalez, J.; Ceballos, G.; Ramirez-Sanchez, I.; Villarreal, F. Sex Related Differences in the Pathogenesis of Organ Fibrosis. *Translational Research*. Mosby Inc. August 1, 2020, pp 41–55. <https://doi.org/10.1016/j.trsl.2020.03.008>.
- (60) Murtha, L. A.; Morten, M.; Schuliga, M. J.; Mabotuwana, N. S.; Hardy, S. A.; Waters, D. W.; Burgess, J. K.; Ngo, D. T. M.; Sverdlov, A. L.; Knight, D. A.; Boyle, A. J. The Role of Pathological Aging in Cardiac and Pulmonary Fibrosis. *Aging and Disease*. International Society on Aging and Disease April 1, 2019, pp 419–428. <https://doi.org/10.14336/AD.2018.0601>.

## Appendix A: Supplementary Tables & Figures

<b>Complete list of human phospho-kinases in proteome profiler kit</b>		
Akt 1/2/3 (S473)	HSP60	PRAS40 (T246)
Akt 1/2/3 (T308)	JNK 1/2/3 (T183/Y185, T221/Y223)	Pyk2 (Y402)
beta-Catenin	Lck (Y394)	RSK1/2 (S221/S227)
Chk-2 (T68)	Lyn (Y397)	RSK1/2/3 (S380/S386/S377)
c-Jun (S63)	MSK1/2 (S376/S360)	Src (Y419)
CREB (S133)	p38 alpha (T180/Y182)	STAT1 (Y701)
EGF R (Y1086)	p53 (S15)	STAT2 (Y690)
eNOS (S1177)	p53 (S392)	STAT3 (S727)
ERK1/2 (T202/Y204, T185/Y187)	p53 (S46)	STAT3 (Y705)
Fgr (Y412)	P70 S6 Kinase (T389)	STAT5a/b (Y699)
GSK-3 alpha/beta (S21/S9)	p70 S6 Kinase (T421/S424)	STAT6 (Y641)
GSK-3 beta (S9)	PDGF R beta (Y751)	WNK-1 (T60)
HSP27 (S78/S82)	PLC gamma-1 (Y783)	Yes (Y426)

## Appendix B: Human Ethics Approvals



**Date:** 29 May 2023

**To:** Dr. Douglas Hamilton

**Project ID:** 6311

**Review Reference:** 2023-6311-80140

**Study Title:** Physical and Biological Factors that Influence the Repair of Skin

**Application Type:** Continuing Ethics Review (CER) Form

**Review Type:** Delegated

**Date Approval Issued:** 29/May/2023 16:14

**REB Approval Expiry Date:** 24/Jun/2024

---

Dear Dr. Douglas Hamilton,

The Western University Research Ethics Board has reviewed the application. This study, including all currently approved documents, has been re-approved until the expiry date noted above.

REB members involved in the research project do not participate in the review, discussion or decision.

Western University REB operates in compliance with, and is constituted in accordance with, the requirements of the Tri-Council Policy Statement: Ethical Conduct for Research Involving Humans (TCPS 2); the International Conference on Harmonisation Good Clinical Practice Consolidated Guideline (ICH GCP); Part C, Division 5 of the Food and Drug Regulations; Part 4 of the Natural Health Products Regulations; Part 3 of the Medical Devices Regulations and the provisions of the Ontario Personal Health Information Protection Act (PHIPA 2004) and its applicable regulations. The REB is registered with the U.S. Department of Health & Human Services under the IRB registration number IRB 00000940.

Please do not hesitate to contact us if you have any questions.

**Electronically signed by:**

Mr. Joshua Hatherley, Ethics Coordinator on behalf of Dr. N. Poonai, HSREB Chair 29/May/2023 16:14

**Reason:** I am approving this document

**Note:** This correspondence includes an electronic signature (validation and approval via an online system that is compliant with all regulations).



# Western Research

**Date:** 2 February 2023

**To:** Douglas Hamilton

**Project ID:** 4988

**Review Reference:** 2023-4988-75696

**Study Title:** Physical, Biological and Pharmacological Factors Influencing human oral cell physiology

**Application Type:** Continuing Ethics Review (CER) Form

**Review Type:** Delegated

**REB Meeting Date:** 21/Feb/2023

**Date Approval Issued:** 02/Feb/2023 12:11

**REB Approval Expiry Date:** 16/Feb/2024

---

Dear Douglas Hamilton,

The Western University Research Ethics Board has reviewed the application. This study, including all currently approved documents, has been re-approved until the expiry date noted above.

REB members involved in the research project do not participate in the review, discussion or decision.

Western University REB operates in compliance with, and is constituted in accordance with, the requirements of the Tri-Council Policy Statement: Ethical Conduct for Research Involving Humans (TCPS 2); the International Conference on Harmonisation Good Clinical Practice Consolidated Guideline (ICH GCP); Part C, Division 5 of the Food and Drug Regulations; Part 4 of the Natural Health Products Regulations; Part 3 of the Medical Devices Regulations and the provisions of the Ontario Personal Health Information Protection Act (PHIPA 2004) and its applicable regulations. The REB is registered with the U.S. Department of Health & Human Services under the IRB registration number IRB 00000940.

Please do not hesitate to contact us if you have any questions.

**Electronically signed by:**

Ms. Nicola Geoghegan-Morphet, Ethics Officer on behalf of Dr. P. Jones, HSREB Chair 02/Feb/2023 12:11

**Reason:** I am approving this document

**Note:** *This correspondence includes an electronic signature (validation and approval via an online system that is compliant with all regulations).*

# Curriculum Vitae

**Sarah Brooks**

## **Education:**

### **B.Sc Biomedical Biology (Honours)**

Laurentian University

Sudbury, ON

2011-2015

### **Ph.D. Candidate**

School of Biomedical Engineering

Western University

London, ON

2016 – Present

## **Honours and Awards:**

Western Graduate Research Scholarship

2016-2021

## **Related Work Experience:**

Student Research Assistant

Northeast Cancer Center

2012-2015

Dental Simulation Clinic After Hours Supervisor

Western University

2019-2020

## **Publications:**

1. Nikoloudaki G., **Brooks S.**, Peidl AP., Tinney D., Hamilton DW. JNK Signaling as a Key Modulator of Soft Connective Tissue Physiology, Pathology, and Healing. International Journal of Molecular Sciences 2020 Febr; 21(3):1015. doi: 10.3390/ijms21031015.

2. **Brooks S**, Mittler S, Hamilton DW. Contact Guidance of Connective Tissue Fibroblasts on Submicrometer Anisotropic Topographical Cues Is Dependent on Tissue of Origin,  $\beta$ 1 Integrins, and Tensin-1 Recruitment. *ACS Appl Mater Interfaces*. 2023 Apr 26;15(16):19817-19832. doi: 10.1021/acsami.2c22381.

### **Presentations and Posters:**

1. Saunders, D.P., Carter, S., Koutsoukis, E., Charette, V., **Brooks, S.**, Hubert, K., Pearce, A., Ishak, F., Szeto, C., Rouleau, T., Fetterly, T. Development of a multidisciplinary, three phased symptom management patient care fact sheet for patients undergoing head and neck radiation therapy. Poster at: MASCC/ISOO International Symposium on Supportive Care in Cancer; 2014 Jun 26-28; Miami, FL.
2. **Brooks, S.**, Hamilton, D. (2017) Investigating the response of human dermal and gingival fibroblasts to changes in substratum compliance: Implications for soft tissue biomaterials development. Poster at: Canadian Biomaterials Society annual meeting; Winnipeg, MN.
3. **Brooks, S.**, Mittler, S., Hamilton, D. (2018) Influence of nanometric substratum topography on human dermal and gingival fibroblast fibrillar adhesion formation. Poster at: Canadian Connective Tissue Conference; Toronto, ON.
4. **Brooks, S.**, Mittler, S., Hamilton, D. (2019) Physiological impact of biomaterial compliance and topography upon gingival fibroblasts. Poster at: International Association for Dental Research; Vancouver, BC.
5. **Brooks, S.**, Mittler, S., Hamilton, D. (2019) Influence of substratum stiffness on the expression of periostin in dermal and gingival fibroblasts. Poster at: FASEB The Matricellular Proteins in Tissue Remodeling and Inflammation Conference; Lisbon, PT.
6. **Brooks, S.**, Mittler, S., Hamilton, D. (2022) Fibroblast Contact Guidance on Sub-Micron Groove Topographies is Dependent on Tissue of Origin. Oral Presentation at: Canadian Biomaterials Society annual meeting; Banff, AB.